In vitro modelling of tongue derived microbial biofilms and their response to treatments

Keith Edward Hewett B.Sc. (Hons)

A thesis submitted in partial fulfilment of the requirements of the University of the West of England, Bristol for the degree of Doctor of Philosophy

This research programme was carried out in collaboration with the

EPSRC and Phillips Research Laboratories UK

Department of Applied Science, University of the West of England, Bristol

April 2018

Abstract

This work concerns the development of a flat plate perfusion model to study biofilms derived from human tongue biota. The model has been derived from a previous sorbarod model, via a flat plate model (used to study wound organisms), to the model described in this thesis. The specific technical objectives were; 1. To measure biofilm pH in real time, 2. To extend VOC analysis by SIFT-MS to six biofilms in parallel and 3. To enable photodynamic interventions and optical monitoring of bioluminescent and non-bioluminescent organisms. The specific scientific objectives were; 1. To validate the model by comparison of *in vivo* and *in vitro* case studies, 2. To characterise the *in vivo* biofilm ecology and compare with ecology *in vitro,* 3. To compare existing and novel anti-malodour preparations and biofilm disrupting agents (including D-amino acids) and 4. To assess and aid the development of a novel handheld surface plasmon resonance based device for measuring oral volatile compounds.

The results demonstrated that the biofilms transplanted from human donors are stable and reproducible, and that profiles of volatile compounds are retained in the transplanted biofilm, with high and low malodour individuals producing high and low malodour biofilms (profiles are indistinguishable by χ^2 analysis at $p < 0.1$). The model was used to evaluate a novel formulation which was shown to be more effective than similar active compounds and controls ($p < 0.05$). In a further experiment, exposure of biofilms to D-amino acids during the growth phase was shown to cause significant ($P<0.05$) effects on microbial and EPS composition compared with controls.

Finally, the model in conjunction with SIFT-MS has been used to assess the performance of a novel surface plasmon resonance based biosensor. This biosensor has been shown to distinguish high and low malodour biofilms both *in vitro* and *in vivo*.

In conclusion it has been demonstrated that the flat plate perfusion system is a stable, reproducible and accurate model covering many of the main aspects of a real tongue biofilm, and it has many advantages when compared with other published biofilm models.

Acknowledgements

I must firstly and foremost thank my supervisor, Professor John Greenman for making this thesis possible. Without his guidance and support since before this particular project even began, I would surely have given up on science long ago.

Secondly, thanks to my mum, the amazing Pearl Hewett. You saw me start, but sadly you never saw me finish.

Thirdly love and thanks to my dad, the amazing Lang Hewett, who's support has been constant through all the good and bad times. And thank you to all the rest of the family, we all support each other wherever we all are.

Thanks to all my friends and colleagues at UWE, for putting up with everything and making it a great place to work in spite of it all. In particular thanks to Saliha Saad firstly for her invaluable friendship, secondly her love of fine food and thirdly of course her irreplaceable role as clinical trials director for the *in vivo* studies. Also, many thanks to Robin Thorn, Darren Reynolds, David Corry and Jasper Morrison.

Thanks to all my other friends and family who have supported me over these years.

And finally, thanks to this PhD itself, for helping me remember that the world is a fantastic place and we all never stop learning.

Table of Contents

List of Figures

List of Abbreviations

AUC	Area under curve
CAD	Computer Aided Design
CCD	Charge coupled device
CDFF	Constant Depth Film Fermente
C-di-GMP	Cyclic diguanylate
CHX	Chlorhexidine
CLSM	Confocal Scanning Laser Microscopy
DGC	Diguanylate cyclases
DLVO	Derjaguin–Landau–Verwey–Overbeek
EPS	Extracellular Polymeric Substances
ET	Electron Transfer
GC	Gas Chromatography
GTP	Guanosine triphosphate
H-NOX	haem NO/oxygen binding
HOMIM	Human Oral Microbe Identification Microarray
HOMINGS	Human Oral Microbe Idenification using Next Generation Sequencing
MDS	Multidimensional Scaling
NCDAA	Non-canonical D amino acids
PCA	Principle Component Analysis
PDE	Phosphodiestererases
PEEK	Poly ether ether ketone
pGpG	linear diguanylate
PT	Proton transfer
PTR-MS	Proton Transfer Reaction Mass Spectroscopy
SIFTMS	Selected Ion Flow Tube Mass Spectroscopy
SPR	Surface Plasmon Resonance
VC/VSC	Volatile Compounds
VOC	Volatile Organic Compounds
VSC	Volatile Sulphur Compounds

1. Introduction

1.1 Microbial Biofilms

It is over three centuries since Antony van Leeuwenhoek described the use of his improved microscope to view a sample of tooth plaque retrieved from an elderly Dutchman (Dobell and Leeuwenhoek 1960). He saw "an unbelievably great company of living animalcules, a-swimming more nimbly than any I had ever seen up to this time". Despite the amount of time passed, knowledge of the prokaryotic world remains meagre to say the least, with barely one percent of existing bacterial species formally described (Pace, 1997). Even within this tiny snapshot of the global microbiome, a large proportion of research has been focused on medically significant bacteria. Most pathogenic bacteria by their nature overwhelm mixed normal flora and predominate at the site of infection. Methods to identify or examine these bacteria have relied on primary isolation and study of a monoculture in vitro, on laboratory culture media. These modes of growth by bacteria are far removed from what is commonly seen throughout nature. For example, surveys of 16S rRNA genes reveal that although approximately 10^7 bacteria exist in one gram of soil, only between 1 and 10% are cultivable (Colwell and Grimes 2000; Kaeberlein *et al.,* 2002). It has been claimed that this is because the correct mix of nutrients or specific conditions that these organisms require has not been supplied, or that they are somehow in a 'dormant' state. However, recent research has shown that some of them have lost the ability to produce crucial compounds such as siderophores and thus rely on their neighbours for growth (Lewis *et al.,* 2010). The mixed culture is thus growing as a microbial aggregate within the soil. If we look wider at examples of microbial colonization throughout nature, we see that diverse complex bacterial communities are ubiquitous. Biofilms exist on

abiotic surfaces such as rocks, minerals and air-water interfaces and almost all biotic ones. The human body itself is colonised by microbial biofilms over the majority of its epithelial surface. They are structurally and dynamically complex biological systems that share many attributes with both macro scale ecosystems and multicellular organisms (Stoodley *et al.,* 2002).

The first stages of biofilm development have been extensively studied both qualitatively and quantitatively. Any surface in contact with liquid containing organic matter will quickly gain a conditioning film of organic molecules (Bryers, 1987). Marshall *et al.,* (1971) were the first to suggest a model based on the Derjaguin–Landau–Verwey–Overbeek (DLVO) theory of colloid stability, which is itself a combination of the effects of Van der Waals attraction and the double layer force. This model has been subsequently developed to include both hydrophobic: hydrophilic and osmotic interactions to give the so-called extended DLVO theory (van Oss, 1995). This theory is however a simplistic approximation of actual processes as it neglects entirely any dynamic effects that are due to directed processes by living organisms. It is these directed processes that have more recently been studied in various species.

Following inoculation, binding and early colonisation, the biofilm develops and matures and nature of it changes in significant ways. Whilst growth has been stochastic in nature, it begins to become more deterministic, as organisms that are capable of interaction and are in close enough proximity begin communication with chemo-attractants and pheromones through quorum sensing. This leads to changes in growth rate and gene expression and the biofilm begins to behave as a true community (Allison et al., 1998). This has been seen in both motile gram negatives such as Escherichia coli and Vibrio spp. and non-motile organisms such as Staphylococcus aureus and Mycobacterium spp. (Stoodley et al., 2002). Microcolonies and water-channels can appear, and cells alter their

physiochemical processes to suit the micro-niches they inhabit; both by autogenic and allogenic succession (Marsh, 2000). In fully mature biofilm, quorum sensing (McLean *et al.,* 1997; Labbate *et al.,* 2004; Parsek and Greenberg 2005) and horizontal gene transfer (Roberts *et al.,* 1999; Hannan *et al.,* 2010) have been demonstrated, along with distinct organismal, ecological and functional organization (Wilmes *et al.,* 2009).

1.1.1 The monolayer biofilm

The initial stage of the formation of complex microbial communities is usually the formation of a monolayer biofilm. This is defined as a biofilm where all cells or small clumps of cells are bound to a surface and none to other cells. Formation initially progresses stochastically with cells attaching, detaching and reattaching. In many species, type IV pili have been shown to be important in this process (Klausen *et al.,* 2003) as have flagellae. *In E.coli* fimbrae such as curli have been shown to also have a role ((Vidal *et al.,* 1998). In other species or variants, surface proteins such as *esp* (Toledo-Arana *et al.,* 2001) *bap* (Cucarella *et al.,* 2001) and Ag43 (Klemm *et al.,* 2004) have been shown to be involved in initial surface binding. As more cells become permanently attached, the process becomes more deterministic. Moorthy and Watnick (2004) showed that in *Vibio cholerae* as type IV pilus attachment progresses, flagella expression is reduced. Van Dellen *et al.,* (2008) suggested that this in turn caused a change in membrane potential that mediated the change from transient to permanant attachment. In *E.coli* the conditionally synthesised EPS adhesin PGA appears to mediate this transition (Agladze *et al.,* 2005). In *Caulobacter crescentus* the flagellum cells are removed by a protease and replaced by a specific holdfast polysacccharide that binds tightly to the surface (Li *et al.,* 2005).

As time progresses, further spread of the monolayer biofilm occurs by both pilus

associated twitching motility and clonal growth (Klausen et al., 2003).Eventually surface colonies merge to form a confluent carpet of cells. In most cases, when sufficient nutrients and other favourable conditions are available, the biofilm will then go on to develop into a complex three dimensional matrix of cells and exracellular material.

1.1.2 Extracellular Polymeric Substances (EPS)

The matrix surrounding and produced by biofilm cells was originally thought to consist almost entirely of polysaccharides, and in fact the abbreviation EPS reflected this. The 'Extracellular Polysaccharides' were seen as a combination of capsule, which was a simple extension of the cell wall, and slime, an amorphous, viscous substance surrounding the cells (Wilkinson, 1958). This misconception was for the most part due to the fact that cells were being examined either in simple plate culture or in the planktonic state. The glycocalyx, as it became known, was well described by Costerton and Irvin (1981) but even in this work and in another published the same year (Costerton *et al.,* 1981), the group was beginning to notice other filamentous structures in the extracellular matrix. As techniques improved, the first indications that it might not be as amorphous as it first appeared then emerged (see Characklis and Wilderer 1989). In the next decade, cryoscanning electron-microscopy (i.e. Cherepin, 1992) , Atomic Force Microscopy (Beech, 1996) and transmission electron microscopy (Jacques and Gottschalk, 1997) using monoclonal antibodies to stabilise the capsule) were all used to image biofilms, with varying degrees of success. In parallel to this work, non-microscopic techniques were providing evidence of the nature of the EPS. A number of studies used genetic mutants that either over or under-expressed polysaccharides (Danese *et al.,* 2000) and alginates (Franklin and Ohman, 1996; Hentzer *et al.,* 2001; Tielen *et al.,* 2005) to examine the nature of the EPS matrix. Additionally, methods of mathematically modelling biofilms, (Wimpenny and Colasanti,

1997; Van Loosdrecht et al., 2002) suggested a heterogeneous mosaic model. However, the underlying problem was that as the matrix consisted of over 90% water, any visualisation techniques which involved dehydration and fixation were bound to destroy much of the 3D structure being studied. Fortunately, it was around this time that Confocal Scanning Laser Microscopy (CSLM) was becoming more readily accessible. The technique, described in more detail later (section 2.5), facilitated an explosion in knowledge and further work (Lawrence *et al.,* 1998; Wingender *et al*., 1999; Neu and Lawrence 2014a; Schlafer and Meyer 2015). It became apparent that not only was there a multitude more constituents to the EPS to be considered, but the function and purpose of the matrix was far more extensive than previously thought.

It is now obvious that a complex three-dimensional structure is probably the most important defining characteristic of a biofilm. The EPS is a combination of polysaccharides, phospholipids, proteins, glycoproteins and nucleic acids. It not only aids adhesion, aggregation, cohesion and retention of water, but it protects the colony, facilitates absorption of organic and inorganic compounds and acts as a nutrient source between species. Perhaps most importantly, though, is the contribution to the ecology of the biofilm. Initially the presence of DNA in the matrix was thought to be merely a contamination from lysed cells, but evidence suggests that in certain species it is important in biofilm formation (Whitchurch *et al.,* 2002) and in some cases is under the release of quorum sensing systems (Allesen-Holm *et al.,* 2006). Acylhomoserine Lactone (AHL) has also been frequently detected in the EPS matrix suggesting other quorum based intercommunication between bacteria (Tan *et al.,* 2015). Factors such as this become unimportant at high maximum specific growth rate (μmax) as organisms tend to downregulate or switch off completely any mechanisms or pathways which are unnecessary when nutrients are in good supply and all conditions are favourable (Magasanik, 1961).

1.1.3 Complex multilayer biofilms

In the conventional model of biofilm growth and development (Figure 1.1) the thick biofilm may be removed by mechanical forces (liquid shear, or toothbrush or other abrasive forces) so that the biofilm continues to grow but reaches pseudo-steady state as parts grow, but other parts are rapidly removed.

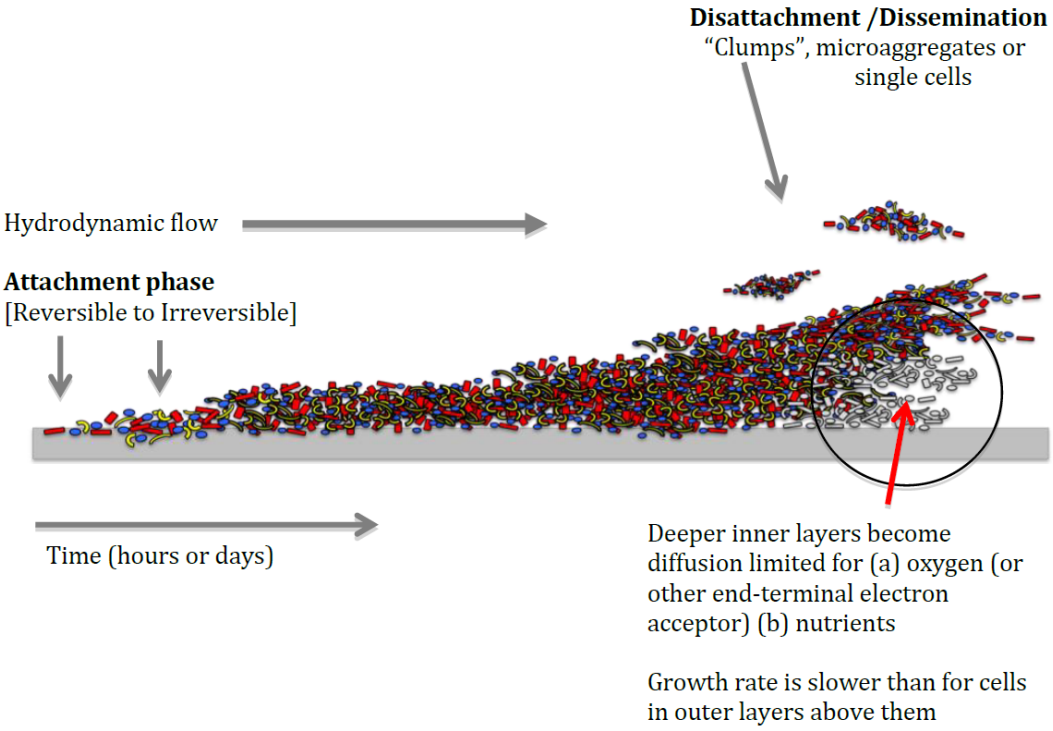

Figure 1.1: Conventional conception of "thick biofilm"

When the removal process is due to fluidic shear, then the removal rate is close to being constant; however the biofilm matrix is heterogeneous due to (a) diffusion layers or gradients for gases (oxygen, carbon dioxide, ammonia) and (b) diffusion layers or gradients for carbon-energy nutrients. Mathematical modelling of diffusion and hydrodynamic flow can show how different microenvironments can favour the growth of some types (e.g. aerobes and anaerobes) and may account for pH changes that form across the depth of the biofilm. The conventional concept considers the substratum (e.g. tooth surface) and biofilm matrix and cells, to be two different entities or compartments.

The finding that perfusion biofilms behave differently to the conventional model (and the repercussions of that finding) suggest that specific conditions can allow for fairly constant steady state conditions to occur which can be maintained for several weeks. The perfusion biofilm can be described as a small vessel of tethered cells within a rapid moving steam of growth medium. The substratum (e.g. cellulosic strands) and the channels and voids are well integrated over the mm-cm scale and the term "biofilm matrix" now includes the substratum as well (figure 1.2).

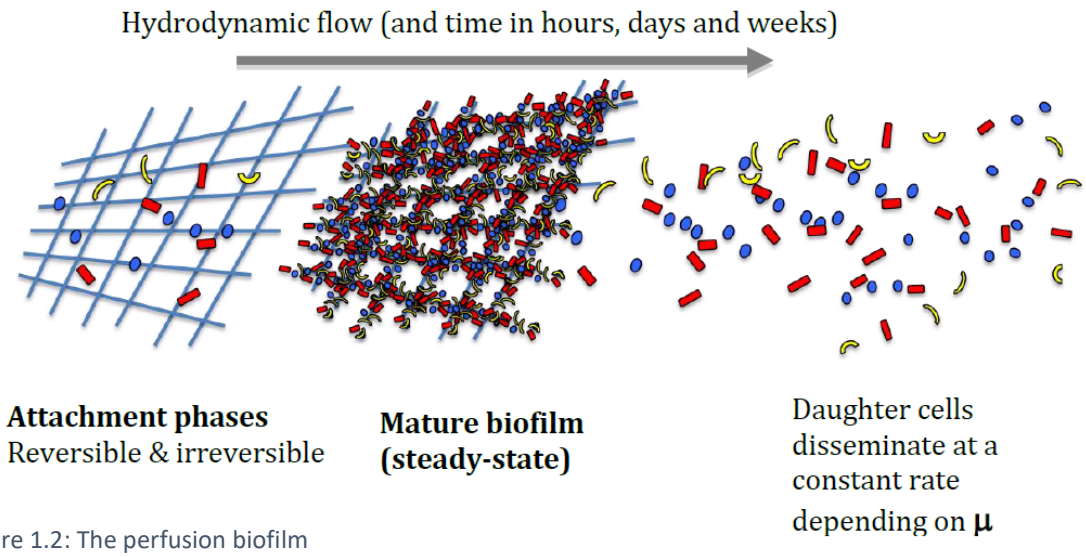

Figure 1.2: The perfusion biofilm

In a thick film biofilm diffusion of rate limiting factors (oxygen and nutrients) will govern the growth rate and metabolism of the cells and are the most important factors that determine the behaviour or physiological state of the deeper parts of the biofilm. This ceases to be the case in a free-flowing loose matrix "perfusion" biofilm where the modelling becomes much simpler since perfusion rate replaces diffusion rate. The consequences of this are that the perfusion biofilm matrix can be considered to be homogeneous (at the mm-cm scale), and that all the cells in the system are formed from the inner attached layer that grows continuously (providing that the physicochemical conditions and flow rate remain constant). At each generation, daughter cells are pushed nearer to the micro-flow channels within the

matrix, and daughter cells are eventually sheared off. Fast growth rates may be achieved in practice (McKenzie, 2007) as well as in theory and it is most likely that the residence time for the mother layer is potentially many years, whilst the half-life of detached cells in the vessel is relatively short, especially at high flow rates. In contrast, a thick film biofilm will increase the diffusion barrier and favour an inner core of anaerobes and an outer core of aerobes, with facultative anaerobes throughout. Cells above the inner layer will continue to grow and multiply within the matrix volume, wherever they may be located in the matrix. The outside layers with shorter diffusion distance to the main nutrient source will grow faster than the inside layers.

Diffusion barriers to the products of microbial metabolism, including acids, bases and hydrogen ions, will increase along with diffusion barriers to substrates. For substrates such as glucose or sucrose the acid production for oral streptococci and other fermentative species would soon create a pH gradient, with the inside layers having a lower pH than the outside layers (McKenzie, 2007). It should be noted that long or tubular perfusion matrix systems can also show marked gradients along the vertical down-flow axis (McKenzie 2007), but this is less so for a flat 1 cm^2-sized matrix where all cells are subjected to all chemical components equally within a short period of time, maintaining overall homogeneity of the micromozaic of microbial aggregates or microcolonies.

The tongue surface is composed of pits, crypts and fissures so that any biofilms that develop deep in a pit are growing constantly and the pressure of growth would tend to push cells towards the lumen end of the pit. However, the biofilm growing on the tongue surface will not have a distinct eternal layer of mother cells because the substratum itself (i.e. the mucosal epithelial cells) are slowly but constantly desquamating producing unattached cells, which may degenerate and lyse, to be ultimately ejected from the micro-vessel pit.

The concepts of compartments is also important in understanding biofilms: For a thick biofilm (such as a thick biofilm on the tongue surface and down crypts or pits) will have (1) bulk salivary phase, (2) a thin salivary surface film that will rapidly flow across the surfaces of the tongue and be rapidly replaced with a mean residence time measured in seconds rather than minutes, (3) the biofilm matrix volume contains fluid (called matrix fluid) which, in contrast to the abovementioned 2 layers has a much slower mean residence time. This slow removal of the inner matrix volume allows reaction products of the cells to build up to a high concentration, and any protein hydrolysis reactions (such as breakdown of glycoproteins) to go more to completion over a given unit of time (e.g. per hour). The matrix volume (matV) of a biofilm for a tongue with low microbial population ($<10^7$ cells cm^{-2}) will be a thin biofilm, ($matV_{thin}$) whilst a population of 10^8-10^9 cells would be denoted as a thick biofilm ($matV_{thick}$). The biofilm area will remain the same, but its matrix volume will be thicker the higher the amount of biofilm components (cells, EPS and solutes). As with a chemostat the dilution rate, D = f/V and its units are expressed as per time unit (h^{-1}).

The effects of thickness, volume and flow rate on the mean residence time (= 1/D) expressed as hours suggests that all reactions will build up to higher degrees of completion, including glucose to lactate, urea to ammonia and bicarbonate to carbon dioxide. In addition carbonic anhydrase can permit phase changing reactions such as HCO_3^{2-} >>> $CO_{2\ (gas)}$ and H_2O with the effect of removing a weak acid (allowing the pH to rise). Likewise the reaction equilibrium between urease and urea is of interest (Mack and Villars, 1923).

$$(NH_2)_2CO + H_2O \xrightarrow{urease} NH_3 + H_2NCOOH \rightarrow 2NH_{3\ (gas)} + CO_{2\ (gas)}$$

Equation 1.1: Urease reaction

Urease is a naturally occurring enzyme that catalyzes the hydrolysis of urea to unstable carbamic acid. Rapid decomposition of carbamic acid occurs without enzyme catalysis to

form ammonia and carbon dioxide (equation 1.1). Depending on the pH, the ammonia will likely escape to the atmosphere unless it reacts with water to form ammonium ion (NH_4^+) according to the following reaction:

$$NH_{3\,(gas)} + H_2O \longrightarrow NH_4^+ + OH^-$$

Equation 1.2: Formation of ammonium ions

The carbon dioxide is reversibly hydrated as shown in equation 1.3 and this reaction is catalysed by carbonic anhydrase (Smith *et al.,* 1999).

$$HCO_3^- + H^+ \longrightarrow H_2CO_3 \rightleftharpoons CO_2 + H_2O$$

Equation 1.3: Carbonic anhydrase reaction

The reaction rate of carbonic anhydrase is one of the fastest of all enzymes, and its rate is typically limited by the diffusion rate of its substrates. Typical catalytic rates of the different forms of this enzyme range between 10^4 and 10^6 reactions per second (equation 1.3), whilst the reverse reaction is relatively slow in the absence of a catalyst. This enzyme is found quite widely in nature including some species of oral bacteria and a mammalian source found in saliva (Supuran, 2004).

It has been shown (Saad, 2006) that by taking tongue scrape samples and re-suspending them into sterile distilled water (rather than weak tryptone buffer) it is possible to measure the matrix pH providing measurements are taken quickly (within 2 minutes of collection). When these data were plotted against malodour scores of 20 subjects, a strong relationship was seen (figure 4.6) with respective R^2 values between 0.7444 and 0.7834. These results suggest that malodour generation is associated with an increase in the mean pH of the tongue biofilm whereas there was only a weak negative correlation (R^2 approximately 0.4) between the pH of saliva and malodour parameters.

Although there are publications regarding the co-measurement of salivary pH and malodour parameters, and reports of tongue surface pH (salivary layer) and malodour, there are none that have been described relating tongue biofilm matrix pH and malodour with the exception of Saad and Greenman (Patent app. WO2008GB02466). The reasons that an increase in biofilm pH may result in an increase in malodour parameters could include: (1) the pH optima for transformation of substrates into VC/VSC could be higher than neutral (2) the higher pH of the tongue favours volatility of VC/VSC (3) the higher pH of the tongue could favour the optimal pH of collective proteolytic activity.

It is also possible that there is no causal relationship between a high pH and malodour but rather the other way round; a high malodour generating biofilm (indicative of protein and peptide metabolism) may have the tendency to cause the pH to increase. A high biofilm density will produce more amines, ammonia or other basic products and produces an alkaline condition. Yet another explanation could be that a thicker biofilm (that correlates with higher malodour) could hold a larger dead space volume of salivary coating/biofilm fluid; analogous to Kleinberg's concept of residual salivary film (Kleinberg and Codipilly, 1995) with a longer mean residence time of molecules than occurring within a thin biofilm. The larger volume of salivary coating coupled with its longer turnover will shift the pH equilibrium towards base as salivary CO_2 is released from the main bicarbonate buffer (CO_2/HCO_3^-).

1.1.4 The Oral Biofilm

In a natural human birth, the neonate leaves the uterus sterile, but as soon as contact is made with the vaginal canal and the outside environment, colonization by bacteria begins (Collado *et al.,* 2012; Costello *et al.,* 2012). As the epithelial surface inside and outside the body becomes exposed to this environment and the organisms in it, a microbiome is built up. By the time this process has completed, prokaryotic cells outnumber eukaryotic

cells by an order of magnitude. The habitats of the human body are extremely varied and this leads to the development of distinct microbial populations. These characteristic populations have varying diversity at the habitat level (alpha diversity) and varying diversity between the same habitats across subjects (beta diversity). Changes in diversity in either direction can be indicative of disease (The Human Microbiome Project Consortium, 2013). The environment of the human oral cavity has been extensively studied and the microbiome found there has been shown to be richer in variety and more conserved than others in the body (Stahringer *et al.*, 2012). The first work to investigate microbial interactions during early biofilm formation was by Kolenbrander with various teams. (Whittaker, Klier and Kolenbrander, 1996; Kolenbrander and London, 1993; Kolenbrander and Andersen, 1986; Kolenbrander, Andersen and Moore, 1990; Kolenbrander and London, 1992). Simple assays utilised the decrease in turbity associated with species-to-species binding to characterise these interactions. The earliest colonizers of the biofilm are overwhelmingly streptococci, followed by *Actinomyces, Capnocytophaga, Haemophilus, Prevotella, Propionibacterium* and *Veillonellae* (summarised in figure 1.3). All of these organisms possess specific cell surface associated adherence proteins which recognise protein, glycoprotein, or polysaccharide receptors on various oral surfaces, including other cell types. This strategy of attaching to bacteria already immobilised to hard or soft tissues may provide secondary colonisers with similar advantages as enjoyed by primary colonizers.

The oral cavity consists of a number of different habitats, including the hard and soft palates, the tongue, cheeks and tonsils, plus the teeth and gingival sulcus, all providing differing conditions and colonized by different populations of bacteria. Overall these comprise of over 600 prevalent taxa (Dewhirst *et al.*, 2010). They are lubricated and irrigated by salivary fluid and this influences biofilm formation both positively and negatively. Some factors inhibit microbial growth and mediate microbial killing (eg. histatin), or bind to

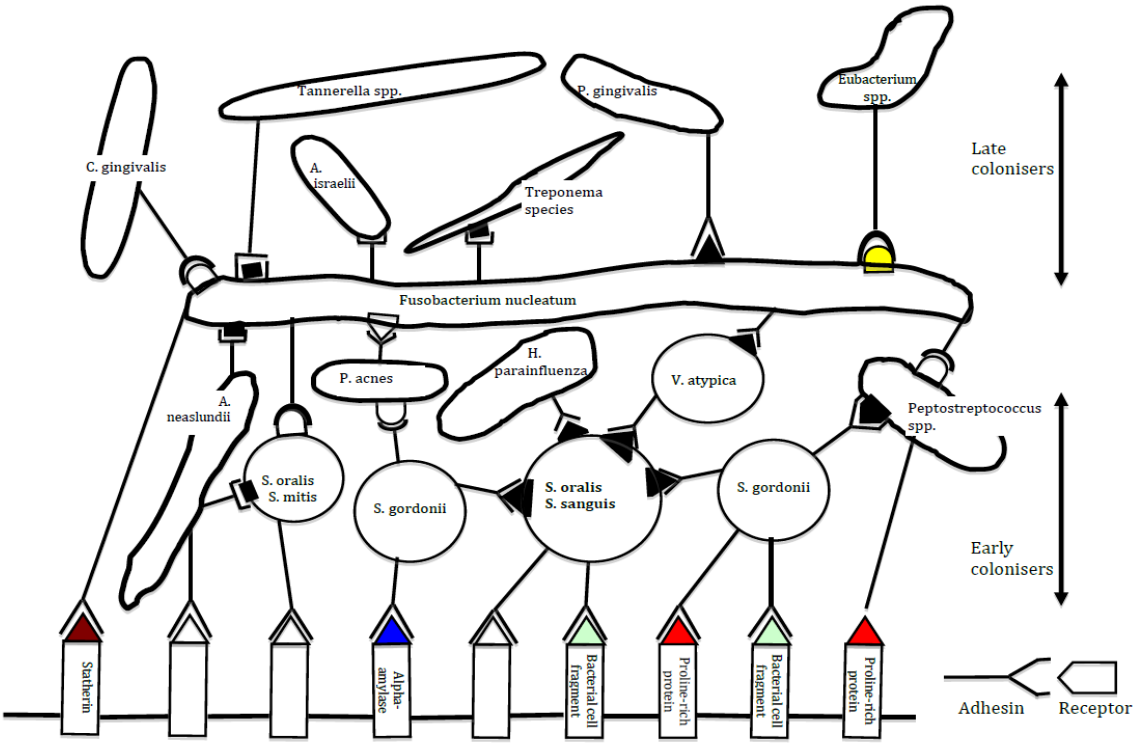

Figure 1.3: Oral biofilm co-attachment showing early colonisers as identified by Kolenbrander *et al.* (1993) (Reproduced with permission of the American Society for Microbiology)

microorganisms to facilitate their clearance from the oral cavity (eg. agglutinins). Conversely, salivary components serve as receptors in oral pellicles for microbial adhesion to host surfaces and serve as microbial nutritional substrates (Scannapieco, 1994)

There are many oral diseases or conditions in which the oral microbiome is implicated, including dental caries, periodontal disease, endodontic infections, dento-alveolar infections, salivary gland infections, tonsillitis and oral malodour. In many of these cases, the etiological agents are not single pathogens but a consortia of microorganisms causing a shift from 'health' to 'disease' (Kuramitsu *et al.* 2007). In the case of oral malodour, its severity is likely to be associated with greater species diversity in the mouth (Donaldson *et al.* 2005).

1.1.5 Bacterial Second Messengers

Second messengers are signalling molecules that act within cells in response to a primary trigger that is external in origin. In eukaryotes this primary trigger is usually a hormone or neurotransmitter, but in microbial cells a wide range of environmental stimuli can act as a primary messenger. Second messengers are thus principle components of intracellular signal transduction cascades. In recent years much biofilm research has focussed on the role of cyclic dimeric (3'→5') guanosine monophosphate (C-di-GMP).

C-di-GMP was first identified as the activator of cellulose synthase in *Gluconacetobacter xylinum* (formally *Acetobacter xylinum*) by Ross *et al.,* (1987). This important molecule has been shown to affect motility, virulence and cause an overall shift to and from planktonic to sessile modes of growth. Tal *et al.,* (1998) showed that intracellular turnover of C-di-GMP is controlled by the dual action of diguanylate cyclases (DGC) and phosphodiesterases (PDE). In the seminal work of Simm *et al.,* (2004), it was shown that these enzymes are identified by GGDEF and EAL domains respectively. These domains had previously been identified in diverse bacterial strains and were designated domains of unknown function; DUF1 and DUF2 (Galperin *et al.,* 2001). Later work by Slater *et al.,* (2000) and Ryan *et al.,* (2017) showed that a further domain, HD-GYP was associated with C-di-GMP downregulation. The cycle is illustrated in Figure 1.4. Briefly, the phosphodiesterases dissociate C-di-GMP into either a linear diguanine polyphosphate (pGpG) or guanosine monophosphate (GMP) which is then converted to guansine trIphosphate (GTP). GTP recycled to C-di-GMP by the diguanylate cyclases. The consequences of up and downregulation of both C-di-GMP and GTP are shown in Figure 1.5.

It is now apparent that a significant messaging and regulation system had been discovered. GGDEF, EAL and HD-GYP motifs have now been identified in all major bacterial phyla (Romling et al., 2013) and over 900 proteins expressing these domains have been

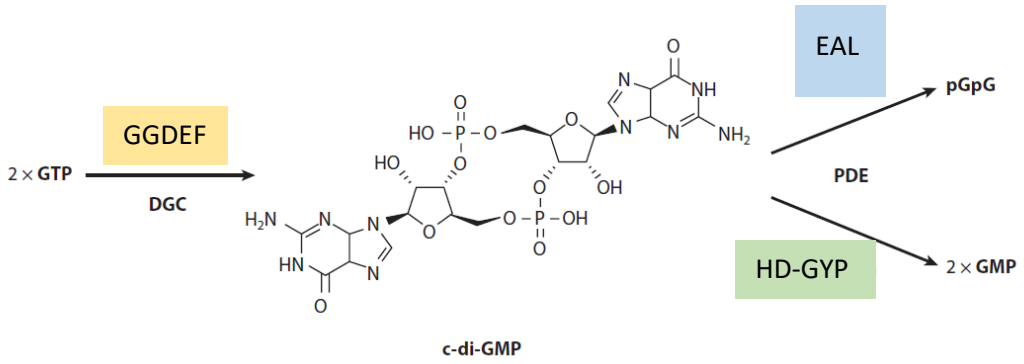

Figure 1.4: Modulation of C-di-GMP by GGDEF, EAL and HD-GYP domain proteins.

identified (Schultz et al., 1998; Tatusov, 2001). Although details vary, the overarching purpose of the C-di-GMP system appears to be the transition between motile and sessile modes of colonisation. Increased C-di-GMP levels correspond to reduced motility and increased production of EPS (particularly alginates and polysaccharides) and fimbriae, and increased cell to cell communication (Römling *et al.,* 2005). However, knowledge of stimuli and effectors of C-di-GMP signalling remains

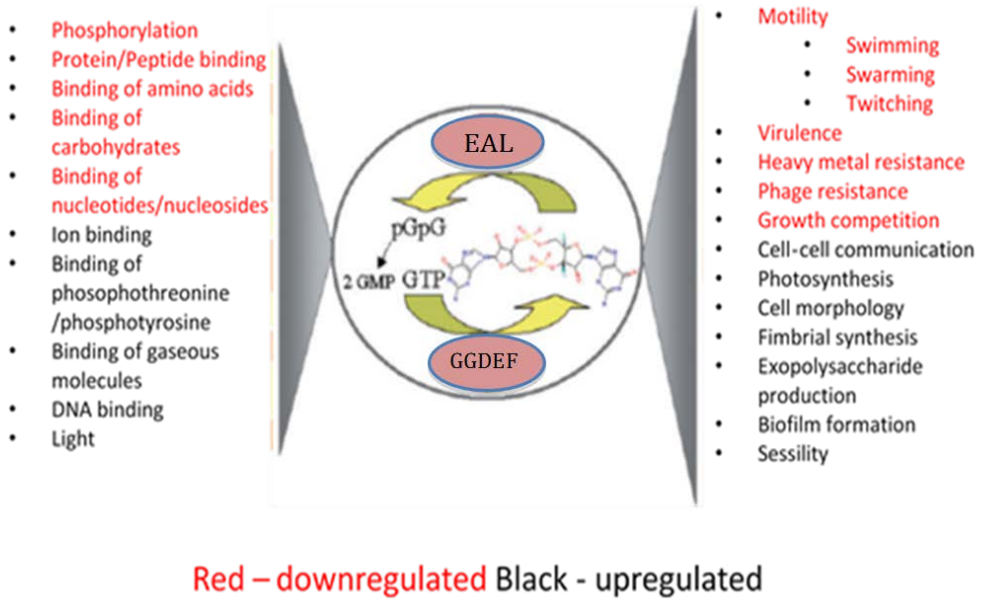

Figure 1.5: Effects in the balance; upregulation and downregulation of C-di-GMP and GTP.

sparse. A number of effectors in various organisms have been shown to carry the PilZ motif (Amikam and Galperin, 2006). This is a ~100 amino acid protein domain that appears to be involved with production of alginate in *Pseudomonas aeruginosa* (Merighi *et al.,* 2007), motility in *Borrelia burgdorferi* (Freedman *et al.,* 2010), *Caulobacter crescentus* (Christen *et al.,* 2007) and *Vibrio cholera* (Pratt *et al.,* 2007) and fimbriae expression and biofilm production in *Klebsiella pneumoniae* (Wilksch *et al.,* 2011). In *Shewanella oneidensis* MR-1, it has been suggested that C-di-GMP acts through MxdB, a membrane associated glycosyl transferase that is essential for cell attachment specifically to the matrix and not the substratum (Thormann *et al.,* 2006). Degenerate EAL and GGDEF domains have also been identified as effectors. LapD is an inner membrane effector protein that binds C-di-GMP via a degenerate EAL domain and induces the expression of biofilm adhesion LapA (Newell *et al.,* 2009, 2011). C-di-GMP has also been shown to bind to riboswitches in limited cases (Sudarsan *et al.,* 2008; Lee *et al.,* 2010). Of the few strict anaerobes studied, *Clostridium perfringens* has been shown to possess C-di-GMP mediated expression of Type IV pili (Hendrick *et al.,* 2017).

The potential hinted at by the ubiquity of C-di-GMP binding domains and the multitude of C-di-GMP dependent systems has yet to be realised. The full extent of this signalling network and the proteins and RNAs that may be involved remains a mystery. A full list of known receptors and effectors can be examined at http://ncbi.nlm.nih.gov/Complete_Genomes/c-di-GMP.html and a summary of current understanding of c-di-GMP binding is given by Chou and Galperin (2016).

In terms of external stimuli a similar state of affairs exists. Few environmental signals that regulate C-di-GMP mediated pathways have been identified. One exception is nitric oxide, which has been shown to increase C-di-GMP levels in *Shewanella oneidensis* (Plate and Marletta, 2012), *Legionella pneumophila* (Carlson *et al.,* 2010) and *Vibrio fischeri* (Wang

et al., 2010) through the GGDEF-EAL domain containing haem NO/oxygen-binding (H-NOX) proteins. Thormann *et al.,* (2005, 2006) have suggested that, in *S. oneidensis*, a reduction in oxygen levels leads to biofilm detachment and dispersal though C-di-GMP pathways, although this is unconfirmed.

It is obvious that these mediators and effectors are merely the tip of a large iceberg and the C-di-GMP mediation network will provide extensive potential for study for many years to come. In this respect the C-di-GMP signalling network within the tongue biofilm has barely been scraped. Oral organisms about which the presence of C-di-GMP related protein domains are known are shown in Table 1.1. This table was created by searching the database referenced earlier (Romling *et al.,* 2013; Chou and Galperin, 2016) for instances of oral organisms from the known oral microbiome (Kilian *et al.,* 2016). Of the organisms showing relevant domains, only *Porphyromonas gingivalis* and *Treponema denticola* have been investigated for C-di-GMP mediated traits. *P. gingivalis* mutants lacking GGDEF proteins showed reduced FimA protein production and fimbrial display, leading to corresponding reduction in biofilm production and host cell invasion (Chaudhuri *et al.,* 2014). Similarly, *T. denticola* deletion mutants for a PilZ-like protein named TDE0214 has been shown to be deficient in biofilm formation and virulence (Bian *et al.,* 2013). Interestingly, one other oral organism, *Streptococcus mutans,* has shown C-di-GMP biofilm mediation and this is through a non-GGDEF domain protein (Yan *et al.,* 2010).

As far as other common oral microbes are concerned, any role of C-di-GMP and mechanisms by which modulation may occur are unknown. A large number of significant oral organisms, such as *Actinomyces* sp*., Bacteroides* sp*., Bergeyella* sp*.,* Enterococci, *Eubacterium so., Fusobacterium* sp*., Neisseria* sp*., Prevotella* sp*., Tannerella* sp*. and Veillonella* sp*.* have simply not been examined for the presence of relevant protein domains, nor investigated for the presence of intracellular cyclases.

Table 1.1: Distribution of GGDEF, EAL, HD-GYP and PilZ domains in the genomes of oral bacteria, where known (compiled from published data)

Do not contain GDDEF/EAL domains	Do contain GDDEF/EAL domains
Actinobacillus succinogenes	*Campylobacter concisus*
Aggregatibacter actinomycetemcomitans	*Halothiobacillus neapolitanus*
Atopobium parvulum	*Halothiobacillus sp.*
Bifidobacterium longum	*Lactobacillus reuteri*
Corynebacterium durum	*Lactobacillus salivarius*
Cryptobacterium curtum	*Porphyromonas gingivalis*
Enterococcus faecalis	*Ralstonia solanacearum*
Filifactor alocis	*Selenomonas sputigena*
Fusobacterium nucleatum	*Staphylococcus epidermidis*
Haemophilus influenzae	*Treponema denticola*
Haemophilus parainfluenzae	
Lactobacillus fermentum	
Lactobacillus helveticus	
Lactobacillus johnsonii	
Lactococcus lactis	
Moraxella catarrhalis	
Prevotella denticola	
Prevotella melaninogenica	
Rothia dentocariosa	
Rothia mucilaginosa	
Streptococcus dysgalactiae	
Streptococcus gordonii	
Streptococcus mitis	
Streptococcus mutans	
Streptococcus sanguinis	
Streptococcus suis	
Streptococcus thermophilus	
Streptococcus uberis	
Tannerella forsythia	
Veillonella parvula	

1.1.6 Treatments based on modulation of C-di-GMP

The ubiquity of C-di-GMP pathways in diverse taxa, and the specificity of the signalling network to prokaryotic cells has led many to suggest C-di-GMP as a potential target for antimicrobial treatment. Effectiveness of hypothetical agents can be proved *in principium* using mutant strains that either over or under express GDDEF and EAL domains. This has been shown with *Ps. putida* (Gjermansen *et al.,* 2006)*, Ps. aeruginosa* (Christensen *et al.,* 2013)*, S. oneidensis* (Thormann *et al.,* 2006)*, Vibrio vulnificus* (Nakhamchik *et al.,* 2008) and others. However, identification of actual agents has proved harder.

Sambanthamoorthy *et al.* (2011, 2012, 2014) have used high-throughput screening to identify compounds that antagonise DGC enzymes, and several of these have shown promising biofilm dispersal properties in V. cholera, Ps. aeruginosa and Staph. aureus. Ma *et al.*, (2011) on the other hand, have protein engineered a potential bioreactive compound. Opoku-Temeng and Sintim's groups have also identified several potential small compounds that can permeate cells and influence C-di-GMP levels in bacteria (Zheng *et al.*, 2014; Opoku-Temeng and Sintim, 2016a, 2016b; Opoku-Temeng *et al.*, 2017). The most promising of these have been hydroxybenzylidene-indolinones . This is an active and promising area of study with the potential to produce novel and important broad-spectrum antimicrobials and anti-biofilm agents.

1.2 Oral Pathology and Malodour

Oral malodour is a common condition defined by the presence of odorous volatile compounds and/or sulphur compounds (VCs, VSCs) on the breath of individuals, noticeable by independent objective judges and considered as objectionable by others. It affects humans worldwide, although tolerance of levels and opinion on what is considered objectionable varies greatly between countries and cultures. Volatile sulphur compounds (VSCs) such as H_2S, CH_3SH and $(CH_3)_2S$ and $(CH_3)_2S_2$ are the main contributors to oral malodour (Tonzetich, 1971). Other VOCs such as indole, skatole, cadaverine and putrescine are also present, but are not considered as objectionable due to their low volatility or high smell threshold (Tonzetich and Richter, 1964;Tonzetich *et al.,* 1967). It is widely accepted that the primary source for the production of these compounds is the microbial community of the dorsoposterior surface of the tongue (Hartley *et al*., 1996b; Hess *et al*., 2008). VSCs are produced through the putrefactive action of microorganisms on sulphur-containing substrates namely cysteine, cystine, glutathione or

methionine within proteins and peptides. Other endogenous and exogenous substrates and precursors in the oral cavity include exfoliated oral epithelium, salivary corpuscules, saliva, blood and food debris (Massler *et al.,* 1951; Tonzetich and Kestenbaum, 1969; Tonzetich, 1977). Figure 1.6: Production of VOCs by oral bacteria shows a schematic summary of these processes.

There have been several microbiological studies investigating the composition of the tongue microbiota of individuals with oral malodour. Additionally, there have been metabolic studies of groups of oral organisms to identify those with the propensity to cause malodour. A summary of this work is shown in table 1.2.

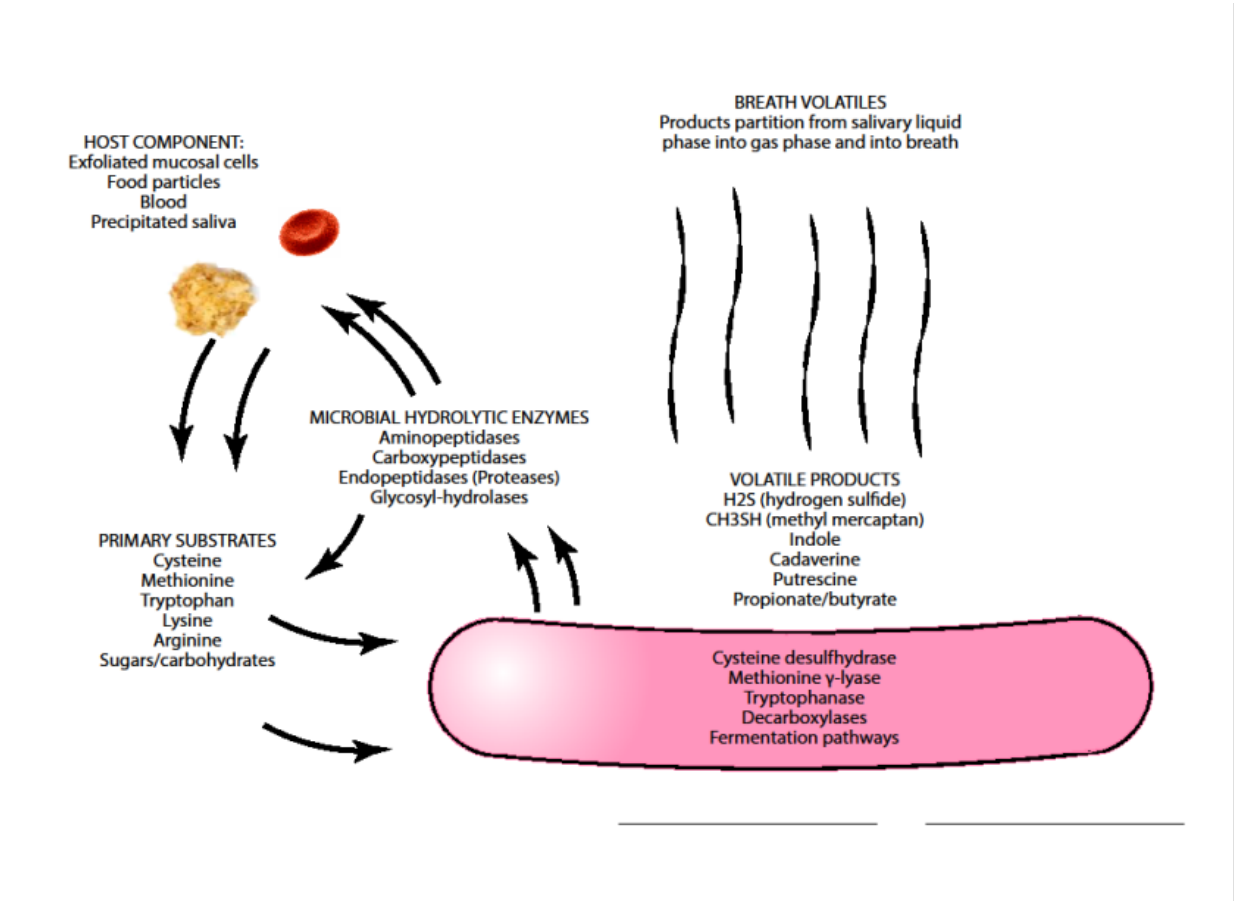

Figure 1.6: Mechanisms of VOC production by oral bacteria

The first of these studies was by Persson *et al.,* (1989) and used gas chromatography to measure the production of sulphides from known species incubated in serum. Next, Hartley *et al.,* (1996) compared samples cultured from the tongue dorsum of low and high malodour individuals. Loesche and Kazor (2002) published a useful summary of the microbiology of halitosis and Tyrrell *et al.*,(2003) published a comprehensive study of eight subjects with oral malodour that gave frequencies of occurrence of a range of VOC producing organisms. Salako and Philip, (2010) used Halimeter and OralChroma to analyse the headspace of vials various organisms to identify VSC producers. Haraszthy *et al.,* (2007, 2008) completed two rRNA based studies that first drew attention to *Solebacterium moorei* as a potential aetiological agent of malodour and Seerangaiyan *et al.,* (2017) also used 16S rRNA gene sequencing in a study study that identified some novel VOC producing organisms.

Table 1.2: Review of organisms linked to malodour

Researchers	Tyrell *et al*	Persson	Loesche	Hartley *et al*	Salako & Philip	Kazor	Seerangaiyan *et al*	Haraszthy *et al.*
Type of study	Microbiological	metabolic	mixed	micro	micro OC	16S rRNA	16S rRNA sequencing	16S rRNA sequencing
Year	2003	1990	2000	1996	2011	2003	2017	20072008
Actinomyces spp.	87.50%							
A. israelii	12.50%							
A. odontolyticus	25.00%							
A. radingae	12.50%							
A. turicensis	62.50%							
Actinomyces sp.	37.50%		*					
Aggregatibacter actinomycetemcomitans					*			
A. segnis							*	
Abiotrophia defectiva								*
Atopobium parvulum		*				*		*
Atopobium vaginae								*
Bacteriodes sp.		*						
Bacteriodes forsythus			*					
Bacteroides stercoris								*
Bacteroides ureolyticus	25.00%							
Bacterionema matruchotii			*					
Bifidobacterium breve	12.50%							
All *Campylobacter* spp.	37.50%						*	
C. concisus	12.50%							
C. gracilis	12.50%							
C. mucosalis	12.50%							
C. rectus	12.50%							
C. ureolyticus							*	
Capnocytophaga sp.				*			*	
Catonella sp.								*
Centipeda periodontii	12.50%	*						
Clavibacter xyli								*
Clostridiales sp.							*	

Researchers	Tyrell *et al*	Persson	Loesche	Hartley *et al*	Salako & Philip	Kazor	Seerangaiyan *et al*	Haraszthy *et al.*
Type of study	Microbiological	metabolic	mixed	micro	micro OC	16Sr RNA	16S rRNA sequencing	16S rRNA sequencing
Year	2003	1990	2000	1996	2011	2003	2017	20072008
Clostridiales sp.								
Collinsella aerofaciens	50.00%							
Dialister sp.						*	*	*
Dialister pneumosintes	12.50%							
Eikenella corrodens	62.50%							
Enterococcus faecalis								
Enterococcus malodoratus								
Eubacterium spp.	87.50%	*						
E. lentum	12.50%							
E. saburreum	62.50%							
E. timidum	25.00%							
E. limosum		*						
E. nodatum								
E. sulci						*		*
Eubacterium group (not identified)	50.00%		*					
Firmicutes sp.								*
Fusobacterium spp.				*				
Fusobacterium nucleatum	62.50%	*						
Fusobacterium periodonticum		*						*
Gemella morbillorum					*			
Granulicatella elegans								*
Haemophilus paraphrophilus								*
Kingella denitrificans								*
Lactobacillus spp.	50.00%							
L. oris	12.50%							
L. plantarum	12.50%							
Lactobacillus sp.	25.00%							

Researchers	Tyrell *et al*	Persson	Loesche	Hartley *et al*	Salako & Philip	Kazor	Seerangaiyan *et al*	Haraszthy *et al.*
Type of study	Microbiological	metabolic	mixed	micro	micro OC	16S rRNA	16S rRNA sequencing	16S rRNA sequencing
Year	2003	1990	2000	1996	2011	2003	2017	20072008
Leptotrichia sp.			*				*	
Leptotrichia buccalis	37.50%							
Luteococcus japonicus								*
Megaspaera sp.			*					
Mobiluncus curtisii								*
Mogibacterium neglectum								*
Neiseria sp.				*				
Neisseria flavecens			*					
Parvimonas sp.							*	
Peptostreptococcus spp.	62.50%						*	
P. anaerobius	62.50%	*						
P. micros	25.00%	*						
Peptococcus sp.							*	
Propionibacterium avidum	25.00%							
Porphyromonas spp.	25.00%		*	*				
P. catoniae	12.50%							
P. endodontalis	12.50%	*						
P. gingivalis	25.00%	*	*		*			
Porphyromonas sp.			*					
Prevotella spp.	100.00%			*			*	
P. buccae	25.00%							
P. corporis	12.50%							
P. dentalis	12.50%							
P. denticola	12.50%							
P. intermedia/nigrescens group	62.50%	*	*		*			
P. loescheii	12.50%	*						
P. melaninogenica	100.00%		*					

Researchers	Tyrell *et al*	Persson	Loesche	Hartley *et al*	Salako & Philip	Kazor	Seerangaiyan *et al*	Haraszthy *et al.*
Type of study	Microbiological	metabolic	mixed	micro	micro OC	16S rRNA	16S rRNA sequencing	16S rRNA sequencing
Year	2003	1990	2000	1996	2011	2003	2017	20072008
P. oris	12.50%							*
P. pallens	37.50%							
P. tannerae	25.00%							
Prevotella sp.	37.50%		*					
Rothia mucilaginosa			*					
Rothia sp.				*				
Saccharothrix australiensis								*
Selenomonas spp.	87.50%						*	
S. flueggei	62.50%							
S. infelix	25.00%							*
S. artermidis		*						
Selenomonas sp.			*					
Solobacterium moorei						*		*
Streptococcus spp.			*			*		
Staphylococcus haemolyticus								*
Staphyloooccus warneri								*
Stomatococcus mucilaginosus								*
SRI							*	
Tannerella forsythia					*		*	
Treponema sp.							*	*
Trepnema dentolica		*	*					
TM7 species							*	*
Veillonella sp.	100.00%							*

Note(1): * indicates presence. % indicates percentage of subjects with strain. Note(2): spp. Indicates multiple species, sp. Indicates single species not fully identified

1.3 Treating Oral Malodour

Approaches to combat oral malodour go back to ancient times and have extended over many cultures and religions throughout history. The use of toothpastes has played a significant part in oral hygiene for many centuries despite early formulations falling short of delivering antibacterial active compounds. Since the introduction of fluorides more than 50 years ago in toothpastes, its role in the prevention of dental caries through a mechanism of remineralisation has become indisputable (Brambilla, 2001). Moreover, other compounds such as metal ions (Zn^{2+}), cetylpyridinium chloride, triclosan, chlorhexidine (CHX), amine fluorides, and stannous fluoride can be added to toothpastes and have shown antibacterial activity *in vivo* (Addy, 1986; Arweiler *et al.,* 2001; Paraskevas *et al.,* 2004) and *in vitro* (Scheie, 2003). It is well accepted that CHX remains a benchmark in dental plaque control and in oral malodour (Addy, 1986; Jones, 1997; Scheie, 2003) and it is often used as a positive control in many studies. However, a long-term side effect of CHX is staining of the teeth (Flötra *et al.,* 1971; Bosy *et al.,* 1994; Quirynen, 2003), so alternative compounds have been used including amine fluoride/ stannous fluoride (AM/SnF) combination. It is believed that fluoride antibacterial action can be enhanced when used in association with cations such as Sn^{2+} or amine (Loveren, 1990). Amine fluoride was shown to reinforce enamel remineralisation and to have an antimicrobial effect (Wiegand *et al.,* 2007). Stannous fluoride is known for its anti-caries effects but is not stable when used alone in mouth rinse preparations or toothpastes (White, 1995). Therefore, it has been used in association with amine fluoride not only to address the instability problem but also to enhance caries protection.

1.4 Modelling the Oral Biofilm

Physical modelling of the oral biofilm can be split into two different systems, batch culture closed systems and open or continuous flow systems. Batch culture closed systems were the first method used historically to model biofilms, consisting of the culture of selected microbial species in a liquid medium with or without a solid substratum of known surface area present. This method has been effective at identifying a wide variety of volatiles from a wide variety of species/samples (Tonzetich, 1971; Tonzetich and McBride, 1981). However, the method is limited by the fact that it does not model the dynamic nature of the *in vivo* biofilm. *In vivo*, the whole physicochemical environment (number of cells, concentrations of substrates, nutrients, products, pH and oxygen tension) is in dynamic equilibrium, whilst these parameters are always shifting as an inevitable consequence of growth in a closed system. Cell populations will expand and products of their metabolism will accumulate leading to unavoidable deviation from initial conditions which is not reflective of the processes occurring in the oral cavity. Research has tended therefore to shift towards continuous flow systems.

1.4.1 Chemostat based systems

The chemostat has been used widely in oral microbiology research and is an ideal device for generating steady-state homogenous culture (Marsh *et al.,* 1983; McKee *et al.,* 1985; Greenman, 1999). However, as the cells remain in the planktonic mode its use for studying biofilms is very limited (Greenman, 1999).

1.4.2 Flow cell systems

Initial flow cell systems consisted of a modified flow cell reactor incorporating recirculation of media across biofilms formed on impermeable substratum (Pilch *et al.* 2005). At various time points, gas samples were withdrawn by small syringe from the head-space of the reactor for gas analysis by GC. These models were used to grow both pure and mixed culture salivary flora. However, these systems are not true continuous flow and can more accurately be described as circulatory batch culture with occasional replenishment. Some VOCs are derived from biofilm cells, but most are produced by the planktonic cells in the circulation loop.

The constant-depth film fermenter (CDFF) has been widely used in studying biofilms, and is a superior example of a continuous flow open system (ten Cate, 2006). Biofilms form within small recesses which are swept periodically to retain a constant depth of material. All other physicochemical parameters (medium, flow rate, atmosphere, temperature and pH) are carefully controlled in the system as a whole. Variability between biofilms is thus minimised (Hope *et al.*, 2012) and many groups have achieved good data regarding the oral microbial ecosystem (McKee *et al.,* 1985; Bradshaw *et al.,* 1989; Kinniment *et al.,* 1996). However, the model is compromised by the fact that all the biofilms share the same bulk planktonic culture, and cell populations on the biofilm can increase by two different phenomena, growth from within or further accretion from without, making growth rates for individual biofilms poorly defined.

1.4.3 Perfusion systems with permeable matrix substratum

A significant development in the *in vitro* modelling of biofilms was the move towards utilisation of a loose matrix substratum-based perfusion system. As outlined in section 1.1.3, perfusion biofilms behave differently to the conventional model in that the substratum and the channels and voids are well integrated over the mm-cm scale. The "biofilm matrix" thus includes the substratum as well as the biomass itself. The first such model was the perfused biofilm fermenter (Gilbert *et al.*, 1989), which used Swinnex filters as the permeable membrane. The working volume of the biofilm in this system is however quite small, and the perfusion model based on the sorbarod system devised by Hodgson *et al., (*1995) is favoured since this model has a biofilm surface many times greater and can be retained in a steady state for periods of several days.

The sorbarod system was the first to be used to study the effects of pH on the development of biofilms and the generation of VSCs from tongue inocula (Taylor and Greenman, 2010). Further work incorporated a carbon veil electrode into the matrix to assess the effects of antimicrobial compounds (Saad, Hewett and Greenman, 2012). Other groups have also used the model to screen anti-malodour agents (Burnett *et al.*, 2011).

1.4.4 Flat-bed perfusion matrix

The flat bed perfusion matrix was originally devised by Thorn and Greenman (2009) to study active surfaces in wound dressings, but with minor modifications has successfully been used to study oral biofilms and their production of volatiles (Saad *et al.,* 2013). The model as originally described is illustrated in figure 1.7.

An inclined slope supports a cellulose matrix comprising of loosely packed strands. Media was fed drip-wise onto the middle of the top surface of the matrix and waste flowed through and over the matrix and exited the enclosure via a drain hole. The only modification required to enable this apparatus to be used to model the oral biofilm was a port to enable the enclosure to be flooded with anaerobic gas and kept under positive pressure.

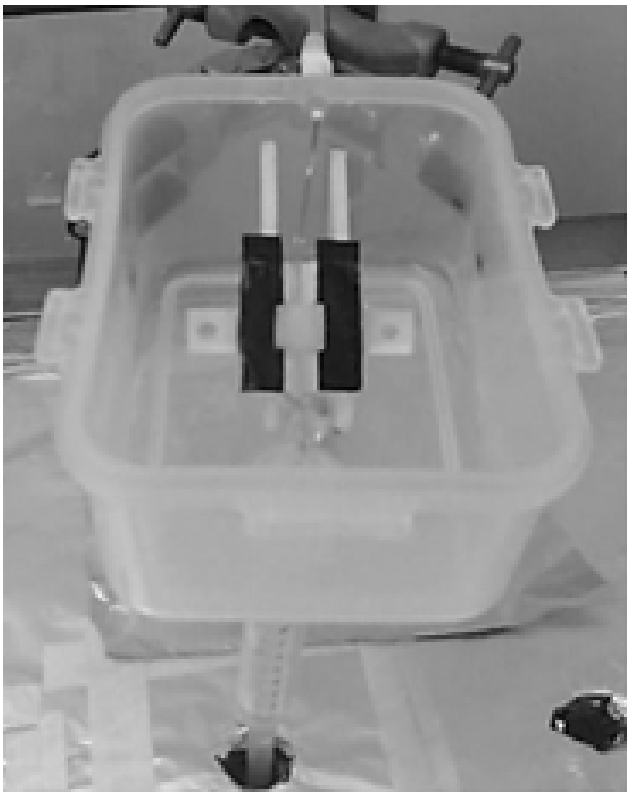

Figure 1.7: Original biofilm slope and enclosure as used by to study the effects of wound dressings (Thorn and Greenman, 2009)

After it was proved that reproducible steady state conditions similar to within the oral cavity could be produced with this method, further modifications were introduced to increased reproducibility between enclosures and runs. Initially, the replacement of the complex arrangement of glued glass, rubber and plastic with milled plastic mounting slopes (figure 2.1) enabled the model to be more resilient to multiple autoclave cycles without distortion or disassembly. This further led to rapid prototyping of the slopes in nanocure autoclavable material and this led to optimisation of the slope shape by computer aided design. A later modification of this design utilised curved slope sides, which allowed for waste to be more efficently channelled into the drain hole preventing build up of media containing planktonic cells inside the enclosure. The temperature of the enclosures has also been more carefully controlled by placing a single box in a dedicated, small volume incubator. Addition of a sampling port to the box allowed sampling of the gases above the biofilm using the instrument based method described in section 1.5. In culmination, these modifications have allowed real time monitoring of volatile organic compounds produced by biofilms by SIFT-MS and are described in more detail in section 2.1.

1.5 Quantifying volatile organic compounds (VOCs)

Historically, detection of volatile compounds produced by biofilms follows the pattern set in breath clinics. The original method was by assessment by a suitably trained human breath judge. Due to the subjectivity of this method, which will be discussed later, instrument based methods were developed. Initially the Halimeter (Interscan) was used, which produced a sensor derived value corresponding to overall levels of VSC (Rosenberg and McCulloch, 1992). After the turn of the millennium, the OralChroma (Abilit), a simplified sensor-based GC system, was developed. This could detect levels of H_2S, CH_3SH

and $(CH_3)_2S$ in ppb to ppm concentrations (Hanada *et al.,* 2003). More recently, the Selected Ion Flow Mass Spectroscopy (SIFT-MS) has been successfully utilised to provide real time detection and quantification of a wide range of volatiles in oral gas samples. These methods will be discussed in more details in the following sections.

1.5.1 Organoleptic assessment

It has been famously repeated that the study of the sense of smell has had a long past but a short history (Boring, 1942). Although our sense of smell has been discussed by philosophers for centuries, objective scientific study of olfaction only really commenced in the last hundred years. Zwaardemaker wrote about the psychology of smell in 1895 and this began the era of interest in this most academically neglected of senses. Early work by Backman (1917) and later Jones (1958a, 1958b) and Jones and Marcus, (1961) attempted to assess detection sensitivities of the human nose to various odorants. It soon became apparent that sensitivity varied hugely to different compounds, and that combinations of compounds had unpredictable consequences. Jones and Woskowt (1963) were the first to use logarithmic scales and mutltivarient regression to examine olfactory response to mixtures of odorants. They concluded that subjective magnitude was neither additive or averaged and suggested that olfaction be described as an "analytical" sense. Berglund *et al.,* (1973) proposed a vector model to describe interaction between pairs of odorants and demonstrated good agreement using selected compounds. This model predicted that the perceived odour intensity of a mixture of compounds A and B, is given by equation 1.4.

$$\psi_{A,B} = (\psi_A + \psi_B + \psi_A\psi_B \cos\alpha)$$

Equation 1.4: Perceived odour intensity of a mixture of two compounds

In the specific case where the perceived strengths of the odours are equivalent, ie $\psi_A = \psi_B$, this equation reduces to;

$$\psi_{A,B} = (\psi_A + \psi_B) \cos\frac{1}{2}\alpha$$

Equation 1.5: Special case of Eq.1 where intensities are equal

This can be used to experimentally deduce values of α for different compounds. This vector model has been successfully applied to qualitatively similar (Berglund *et al.,* 1973) and dissimilar (Cain and Drexler, 1974) compounds and to mixtures of up to four substances (Berglund, 1974; Laing *et al.,* 1993).

The inherent problem with all methods of malodour detection or diagnosis stem from the fact that categorisation by human judge is of course subjective, and some odours are considered more objectionable than others. This has led to the use of the so called "hedonic" scale (ASTM 1968) which scores odours based on how pleasant or unpleasant the odour is. From a clinical point of view this is useful on the one hand as a subjective assessment of the problem, but does not give information about actual compounds present and by inference the biological processes involved in their production. The organoleptic scale (Allison and Katz, 1919; Rosenberg, Kulkarni, *et al.,* 1991; Rosenberg, Septon, *et al.,* 1991) is therefore considered more relevent and an extensive evaluation of its use

is given by Greenman *et al.,* (2004). Because of the attempt to standardise through training the subjective nature of the measure, it is still considered the gold standard assessment for most clinical trials. However, instrument based measurements are by nature more objective and are therefore more useful when it comes to understanding the biological and chemical processes involved in VOC production.

1.5.2 Halimeter

The halimeter was developed by Interscan in the late eighties as a relatively low cost alternative to the standard GC-MS methods of gas analysis. It enabled dental and medical surgeries as well as researchers the ability to assess malodour in a standardised reproducible way (Rosenberg and McCulloch, 1992). A gas pump draws air through an inlet tube and across a sensor at a continuous flow rate. This sensor is comprised of a metal film sensing electrode coupled to a reference counter-electrode. A bias voltage is applied to favour oxidation of hydrogen sulphide at the sensing electrode, although other sulphides such as methyl mercaptan and dimethyl sulphide will also be oxidised. The instrument can therefore give a VSC level in parts per billion without discrimination between different sulphur compounds. It can also suffer from false positive response to other compounds that may be present in the sample such as ethanol, giving a fairly crude evaluation of oral malodour. It has however been widely and extensively used in clinical and microbiological studies.

1.5.3 OralChroma

First decribed by Hanada et al., (2003), the OralChroma is a simplified gas chromatograph that uses a gold doped indium oxide sensor and a specifically constructed column to create a relatively portable instrument for detecting VSCs. It detects H_2S, CH_3SH and $(CH_3)_2S$ in breath to around 100ppb levels and has been well reviewed in the

literature, for example by Tangerman and Winkel (2008). The instruments suffers from two issues, one is due to the interference of acetone, ethanol, isoprene and acetylaldehyde if present in high amounts on the breath of the subject. This problem can be minimised by strict conditions on food and drink ingested prior to testing. The second issue is due to software related issues leading to incorrect identifying of peaks and their measurement. This can be minimised by analysing the raw data produced from the sensor rather than the software's interpretation. If standard gases are available, calibration curves can be generated from the area under the peaks produced from known dilutions, giving far superior sensitivity and reproducibility.

1.5.4 SIFT-MS

The technique was first developed by Adams & Smith (1976) to study gas phase ion–neutral reactions in the laboratory. These reactions between charged ions and uncharged molecules occur in a number of terrestrial (Thomas, 1974), extra-terrestrial (Huntress 1974;Wayne, 2009) and extra-solar (Smith, 1992;Anicich, 2003) environments. The SIFT method was a development of the flowing afterglow (FA) method in use at the time which was itself was an improvement on stationary afterglow analysis. In order to study the reactions between ions and neutral atoms in these remote environments, a method was required to model the reactions in the laboratory. In the afterglow methods, ions are created by electrical discharge in a carrier gas such as helium and these ions are then reacted with neutral species in an introduced sample. A mass spectrometer can then be used to measure loss of the primary He^+ ions and a corresponding increase in product ions. In the FA method, the carrier gas is relatively fast flowing enabling samples to be introduced downstream of the ionisation event and other reactant gases to be introduced downstream of the ionisation but upstream of the sample. These gases react with the He^+ plasma to produce different

primary reactant ions (figure 1.8). The ability to sequentially add several reactant gases and thus produce many reactant ions, both positive and negative, proved to be both an advantage and a disadvantage to this method. It was extraordinarily flexible, but secondary reactions between reactant ions and parent gases caused huge complications in identification of ion products and precise quantification of their reaction coefficients.

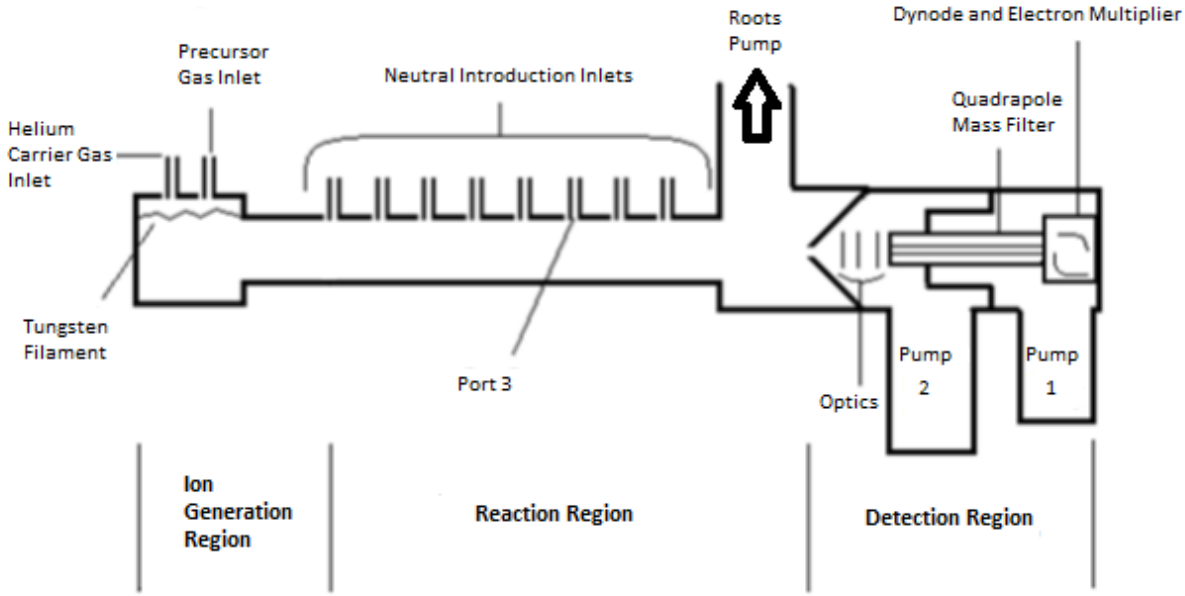

Figure 1.8: Flowing afterglow mass spectroscopy

The SIFT technique incorporated a significant and novel modification in that reactant ions were generated by an ionisation method within a seperate chamber (known as the SIFT chamber) and then selected using a quadropole mass filter. As the pressure in the downstream sample chamber, or flow tube, can be kept relatively high, there is little contamination of this chamber by any stray products of the ionisation process. This means that the reaction paths are much more well defined and therefore reaction coefficients can be measured with greatly increased precision and accuracy. This lead to an explosion in modelling of diverse plasmas such as those produced inside gas lasers and during plasma

deposition and etching. However, work with the technique also revealed its power as a analytical and diagnostic device.

The D region of Earth's troposphere contains a few postive ion complexes that prove to be stable and relatively unreactive with the major molecular components of the atmosphere. These include most notably the hydronium (H_3O^+), nitrosium (NO^+) and dioxygenyl (O_2^+) ions. The unreactive nature of these ions means that they are perfect for analysing trace gases in sample of moist air. By generating and selecting for these ions in the SIFT chamber, samples from many sources can be analysed. Where reaction coefficients are unknown, they can be determined with simple techniques. By controlling and knowing precisely the nature and concentrations of sample gases introduced into the instrument, reaction coefficients for numerous molecules and compounds can be deduced. Smith and Španěl performed a number of experiments of this kind before the turn of the millennium (Španěl e*t al.,* 1995; Španěl *et al.,* 1997; Smith and Španěl, 2011a, 2011b), leading to even more potential applications.

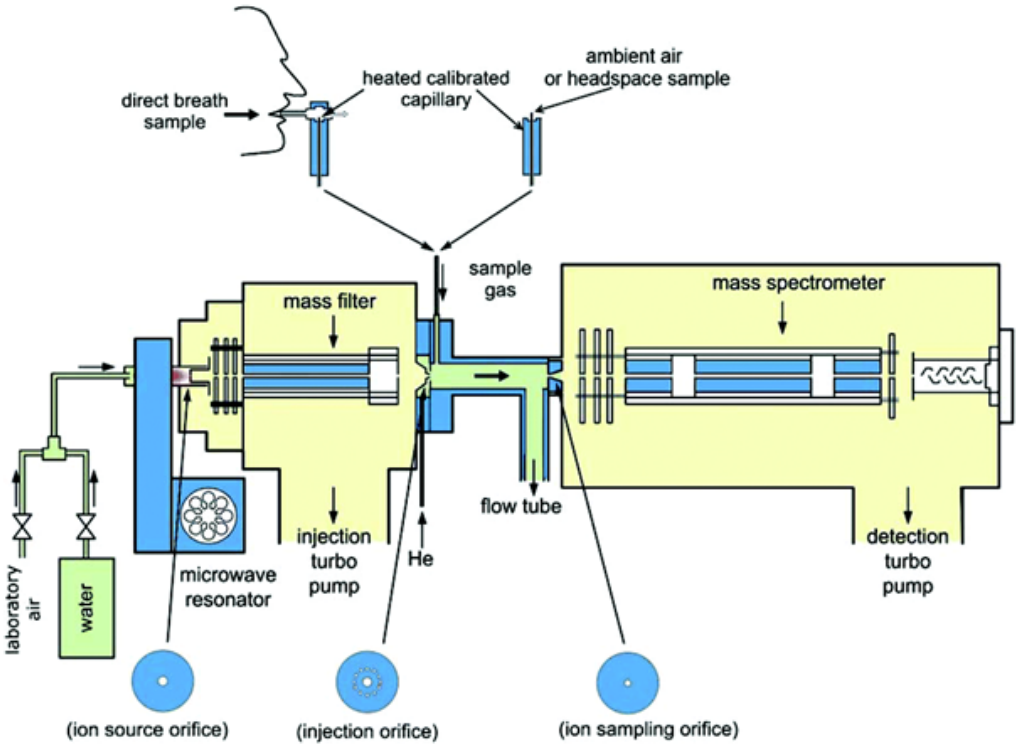

Figure 1.9: Profile3 SIFT-MS schematic (Smith and Španěl, 2011a) (Reproduced with permission from the Royal Society of Chemistry)

Smith and Španěl had direct involvement in the evolution of the SIFT-MS instrument up to and including the production of the Profile3 device by Instrument Science. This utilised a microwave resonator to generate the three positive reactant ions from humid air. After selection by the mass filter and reaction in the flow tube, products are sorted by mass spectrometer and enumerated by multiplier/pulse counter. Rate coefficients are calculated by the decay rate of precursor and increase of product counts, and from these gas levels in the sample are determined (Španěl *et al.,* 1997; Smith and Španěl, 2005). Their own diagram of the Profile3 instrument can be seen in figure 1.9.

Like other modern direct-injection mass spectrometric (DIMS) methods volatile compounds can be measured quantitatively in real time. Of the DIMS techniques, SIFT-MS is most often compared to proton-transfer-reaction mass spectrometry (PTR-MS). SIFT-MS tends to lose out in sensitivity to PTR-MS as with the latter technique a high intensity high purity H_3O^+ beam is injected without selection or dilution in a carrier gas. This leads to a sensitivity two orders of magnitude greater than by SIFT-MS (Blake *et al.,* 2009). SIFT-MS however, by allowing pre-selection of reagent ions, avoids the pitfall of not being able to ionize compounds whose proton affinity is smaller than that of H_2O (Jordan *et al.,* 2009). Also, SIFT-MS allows fine control of experimental conditions and thus determination of rate coefficients that can be routinely used for quantitative analysis (Biasioli *et al.,* 2011). Literature data on rate coefficients at approximately room temperature can be used for SIFT-MS, but is of questionable value for PTR-MS (Cappellin *et al.,* 2010). Also, rotation of reagent ions gives more selectivity and resolution between compounds using SIFT-MS.

Since Smith and Španěl ceased direct involvement, the technology has been further refined and improved to give the Voice200 instrument constructed by Syft Technologies of New Zealand. The significant improvements brought have been stable flow tube

temperatures and the ability to generate negative ions in the SIFT chamber. As with the positive ions, the ions that have been selected are those that are relatively stable and unreactive in moist air. This recent development has the potential to produce a wealth of new data and applications for the SIFT-MS technique. So far it has mostly been used in industry due to the ability to quantify inorganic compounds such as hydrofluoric, hydrochloric and other acids. Table 1.3 shows the mechanisms by which positive and negative ions react in modern SIFT-MS techniques.

Table 1.3: Mechanisms of positive and negative reagent ions reactions in modern SIFT-MS

Mechanism	H_3O^+	NO^+	O_2^+	OH^-	O^-	O_2^-	NO_2^-	NO_3^-
Proton transfer (PT)	yes	no	no					
Electron transfer (ET)	no	yes	yes					
Dissociative ET	no	yes	yes					
Hydride abstraction	no	yes	no					
Association	yes	yes	no	yes	yes	yes	no	no
Proton Abstraction				yes	yes	yes	yes	yes
Electron attachment				no	no	yes	no	no
Associative Detachment				yes	yes	yes	no	no
Displacement/Elimination				yes	yes	no	no	no

1.6 pH and the biofilm

The pH of the tongue biofilm is likely to influence both the microbial composition and activity of some transformations (e.g. sulphur compounds into VSC) over others. McKenzie (2007) first used the Sorbarod perfusion model to study the interdependence between pH and glycolysis in *Streptococcus mutans* biofilms, showing reductions in pH occurring to varying degrees with various sugars. No effect was seen, however, with substances which tended to raise pH such as urea as this organism does not possess urease. Taylor and Greenman (2010) used the same model to study the effects of pH on both a mixed species biofilm community and the production of hydrogen sulphide. Six replicate biofilms (inoculated from a single suspension of tongue scrape sample) were perfused with basal

medium at 6 different pH values and the ensuing mixed community biofilms were analysed using conventional microbial viable count techniques, but also community level physiological profiling (CLPP) using Biolog AN plates. Highest levels of H_2S were produced at pH 7.5 which were significantly higher ($p < 0.05$) than biofilms at pH 7.0 and 8.0. Biofilms at pH's 6.5, 6.0 and 5.5 produced decreasing concentrations of H_2S with lower pH. It was concluded that the optimum pH required for highest transformation of sulphur-containing substrates to H_2S occurs between pH 7.0 and 8.0, which correlates with the known pH optimum characteristics of cysteine desulfhydrase systems that change thiols into H_2S with optima between 7.6 to 8.5 (Greenman 1999; Mhlenhoff *et al.,* 2004; Tchong *et al.,* 2005; Wu *et al.,* 2008). The authors conclude "The effects of pH on tongue-derived biofilm are therefore likely to have a multi-factoral effect on the ecological diversity of H_2S-producing organisms and their physiology".

1.7 Confocal Laser Scanning Microscopy

The origins of CLSM can be traced to improvements in microscopy developed by Marvin Minsky (Minsky, 1955) at Harvard. The problem with traditional wide-field fluorescence microscopy is that the subject is illuminated all at once, and each image point, however viewed, is partially obscured by aberrant scattered light from other image points not being viewed. Minsky realised that the way to avoid this would be to image each point separately and individually in turn, and this would lead to greatly increased resolution and contrast. A second microscope could be used instead of a condenser lens to focus a pinhole aperture at the imaged point thus eliminating all rays not focussed on this point. Focal brightness is thus retained but with a huge reduction in errant light in the specimen. A second pinhole beyond the usual objective lens further eliminates errant light that was originally focussed on the

image point but became scattered by out of focus points in the specimen. This gives an elegant symmetry with pinholes and objective lenses either side of the specimen. It is obvious how these single point illumination techniques give can achieve far greater resolution and contrast but the problem is that each point must be imaged or 'scanned' in turn. In order for this to occur quickly enough to be practical, the illumination must be much brighter than standard light sources supply. Minsky first used carbon or zirconium arcs, and output was passed through a photomultiplier circuit before being visualised on a long-persistence phosphorescent screen. This arrangement was patented by Minsky with the help of his brother-in-law Morton Amster in 1957 (Minsky, 1988).

From these beginnings, confocal microscopy took perhaps three decades before the potential began to be fully realised. One of the reasons for this was, as admitted by Minsky himself (Minsky, 1988), due to the poor imaging system. Much of the resolution and clarity that Minsky obtained was lost on the crude phosphorescent screen, and there was no way of obtaining a permanent copy. Since then, there have been both huge advances in digital imaging with charge-coupled devices (CCD) and exponentially faster computer processing power to analyse these images (Inoué, 2006). However, the primary advance for the technique was the development of the laser (Gould, 1959). The production of intense beams of coherent light enabled faster scanning and subsequent improvements in imaging. Commercially successful microscopes began to appear and were used to image immuno-fluorescently labelled specimens (White *et al.*, 1987). The ability of the device to scan in optical sections was invaluable and montages of the Z-series of scans could be examined. As computing power increased, the Z-series of stacks could be reconstructed into 3D representations of the specimen. Still later time-lapse sequences could be animated and rotated in real time giving true four dimensional imaging (Stephens and Allan, 2003). For a comprehensive review of methods of CLSM of biofilms the reader is directed to Neu and Lawrence (2014).

1.8 Aims and Objectives

The main technical aim of this thesis was to improve and further develop the in vitro flat-bed perfusion matrix biofilm model. This was to enable the model to be used to study a wider range of biofilm conditions and states, and to facilitate the testing of a wider range of interventions and biologically active compounds (See chapter 3). The specific objectives were as follows;

1. To measure biofilm pH in real time.
2. To extend VOC analysis by SIFT-MS from one unit at a time to six.
3. To enable biofilm interventions based on photodynamic therapies.
4. To enable biofilms incorporating bioluminescent organisms to be monitored in real time using optical recording.

The main scientific aims of this thesis was to study the behaviour of different antimicrobial compounds on biofilm growth, physiology and metabolism, and compare with in vivo work. These studies also included compounds with biological activity but not direct antimicrobial effects. A further aim was to show the utility of the model as a test-bed for comparative assessment of other instruments or devices. The specific scientific objectives were as follows;

1. Validation of the model by comparison of in vivo and in vitro case studies.
2. Characterisation of *in vivo* biofilm ecology and further comparison with the microbial ecology *in vitro.*
3. Comparison of currently available over-the-counter antimalodour preparations *in vivo* and *in vitro*.
4. Use of the model to assist and assess the development of a novel handheld surface plasmon resonance based device for measuring oral volatile compounds.
5. To investigate the effects of non-antimicrobial biofilm disrupting agents such as D-amino acids.

2. Methods

2.1 The Flat Bed Perfusion Matrix Model

2.1.1 The biofilm enclosure

The methodology followed is a further modification of that described in detail by Saad, Hewett & Greenman (2013). The biofilm enclosure consists of a modified polypropylene freezer box (Lock and Lock, Amazon, UK) within which a previously inoculated loose fibred 1cm^2 cellulose matrix is held in place on a specially constructed slope. The development of this slope in particular is detailed below. Media is fed drip-wise by peristaltic pump (Watson-Marlow, Falmouth, UK) via a 23G hypodermic syringe (Terumo, Japan). The feed line for this syringe is connected to the pump via a grow-back inhibitor constructed as shown in 2.1. The standard media used was one seventh strength brain heart infusion (Becton-Dickinson, New Jersey, USA) supplemented with haemin (0.0001 g/100ml), dithiothreitol (0.005 g/100ml) and cysteine (0.1 g/100ml w/v) all supplied by Sigma-Aldrich, UK. pH was adjusted to 7.4 prior to autoclaving. Waste flowed out of the box via silicone tubing attached to a PTFE elbow connector under the box. The box was filled with anaerobic gas (90% nitrogen, 10% carbon dioxide) from a cylinder of compressed gas (BOC) and kept under positive pressure by peristaltic pump. Gas sampling takes place through Poly-Ether Ether Ketone (PEEK) tubing of 1/16in external diameter and 0.055in internal diameter (Supelco, Penns., USA). This is introduced through the front of the enclosure and protected from contamination by a 1ml pipette tip (figure 2.2).

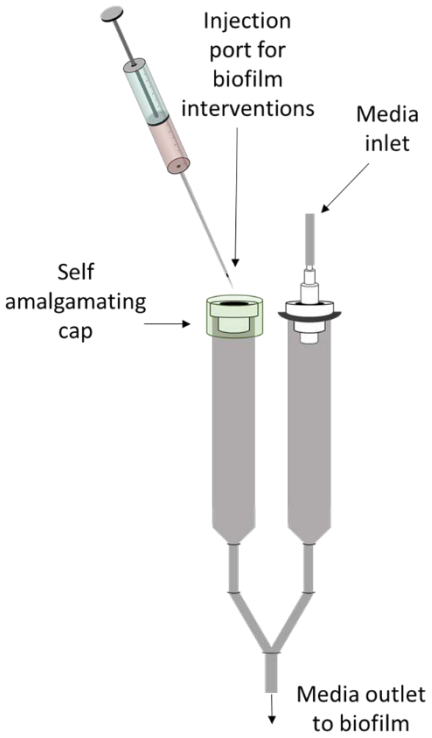

Figure 2.1: Growback inhibitor and injection port

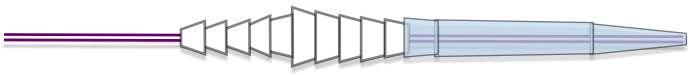

Figure 2.2: PEEK tubing protected by pipette tip

2.1.2 The matrix mounting slope

The initial design of the matrix mounting slope was the same as that used by Thorn and Greenman (2009). This consisted of a glass microscope slide cut to shape using a diamond cutter. This was glued to polypropylene supports that were then attached to the base of the enclosure by M1 countersunk machine screws. To retain the matrix in place, supports were cut from rubber sheeting and attached with extreme temperature glue (Bostik, UK). This slope is shown in figure 1.7. Unfortunately repeated autoclaving of this design caused the glued bond to break down and come apart.

The glass slope was then replaced with polypropylene to allow an adhesive specifically suited to low surface energy plastics to be used (3M, UK). This led to increased resilience to repeated autoclave samples, but bond failure still occurred. Next, solid plastic supports were milled by Philips UK using an in house CNC process. These slopes are shown in Figure 2.3. These proved far more reusable, but due to the planar surface of the mounting area, drips of media could run sideways across the slope and fail to exit the enclosure via the waste tubing. This led to a build-up of contaminated waste fluid in the enclosure which in tur led to artefactual VOC production from planktonic cells in suspension. To prevent this from happening the slopes were redesigned using CAD (Solidworks, Dassault Systems, Massachusetts, USA) and 3D printed in Nanocure (envisionTEC, Michigan, USA) as shown in figure 2.4. The U-shaped channel pictured prevents overspill and ensures that waste exits the enclosure via the waste tube.

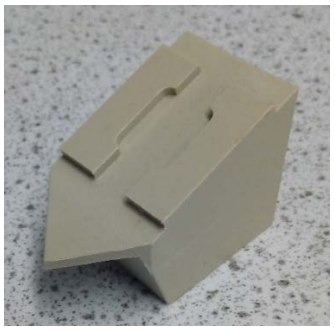

Figure 2.3: CNC milled polypropylene slope.

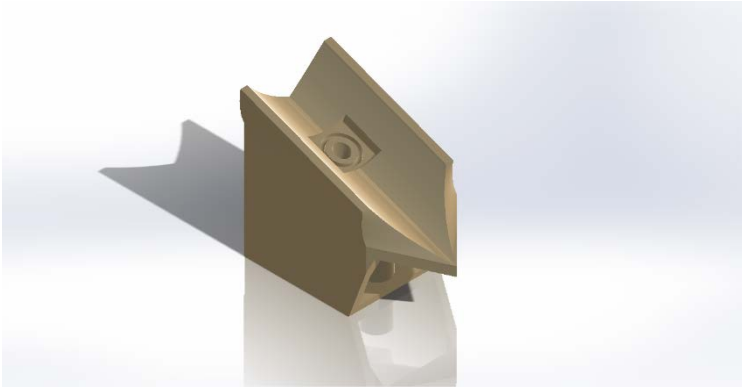

Figure 2.4: CAD slope proptotyped in NanoCure

2.1.3 Inoculation of the matrix

The inoculation of the matrix is performed as follows; a sample was typically taken from one individual volunteer by dorsal tongue scrape using a sterile toothbrush with soft nylon bristles of size $1cm^2$. Volunteers for this process were selected after assessment by trained organoleptic judge. The sample was inoculated directly into degassed brain heart infusion and vortexed. The cellulose matrix was placed on the surface of a fastidious anaerobic agar plate and a 300µl aliquot of the tongue scrape suspension applied to the surface. The inoculated matrix was pre-incubated anaerobically for 24 hours and then transferred to the support slope within the airtight autoclavable growth chambers.

2.1.4 Incubation of the enclosure

The biofilm enclosures were mounted into a modified shelf and placed inside a mini incubator (VWR International Ltd., Lutterworth, UK). The front panel of these incubators was replaced with a laser-cut polycarbonate panel allowing inlet ports for gas and media, and outlet ports for waste and VOC analysis. Additional ports allowed power to be supplied to LED illumination units and for access by pHOptica fibres. (See section 3.2). The top port of the incubator was reserved for temperature measurement by either standard glass thermometer or pHOptica thermocouple.

2.1.5 Introduction of fluid intervention pulses

At a distance of 15cm from the enclosure the media feed line was split to allow the incorporation of both a growback inhibitor and a port for the introduction of fluid interventions. This arrangement is seen in figure 2.2. Both branches were constructed from syringe bodies. The top of the grow-back inhibitor consisted of a drilled bung through which the media line was inserted. The top of the injection port consisted of a self-amalgamating bung from a blood vacutainer (Becton-Dickenson, New Jersey, USA).

To introduce fluid pulses, the media line was closed by tube clamp, and the media line below this point flushed through using a syringe of anaerobic gas. Fluid was then introduced by second sterile syringe. The time taken for the fluid injected to flow over the biofilm was measured by laboratory timer.

2.1.6 Sampling the biofilm enclosures

Gases produced by the biofilms were monitored in real time with the use of either a Profile 3 SIFT-MS (Instrument Science, UK) or, later, a Voice200 SIFT-MS (Syft Technologies, Canterbury, New Zealand). Gas sampling was through a protected port in the biofilm enclosure described above. To ensure more sensitive detection of indole and methyl-indole by the Profile3 instrument, the primary stainless steel inlet tube was removed and replaced with Polyether ether ketone (PEEK) tubing to reduce adsorption of these compounds to the surface. An inner and outer jacket was constructed from metal foil with the inlet heater placed inside. This allowed heating of the inlet tube and vaporisation of any water vapour. These modifications were similar to those performed (Ross and Esarik 2013) for indole detection. To enable experiments to be performed with several biofilms at one time, a sequential sampling system was constructed. Details of this are provided in chapter 3.

2.2 Microbiological methods

2.2.1 Tongue scrape sampling for *in vivo* studies

Tongue scrape sampling was based on the method originally described by Hartley *et al.*, (1996b). A standard, soft- bristled toothrush was trimmed to give 1cm^2 contact area and autoclaved. This was then pressed and brushed gently over a 4cm^2 area of the tongue dorsum of a donor individual. The tongue biofilm material was then transferred to 10ml of

degassed brain heart infusion (BHI, Becton-Dickenson, UK) first by manual agitation on the inner surface of a glass universal followed by vortex mixing at full speed for 30 seconds.

2.2.2 Destructive sampling of biofilm matrices

Biofilm matrices were removed from their enclosures by sterile forceps, placed into 10ml of BHI and vortexed for 30 seconds at full speed. Serial dilutions were performed in BHI and plated as above.

2.2.3 Anaerobic plate counts

Anaerobic plates counts were performed on tongue scrapes, biofilm eluates and biofilm matrices as required. Two media types were used, fastitidious anaerobe agar (FAA, LabM, Bury) at a concentration of 46g per litre, enriched with 50ml defibrinated horse blood and the same agar with Vancomycin at a concentration of 0.00025% w/v (Oxoid, UK). In this way strict anaerobes can be distinguished by growth on both plates. Serial dilutions were performed in BHI and plated by spiral plater (WASP, Don Whitley Scientific, Shipley, UK.)

2.2.4 Basic identification of organisms

Organisms were first categorised by colony type. Further identification was performed by Gram's stain. Catalase reaction was performed to presumptively identify streptococci when required.

2.3 HOMIN and HOMINGS analysis of the oral microbiome

DNA extraction and pyrosequencing was carried out fully at Molecular Research (MR DNA), Shallowater, Texas, and sequencing was performed at the Forsyth Institute, Cambridge, USA. In summary; 50ng of DNA was extracted by Nextra DNA sample Preparation Kit (IIlimina). The 16S rRNA V4 variable gene region PCR primers 515 /806 (Caporaso *et al.*, 2011) were used in a single-step 30 cycle PCR using the HotStarTaq Plus Master Mix Kit (Qiagen, USA) (94°C; 3 minutes, followed by 28 cycles of 30 seconds, 53°C; 40 seconds, 72°C; 1 minute then 5 minute elongation step). Sequencing was performed on an Ion Torrent Personal Genome Machine (PGM) and data were processed using a proprietary analysis pipeline. OTUs were defined by clustering at 3% divergence (97% similarity) and taxonomically classified using BLASTn against a database derived from GreenGenes (http://greengenes.lbl.gov/cgi-bin/nph-index.cgi), RDPII (http://rdp.cme.msu.edu) and NCBI (www.ncbi.nim.nih.gov).

The resultant percentage frequencies of target taxa to be determined were visualised using Circos software (Krzywinski, 2009). Taxa were plotted radially around the circos plot and the samples were ordered from low to high malodour starting at the centre of the plot. Each point was coloured by heatmap ranging from pale to dark red based on the percentage frequency. This meant that darker red at the outside of the circular plot corresponded to association with those organisms with malodour. Both Pearson's Coefficient of Skewness and Kelly's Coefficient of Skewness were calculated for each organism and plots created showing organisms showing positive or negative association with malodour.

To investigate potential interactions between species in the oral microbiome, probabilistic co-occurrence tables were generated using a probabilistic model (Veech, 2013) implemented in Rstudio (Boston, USA) (Griffith *et al*., 2016).

2.4 Analysis of the biofilm EPS

Microbial EPS is notoriously problematic to analyse due to its complexity. The constituents of the EPS must be separated from the cells and dissolved into solution without damaging the cells and releasing their contents. After study and experimentation the following procedure was used.

The biofilm matrix was suspended in EPS extraction buffer (2 mM Na_3PO_4, 4 mM NaH_2PO_4, 9 mM NaCl and 1 mM KCl at pH 7) and vortexed for one minute. A 1ml aliquot of this suspension was taken for microbial culture and 1ml for dry weight determination. The remaining 8ml was treated with, 0.06ml of 36.5% formaldehyde (Fisher Scientific, UK) and shaken at 4°C for 1 hour. This was followed by 4ml of 1M NaOH, again at 4°C with shaking, for 4 hours. This was then centrifuged at 20,000 G for twenty minutes and filtered through a 0.2µm membrane. The final purification stage was to dialyse the solution through a 3500 Dalton membrane at 4°C for 24 hours.

Following extraction, EPS solutions were assayed for polysaccharides and proteins by Dubois (1960) and modified Lowry methods. The extraction method was performed on sterile distilled water samples to provide a baseline for calibration.

2.4.1 Dubois assay for polysaccharides

For the Dubois assay, 0.05ml of 80% phenol solution was added to 2ml of EPS solution in 20mm boiling tubes. To this was rapidly pipetted 5ml of concentrated sulphuric acid. The acid was pipetted by modified 5ml pipette to enable fast dispense, and directed directly at the fluid surface to ensure fast efficient mixing and uniform heating. The tubes were allowed to stand for 10 minutes then shaken and place in a waterbath at 30°C for 20 minutes. Absorbance was measured at 480nm and compared to distilled water blanks. A calibration curve was generated using known dilutions of a standard glucose

solution. The amount of polysaccharide is therefore given in glucose equivalents to compare EPS extractions rather than absolute quantitative measurement of individual sugars.

2.4.2 Modified Lowry assay for protein

For the modified Lowry assay, 2.2ml of Biuret Reagent (Sigma-Aldrich, UK) was added to 0.2ml of EPS extract in a clean sterile test tube, mixed and let to stand for 10 minutes. 0.1ml of Ciocalteau's Phenol Reagent (Sigma-Aldrich, UK) was added, mixed and allowed to stand for 30 minutes. Contents were then transferred to cuvettes and absorbance read at 720nm using a Jenway 6305 spectrophotometer (Cole-Palmer, UK). Blank samples were aliquotted from 0.85% sodium chloride. A calibration curve was plotted using standards prepared with bovine serum albumin (Sigma-Aldrich, UK) and used to calculate protein levels in the EPS samples.

2.5 Confocal microscopy of the biofilm

To enable visualisation of the oral biofilm by confocal laser scanning microscopy (CLSM), it was necessary to mount and stain samples in a reproducible way. As cellulose fibres auto-fluoresce when excited by most wavelengths of laser light, portions of biofilm had to be separated from the main bulk of the material to be examined. To achieve this, 10mm diameter round glass coverslips (Fisher Scientific, UK) were first sterilised by autoclave and then placed underneath mature biofilms. They were incubated along with the biofilm in the normal way and removed after varying time periods. The coverslips were then inverted and placed onto glass slides. Various fluorescent stains at varying concentrations were added by pipette to the edge of the coverslip and allowed to migrate by capillary action.

Table 2.1: Fluorescent stains used in CLSM of the biofilm matrix

Stain	Supplier	Target	Concentration	Incubation time	Excitation wavelength	Emission wavelength
Hoesch 33258	Sigma Aldrich, UK	Intracellular DNA	1µg/ml	1 hr	350nm	461nm
Congo Red	Sigma Aldrich, UK	Polysaccharides Amyloids	15mg/ml	30 min	497nm	614nm
Calcofluor White	Sigma Aldrich, UK	Polysaccharides Amyloids	3.5 mg/ml	30 min	300-440nm	355nm
Sypro Orange	Sigma Aldrich, UK	Proteins	1µg/ml	30 min	470nm	570nm
Thioflavin T	Sigma Aldrich, UK	Extracellular Amyloid	7.5µM	30 min	385nm	450nm
Fluor-conjegated lectins (ConA, WGA, AAL)	Vector Labs, Uk	Various	100µg/ml	30 min	495nm	519nm

The slides were then incubated under anaerobic conditions for up to 1 hour, before examination using an Ultraview FRET H confocal microscope (Perkin Elmer, UK). Table 2.1 shows the various fluorescent stains used along with concentrations and incubation times.

2.6 Sampling the oral cavity

2.6.1 Trained Organoleptic Judge

Organoleptic scoring by trained judge was used to assess malodour. The mouth was kept closed for two minutes to allow formation of headspace equilibrium in the oral cavity, then the head was inclined backwards and the mouth opened to allow assessment by judge. Malodour was categorised from 0-5 where 0 = no odour, 1 = barely noticeable, 2 = slight odour, 3 = moderate odour, 4 = strong odour and 5 = very strong odour
(Rosenberg and McCulloch 1992; Greenman et al., 2004)

2.6.2 The OralChroma

Samples were collected from the human volunteers as recommended by Abilit Corporation, Japan. A 2ml volume of air from the oral cavity was collected by gas syringe (B. Braun Medical Ltd, Sheffield, UK) and injected into the injection port of the gas chromatograph (OralChroma^{TM} Abilit Corporation, Japan). The area under the peaks was used to calculate levels of hydrogen sulphide and VSC concentrations from a calibration curve. This curve was created by diluting hydrogen sulphide from a standard cylinder at 3ppm (BOC gases, UK) using a precision gas diluter (Custom Sensor Solutions, Arizona, USA). A calibration curve is shown in figure 2.5.

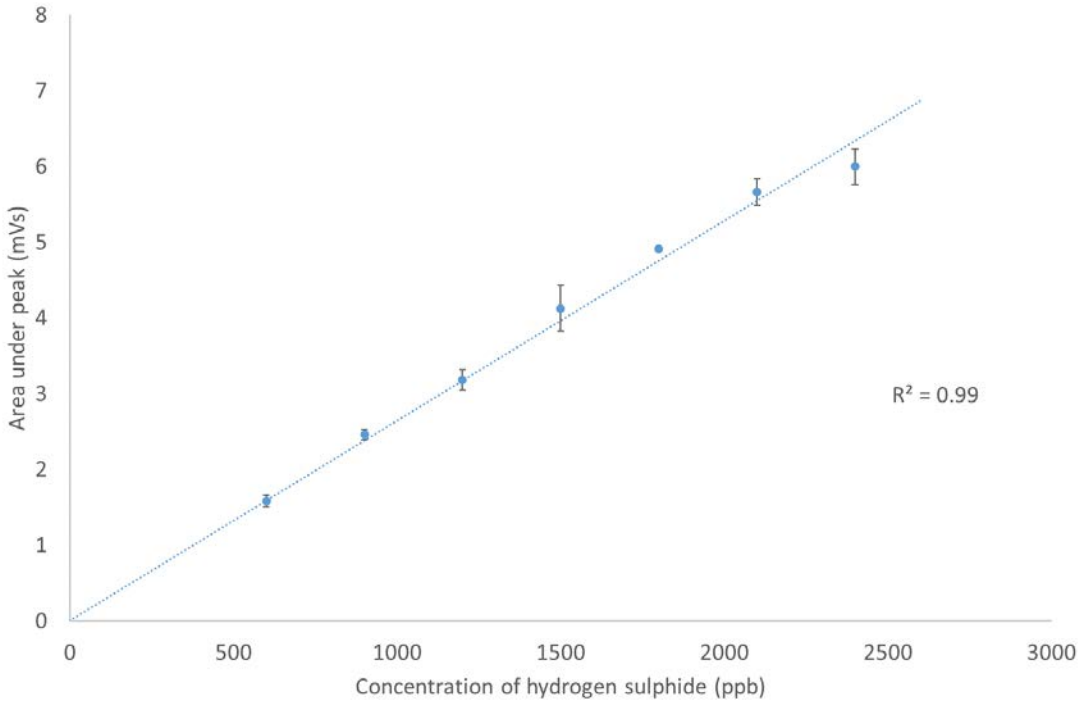

Figure 2.5: OralChroma calibration curve. n=3, bars represent standard error.

2.6.3 SIFT-MS

The Profile3 instrument was used with a source pressure between 0.26 and 0.30. Quadrapole currents were between 5 and 7nA and 20 to 30pA. Full scans with the selected reagent ion (H_3O^+) were performed at the start of each run, and counts at 19, 37 and 55 and 73 m/z positions compared with expected values. Sample inlet capillary was regularly checked and replaced when helium off pressure dropped below 0.07 Torr.

The Voice200 instrument had capped and uncapped pressures checked each time before use, along with calibration gas pressure. These values were recorded. Validation with standard gases as recommended by the manufacturers was performed before all testing. Full scans were checked regularly for optimum performance of the instrument. Time and count

limits were 100ms and 10,000 counts. All settings for both instruments can be seen in appendix 3.

It was necessary to modify the sampling inlet of the SIFT-MS to measure VOC levels in the oral cavity. The rear port of the sampling head was connected to a mini diaphragm pump. The front inlet was adapted to hold a disposable straw that could be introduced into the oral cavity. Air was thus drawn from the oral cavity and this stream was then subsampled by the SIFT-MS. A diagram is shown in figure 2.6. This method reduces disturbance introduced by breathing and minimises unwanted sampling of systemic gases. Dynamic calibration by flow rate adjustment was performed during sampling to give 6% water content in breath (Profile3). This was not necessary with the Voice200 due to the validation procedure with standard gas being performed for each run.

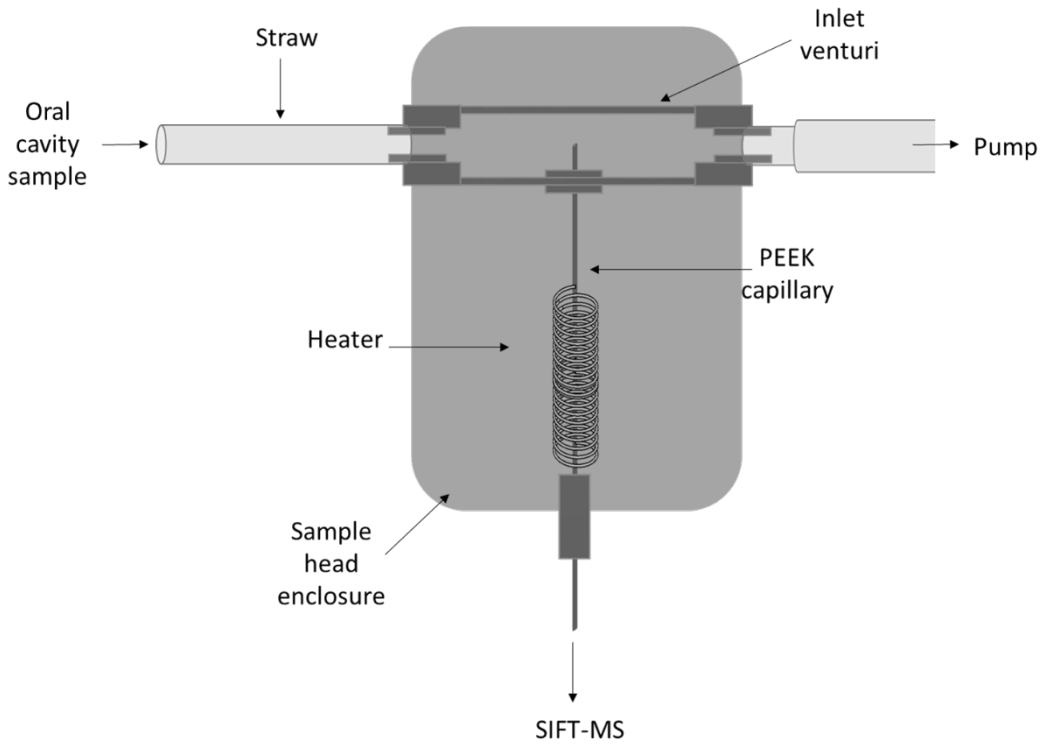

Figure 2.6: Modifications to the Profile3 SIFT-MS sampling head

The subject was instructed to close their mouth and breathe through their nose for a period of two minutes, then to insert the straw into their mouth so that the instrument sampled from above the dorsal area of their tongue. They were then instructed to rest their lips loosely against the straw and breathe gently through their nose for the sampling period of one minute. A 40 second sampling period was recorded which would typically include six data points for each compound.

2.7 Selection of individuals for *in vivo* trials

The effect of novel anti-malodour compounds on the biofilm was compared with the effect of these compounds on human volunteers. In these cases the general protocol was used with modifications for specific product trials. The clinical trials director responsible for volunteer selection and screening was Dr. Saliha Saad (UWE, Bristol).

Volunteers were selected from a larger group who have been previously screened for inclusion in malodour trials. In the laboratory, organoleptic, OralChroma and SIFT-MS assessments were made of their malodour status. On the basis of this screening, a health questionnaire was completed to determine any exclusion criteria (Table 2.2). In order to maintain anonymity, each subject was assigned a code number which was recorded on the questionnaire. All relevent documentation regarding the ethics and permissions for samples used can be examined in Appendix VI.

Table 2.2: In vivo study exclusion criteria

Eligibility criteria	Exclusion criteria
Voluntary participation confirmed by consent form	Recent medical history of infectious disease
Availability during specified times to comply with sampling intervals	Antibiotic medication within 1 month of the trial start date including medicated sweets
Organoleptic score above 2 and greater than 100 ppb H_2S by SIFT-MS	Any change in oral hygiene practice during the trial prior to sampling
	Substantial false dentition
	Use of highly perfumed cosmetics at time of sampling
	Advanced uncontrolled caries, gingivitis, peridontitis or oral candidosis

Trails were performed by crossover design with eligible volunteers assigned a randomised treatment schedule. Each subject was randomly assigned a numeric label and each treatment was allocated a code letter.

Microbiological analysis was performed on tongue scrape samples before treatment and after treatment according to the specific schedule of the trial. Relevant dilutions were plated on fastidious anaerobe agar (LabM, Bury, UK) with and without vancomycin ($2.5mgl^{-1}$ Sigma-Aldrich, UK) and incubated anaerobically for seven days. Plate counts were performed for strict and facultative anaerobes as well as total viable organisms.

All statistical analysis used Prism software (Prism 5.0, GraphPad, San Diego, US) which was also used to calculate P-values for nonlinear regression coefficients, and confidence levels.

3 Technical developments

3.1 Introduction

The *in vitro* oral biofilm model as described has been successfully used to investigate the efficacy of anti-malodour compounds on volatile production (Saad, Hewett, & Greenman, 2013). During this process, some shortcomings of the model were identified. Moreover, technical adaptations were devised that would enable the model to be both more flexible and efficient. These elements will be discussed individually.

3.1.1 Physiological conditions of multiple biofilms

It was hitherto discovered that if several biofilm enclosure units are incubated together in one incubator, reproducibility is adversely affected (figure 3.1). Fan based air circulation in a relatively large internal area leads to temperature variation between the enclosures causing significant differences in both volatile production and uniformity of the

Figure 3.1: Several biofilms incubated in a single large incubator with fan circulation

biofilms. This issue was exacerbated by opening the door to facilitate any kind of sampling. Not only could only one biofilm be sampled at a time, but due to the time required for the conditions within the chamber to stabilise, interventions of any sort could only be performed after a significant time delay between each sample. The increased time and variability caused by these factors was found to severely limit the amount of reliable data that could be generated from the model. Techniques to overcome these sampling issues were required.

3.1.2 pH monitoring of the biofilm

As described in section 1.6, pH of the biofilm affects both microbial composition and chemical transformations that occur. A way of monitoring the pH within the biofilm could provide interesting data above what can be gleaned from mere pH measurement of media flowing into and out of the system. MacKenzie (2007) had experimented with pH microprobes but it was thought that a less invasive method may be superior.

3.1.3 Bioluminescent organisms as reporters of metabolic activity

Bioluminescent indicator organisms are strains of bacteria into which have been cloned lucifierases from other light-producing organisms. They are powerful tools for studying both microbial metabolism and the action of antimicrobial substances as their production of light reflects the actual metabolic rate of microbial cells (Beard *et al.*, 2002; Koga, Harada *et al.,* 2005; Vesterlund *et al.,* 2004). Plasmids pGLITE and pMCS5-LITE containing the luxCDABE operon of *Photorhabdus luminescens* under constitutive control of the *lac* promoter have been used previously in perfusion based models (Lewis *et al.*, 2006; Parveen *et al.*, 2001). Modification of this flat plate system to allow the use of bioluminescent

organisms paves the way for interesting work examining the effects of novel antimicrobials in real time.

3.1.4 Photodynamic therapy

The effect now known as Photodynamic Therapy (PDT) was first noticed, and famously described by Paul Ehrlich, at the turn of the century when certain combinations of dyes and illumination was shown to kill bacteria. The treatment depends upon a combination of dye with a corresponding frequency of light which leads to the production of cytotoxic free radicals and found success and acceptance in the treatment of carcinomas (Robertson, Evans, & Abrahamse, 2009). However, Photodynamic Antimicrobial Chemotherapy (PACT) has found limited applications other than its use in the sterilization of blood products (Ben-Hur & Horowitz, 1995). This may change since research has shown that this type of therapy can be very effective against biofilms (Hamblin & Newman, 1994; O'Neill, Hope, & Wilson, 2002). Phenothiziniums such as methylene blue (MB), and toluidine blue O (TBP), azure A-C and thionin have all been used as photosensitisers effective in the wavelength range of 600-660nm (Wainwright, 2007; Wilson, 2004). MB absorbs most effectively at 656nm and has been shown to be non-toxic to mammalian cells up to 1% w/v (Creagh *et al.*, 1995). These factors and recent reductions in costs of high intensity LED light make this an important area of study with potential applications in oral healthcare.

3.2 Materials and methods

3.2.1 Stabilisation of conditions and serial biofilm sampling

Biofilms enclosures were incubated in INCU-line Digital Mini incubators (VWR International, UK). Sequential sampling of several biofilms incubated at the same time in one experimental run was implemented by constructing a software controlled, solenoid-operated multivalve. A PEEK bodied valve (Cole-Palmer, Bedfordshire, UK) was selected to minimise contamination by volatiles, and this could be connected by PEEK tubing to both the biofilm enclosures and to the SIFT-MS instrument. Actuation of the solenoid valves was by relay board (Circad Design Ltd., Suffolk, UK). Communication with this board was by USB, and both board and cable were powered by the same 24VDc power supply.

The relay board was controlled by ASCII text sent serially over USB by an application written in Python (PSF, Delaware, USA). The GUI front end was designed using Glade3/GTK+ (GNU/GPL public license). A screen shot of the application can be seen in Figure 3.2.

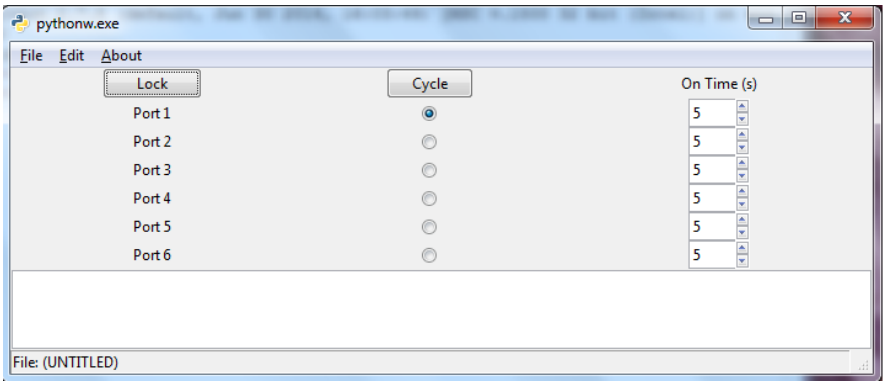

Figure 3.2: Multivalve solenoid valve control application

Ports could be selected individually or cycled in sequence, with each port remaining on for a chosen time period. All switching was logged in a comma separated text file with timestamp, allowing port state at any given time to be known. A schematic diagram of the multiport valve is shown in figure 3.3.

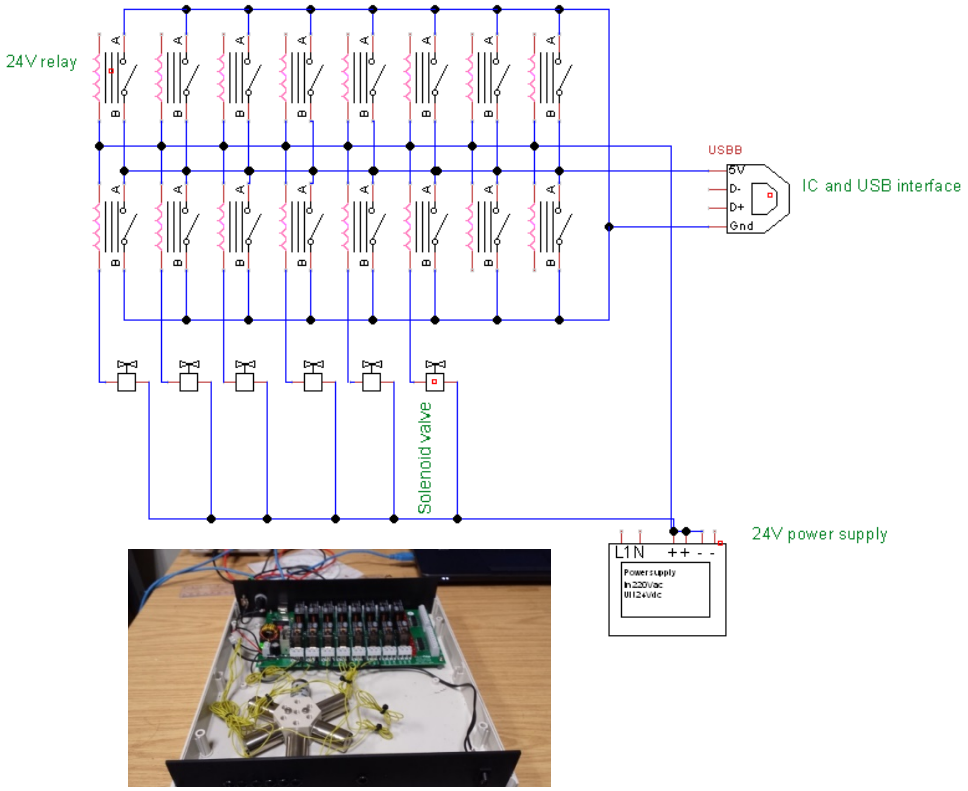

Figure 3.3: Multiport valve schematic diagram and photo.

3.2.2 pH measurement of the biofilm

In order to measure the pH of the biofilm in real time, a pHOptica optical measurement system was employed (see chapter 2, General Methods). This system relies on a paper optrode containing two embedded fluorophores, one whose fluorescence depends on pH and the other a reference to compensate for any drift. The exact nature of these fluorophores is proprietary information protected by the manufacturers. Excitation and measurement is performed by glass and fibreoptic waveguides. In order to incorporate this

system into the flat-plate biofilm system, it was necessary to redesign the slope by CAD and re-prototype in Nanocure^{TM}. A close fitting channel was made into the slope with a channel for sealing around the hole necessary in the base of the biofilm enclosure. At the top of the channel under the biofilm was a recess to accept a 10mm glass microscope coverslip with a further recess to allow sealing with autoclavable sealant. This arrangement is illustrated in Figure 3.4 and figure 2.4 in the previous chapter. Biofilms were incubated for two days after innoculation before the optrode disc was carefully place aseptically underneath the cellulose matrix over the glass window. The waveguide and attached fibreoptic cable was then inserted under the channel and attached to the pHOptica device. Calibration information was supplied by VWR for each batch of optrode discs used. The reference temperature probe from the instrument was inserted into the incubator by the top port. A laptop running pHoptica software was attached and readings taken at 1 second intervals.

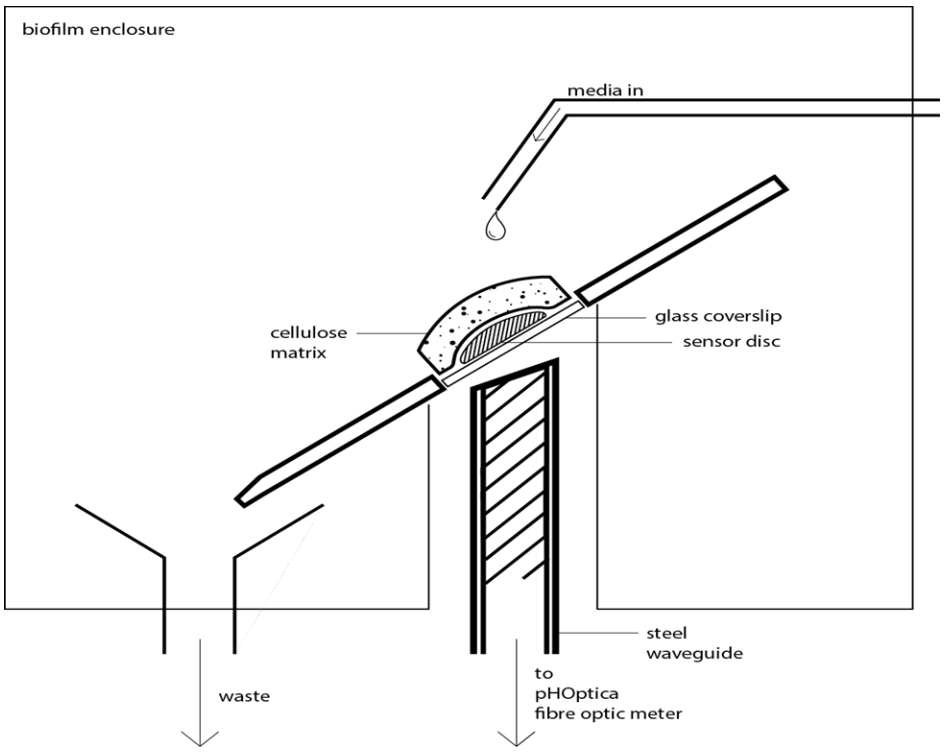

Figure 3.4: Diagram of biofilm enclosure showing port for fibre optic cable

3.2.3 Modifications to allow study of bioluminescent biofilmss

To enable the flat plate perfusion system to utilise the reporter organisms described in section 3.1.3, one biofilm incubator was further modified to allow an overhead camera to record and measure light intensity. A window was cut in the inner and outer top covers of the incubator and a Perspex panel glued, sealed and bolted into place (figure 3.5). Preliminary experiments with bioluminescent *E. coli* strain DH5α showed that bioluminescence could be monitored in real time by CCD device.

Figure 3.5: Modifications to allow the use of bioluminescence reporter organisms in the flat plate biofilm model

3.2.4 Time lapse recordings

An additional advantage of the windowed incubator is that time lapse recordings of biofilm maturation and development could be made. This was achieved using a Galaxy S4 smartphone equipped with the Android based Framelapse Pro software.

3.2.5 Modifications to allow *in vitro* photodynamic treatment

A glass window was installed in the top of the enclosure to enable a high power LED to illuminate the biofilm. This could be accompanied by injections of photodynamic agents. Power could be supplied to each LED at a time on up to six enclosures. Voltage was controlled by variable laboratory supply (EL301R, Thurby Thandar Instruments Ltd., Cambridgeshire, U.K.). The LED housings could be used with a number of different fixed wavelength LED units (Mouser, USA). The LED installation can be seen in figure 3.7

.

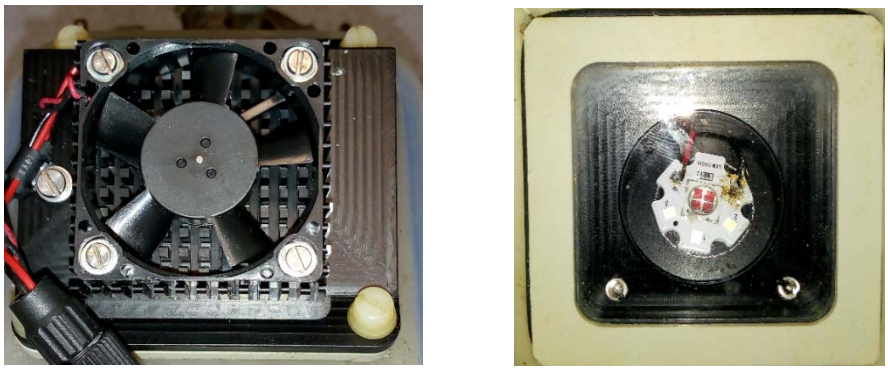

Figure 3.6: LED apparatus installed in biofilm enclosure window, shown from above (left) and below (right)

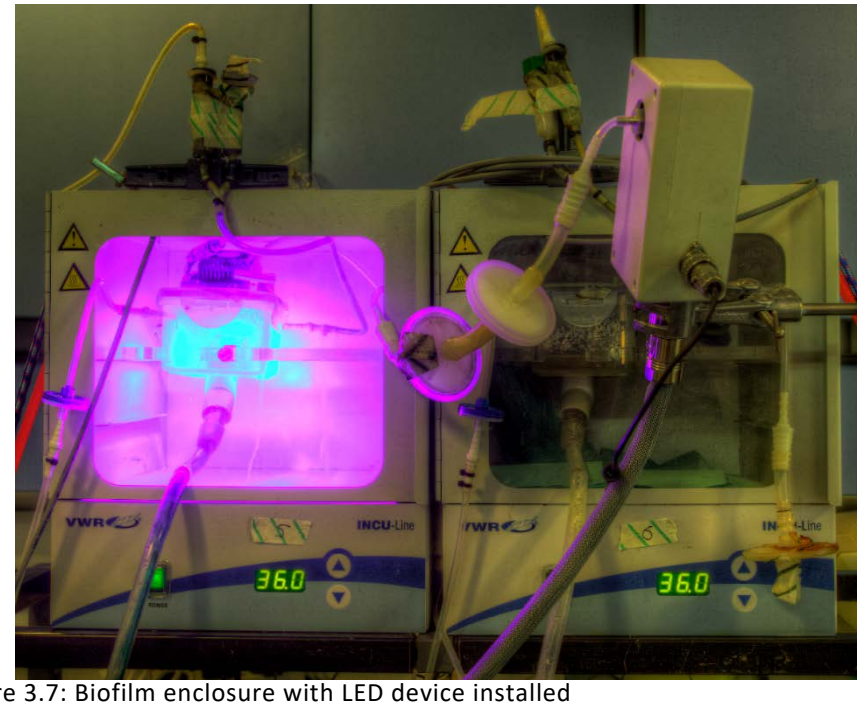

Figure 3.7: Biofilm enclosure with LED device installed

3.3 Results

3.3.1 Multisampling

Six incubators can be seen in figure 3.8, showing PEEK tubing entering through each front panel. A spike in signal was often seen when switching from one biofilm to another, and this was trimmed out at the data analysis stage. These spikes can be seen in Figure 3.9: Example trace by SIFT-MS during sampling of four biofilms.

An example of the trace obtained by SIFT-MS during a sampling period can be seen in Figure 3.9. These traces were separated into data from each biofilm, with all spikes or interference removed using iterative functions written in MATLAB code.

Figure 3.8: Six incubators showing equal length PEEK tubing entering each through the front panel.

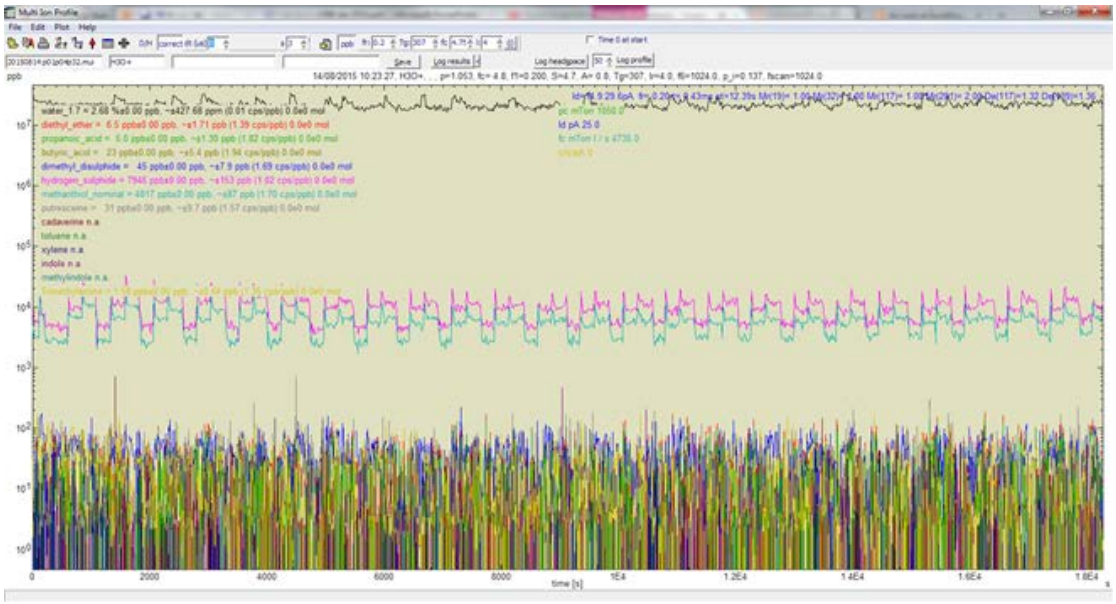

Figure 3.9: Example trace by SIFT-MS during sampling of four biofilms.

3.3.2 Real time pH measurement

It was shown that the pHOptica sensor could be used to measure the pH of an *in vitro* biofilm in real time whilst simultaneously measuring volatiles produced using SIFT-MS. Figure

3.10 shows example traces of volatile production accompanied by pH readings by the fibre optic sensor. There were however reproducibility problems with this method and this will be discussed later.

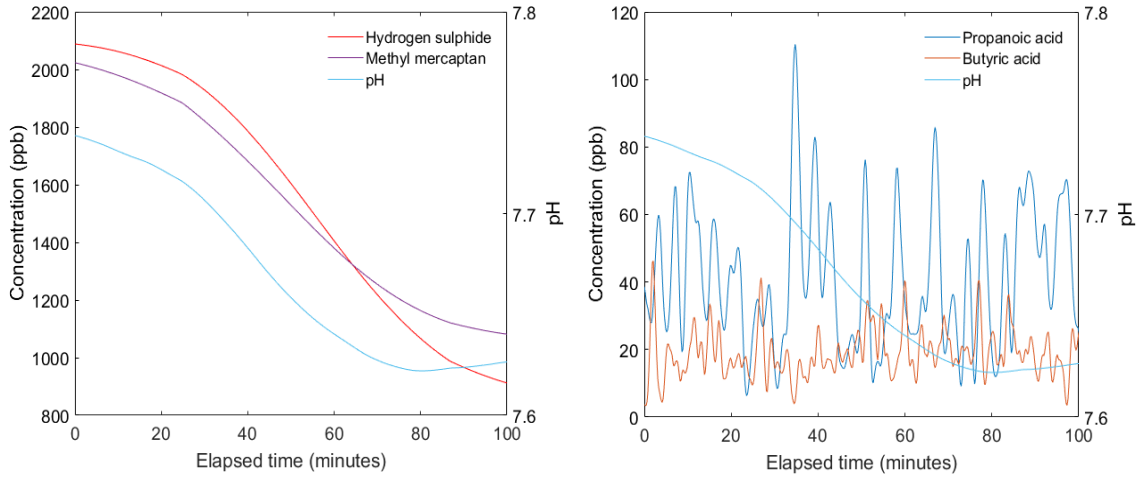

Figure 3.10 Production of sulphides (left) and acids (right) from an *in vitro* oral biofilm immediately following a pulse of 2ml 200mM glucose

3.3.3 The bioluminescent biofilm

A graph of preliminary results can be seen in figure 3.11. In this example, methyl mercaptan levels from a DH5α strain of *E. coli* are monitored along with light intensity, and the production of both appear to be related in this instance. This was intended as a proof of principle experiment, and potential uses for this are discussed in chapter 8.

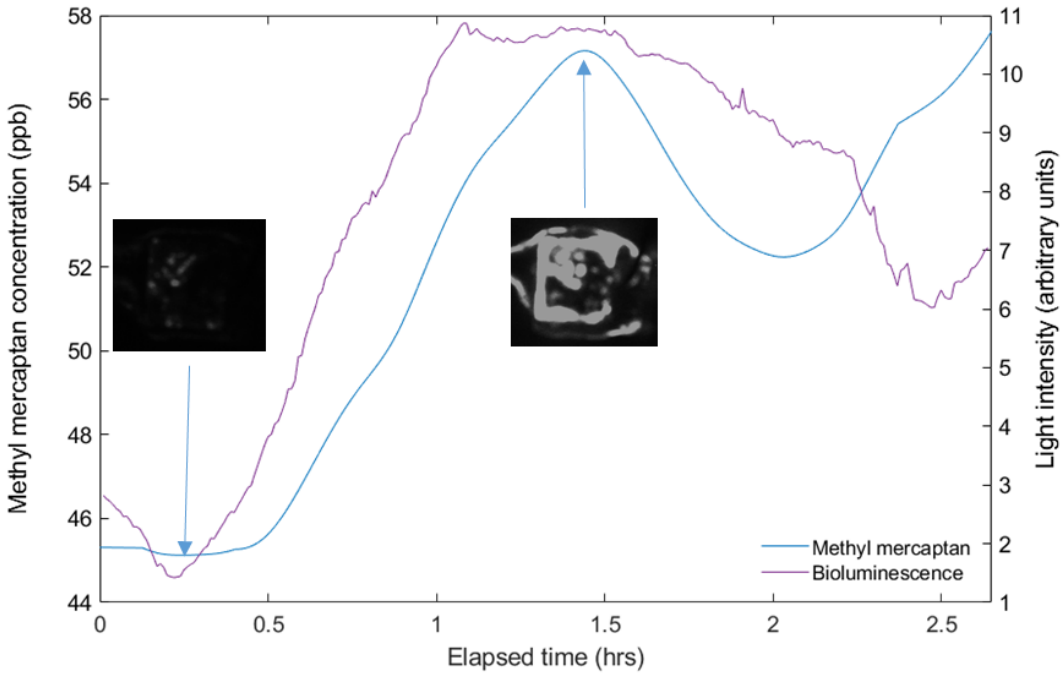

Figure 3.11: Methyl mercaptan and light intensity in bioluminescent *E. coli* DH5α

3.3.4 Time lapse recordings

Figure 3.12 shows the development of dark metal sulphide compounds (e.g. ferrous sulphide) whilst using SIFT-MS to monitor the levels of hydrogen sulphide and methyl mercaptan, to demonstrate a potential relationship between pigmentation and sulphides. The pigmentation is not visible at the introduction of the inoculated cellulose matrix (figure 3.12A).

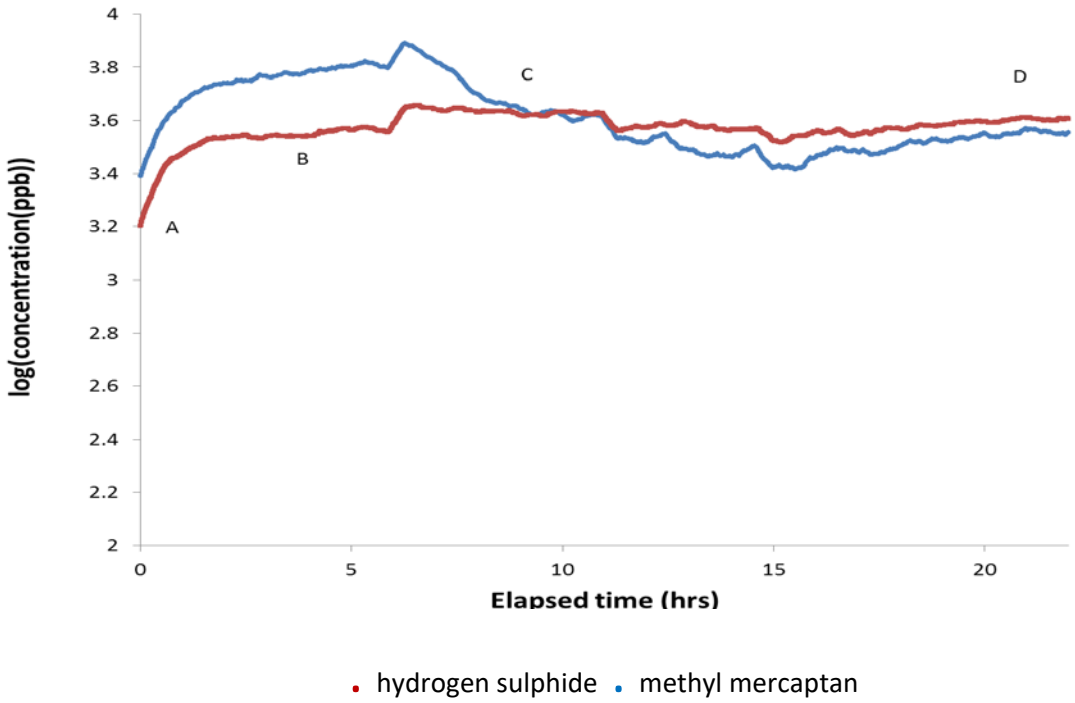

Figure 3.12: Graph showing sulphides produced by a maturing biofilm with accompanying timelapse images from timespoints A, B, C and D.

Pigment is clearly visible at 4 hours of constant medium flow (figure 3.12B) and become most marked by 8 hours (figure 3.12C). The pigmentation remains high (figure 3.12D) until the end of the experimental run (at 21 hours). This method can be used to identify possible causes of variations in VOC production during maturation of biofilms as complex structures and pigmentation changes occur. A similar approach of time-lapse can be used to describe other processes such as *in situ* "viable" staining methods, effects of fluorescent dyes and other colour absorption/desorption processes, which can be monitored over minutes, hours or days of operation.

3.3.5 Photodynamic therapy

Preliminary work showed a dose response with the photosensitizer methylene blue, but at concentrations and staining intensities too high for therapeutic use. The dose-response curve for methylene blue on sulphide production is shown in figure 3.13. If compared to the effects on biofilm volatile production seen with proprietary mouthwash formulations, such as seen in figure 4.9 in section 4, it can be noticed that reductions are relatively inconsequential. !fă2Σ ůḰŜ Ŏoncentration of methylene blue used was high enough that staining of the oral cavity was likely. It is for this reason that this particular avenue was not followed further.

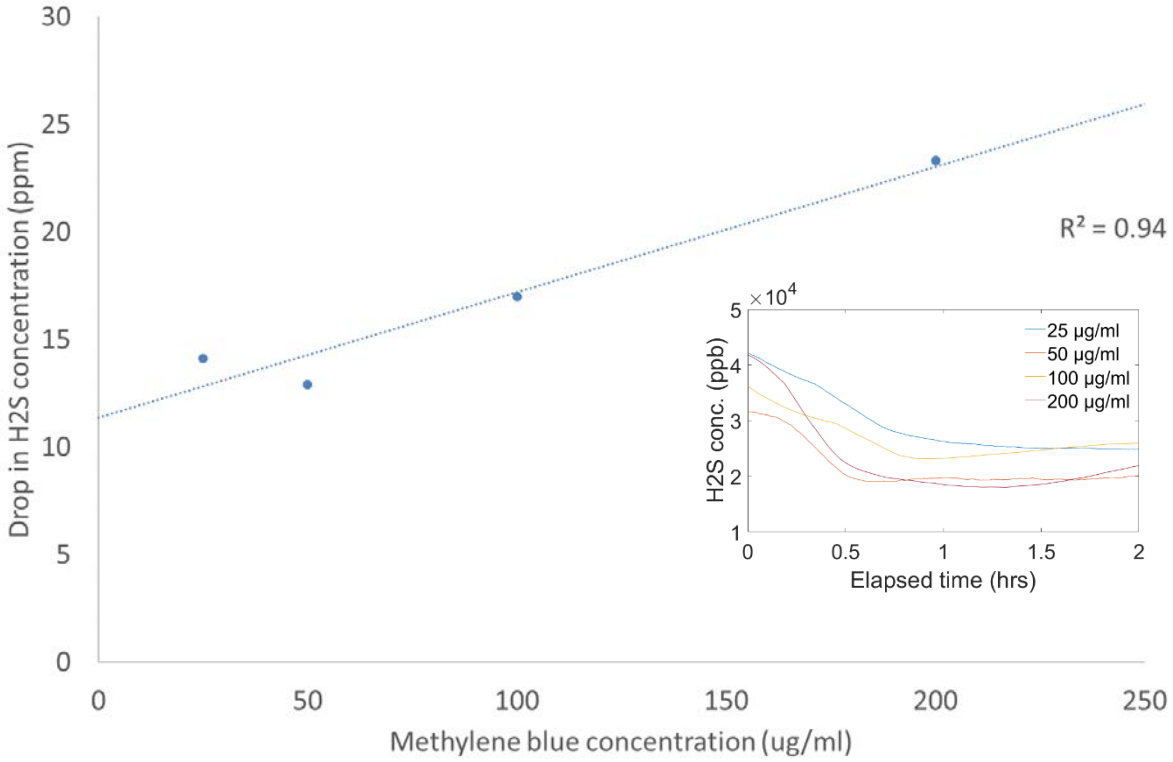

Figure 3.13: Dose response for methylene blue and 660nm light at an intensity of 64 $mWcm^{-2}$.

3.4 Discussion

Through these developments and experiments it has been shown that the flat plate perfusion model is a stable and versatile test bed for in depth analysis and examination of microbial biofilms *in vitro*. The ability to inoculate and mature several biofilms in parallel from an identical tongue scrape sample and monitor them sequentially by SIFT-MS provides a versatile test bed for the examination of the effects of many types of interventions. It has further been shown that the model itself can be used to study bioluminescent organisms thus making available the insights into biofilm physiology that this provides.

Whilst the particular photodynamic therapy investigated here showed issues that suggests the development of a therapeutic regime unlikely, the model itself can certainly be

used to investigate the many promising combinations of light and photosensitiser that have been suggested elsewhere.

In respect of the real time pH measurement that has been demonstrated, it is obvious that such a method would be an extremely useful way to investigate the complex interplay between pH, VOC production, and other aspects of biofilm physiology. However, much more work is needed in this area to validate and standardise the optrode based method to achieve reproducible results with multiple biofilms. Incorporating the optrode into the biofilm matrix in a standardised way that would still enable interrogation by fibre optic cable would need to developed and validated and this proved to be beyond the scope of this project.

In conclusion, whilst not all avenues outlined in this chapter have been explored fully, there is ample potential for further study of both biofilm physiology and the effect of treatments or interventions thereon. The next chapter will outline further validation of the model and examination of the nature of the oral biofilm, and further chapters will describe the use of the model to evaluate both some specific treatments and a novel biosensor system.

4 The oral microbiome and volatilome

4.1 Introduction

By around the time of puberty the community of human oral bacteria has reached microbial homeostasis (Marsh, 1989) . This is a dynamic equilibrium involving the interaction of a large number or organisms and the human host. This microbiota is remarkable stable once established and has been shown to vary little over many years (David *et al*., 2015; Rasiah *et al.*, 2005), and is probably the most stable of all sites of microbial colonisation on the human body (Zhou *et al.*, 2014). However, whilst this core body of species remains stable over long timescales, a degree of variation over shorter timescales is common (David *et al.*, 2015). This is reflected in the profile of volatile gases that the oral biofilm produces, as it is affected by not only microbial composition of the biofilm, but the particular metabolic activity it has at a given time point. The amount of dissolved hydrogen sulphide and methyl mercaptan in solution is highly pH dependant, whereas dimethyl disulphide is less so. This explains the dominance of these first two sulphides since acids are typically produced from food or saliva through microbial metabolism. The aetiology of caries is also inextricably linked to the pH of the oral cavity. Since experiments involving gastric tube-feeding of both animals (Haldi *et al.,* 1953; Bowen *et al.,* 1980) and humans (Littleton *et al.,* 1967; Cooke *et al.,* 1982; Ellison *et al.,* 1982) it has been known that oral ingestion of carbohydrate components leads to carious lesions, and that this is dependent on the presence of oral microorganisms on the dental surfaces. It is now well understood that sucrose has the greatest effect, and that the major glycolytic,

acid tolerant organisms in the oral cavity are streptococci such as *S. mutans* (Lemos, Abranches and Burne, 2005). Imfeld and Lutz (1980) first used pH telemetry with electrodes implanted in dental appliances to demonstrate reductions in pH following ingestion of carbohydrates. Following ingestion of sucrose solutions, intra-oral pH is seen to fall from 7 to under 5. The association between pH and oral malodour has been less well studied, and there is still disagreement about how salivary pH may be an important factor in malodour. Saad (2007) showed no strong relationship between salivary pH and malodour, but it has to be accepted that the site of highest VSC production is the tongue biofilm interface; not the reactions in saliva. The biofilm matrix contains fluid, which is a completely different compartment with a different composition from saliva. The following compartments have been described on the tongue: (1) Bulk salivary volume (2) Rapidly exchanging thin salivary coating layer (3) the biofilm and biofilm matrix fluid (4) tongue epithelium substratum. By blotting the surface of the tongue, the bulk saliva and thin layers are removed. A sterile toothbrush is then used to take two or three tongue dorsum impression samples, which are pooled in a small volume (2 ml) distilled water. It is the resultant pH of this suspension that was used by Saad (2007) to show that there is indeed a fairly strong relationship between the pH of the tongue biofilm matrix and malodour (figure 4.1) but that this is not seen from salivary samples. Thus the oral microbiome, whilst more conserved and stable than other sites in and on the human body, varies significantly between individuals. Each individual microbiome will respond differently to stimulus, nutrients and pH and thus will contribute in a different way to the volatilome that is produced. This chapter describes experiments that were performed to investigate the nature and differences of the oral biofilm both *in vivo* and *in vitro.*

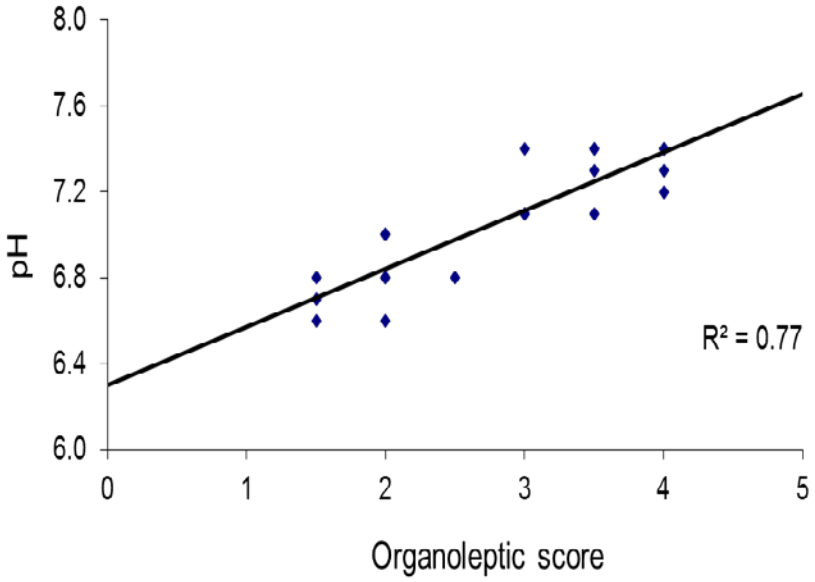

Figure 4.1: Relationship between organoleptic score and pH of tongue biofilm (Saad and Greenman, unpublished)

4.1.1 Periodontal malodour

Periodontal disease is a chronic bacterial infection causing persistent gingival inflammation, and in some cases connective tissue destruction and bone resorption around the teeth. It is also characterised by pocket formation and recession. Although oral malodour is not caused by periodontal disease, there is ample evidence to suggest that periodontal disease increases the severity of malodour and also contributes to an increased tongue coating and higher production of VSC (Bolepalli *et al.*, 2015). Previous research has shown that chronic periodontitis patients exhibited about four-time higher amount of tongue coating compared to healthy control subjects (Yaegaki and Sanada, 1992). Moreover, oral malodor is more strongly associated with tongue coating rather than the severity of periodontitis (Morita and Wang, 2001a, 2001b). In addition, there are significant

correlations reported in the literature, where periodontal malodour has been associated with (1) increased number and depth of periodontal pockets (Yaegaki and Sanada, 1992), as well as (2) increased gingival crevicular fluid (GCF) flow rate(Morita and Wang, 2001a), (3) increased radiographic bone loss, (Morita and Wang, 2001b) and (4) presence of periodontal pathogens (Loesche and Kazor, 2002). In a study by Yaegaki (1997) an association between pocket depth of gingival pockets, amount of VSC and the CH_3SH/H_2S ratio was established.

The collective evidence from numerous *in vitro* and *in vivo* studies suggests that the persistence and diversity of the resident oral flora is dependent upon the range and rate of supply of nutrients provided by the host. For example, the salivary mucins (glycoproteins) act as the main source of carbohydrates for plaque and tongue biofilm bacteria. The degradation of the oligosaccharide side chains depends upon the concerted action of consortia of different species, each with complementary profiles of glycosidase activity (Beighton, Smith and Hayday, 1986; Ter Steeg *et al.*, 1988; Van der Hoeven and Camp, 1991; Bradshaw and Marsh, 1998). Furthermore, the growth of some species can be dependent on the provision of nutrients by other species, such as the supply of short-chain fatty acids by *Fusobacterium* sp. to *Viellonella* sp.

The specific theory of oral malodour suggests that specific microbial species are responsible (i.e. aetiological) whilst the non-specific theory suggests that the tongue biofilm "as a whole" is important, without the need for a specific agent (i.e. amount is more important than specific composition). In a diverse biofilm there may be many species that can transform substrates to VSC and many species can "substitute for others" in different cases. From a modelling perspective, the tongue surface biofilm may be classed as a continuously perfused matrix biofilm system. However, in periodontal disease there are

clear differences to tongue biofilms, both in the ecological composition and likely source of nutrition. The location of the periodontal microflora is at the interface of hard tissue tooth surfaces and the non-keratinised sulcular epithelial cells. This forms the sulcus or gingival crevice. Most importantly, the microbes gain nutrition mainly from gingival crevicular fluid sources rather than from saliva. In health, the subgingival flora may be supplied with nutrients from a mixed domain of saliva and crevicular fluid, since the diffusion rate of crevicular fluid is slow. This is because flow across intact junctional epithelial cells is dependant on the surface area of non-keratinised epithelia, and its ratio with the volume or mass of microbial cells that the fluid supplies within the crevice. As periodontal disease progresses, the gingival crevice volume extends deeper towards the roots of the teeth and increases in size, to develop into what is described as a periodontal "pocket". The microbial populations increase, and in addition, the microbes respond to the changing conditions (i.e. change their physiological state) producing more tissue-destroying hydrolytic enzymes as well as cytotoxic and inflammatory agents. The joint effect is to exacerbate tissue damage and continue to enlarge the pocket.

4.1.2 Characterisation of the oral microbiome by nucleic acid sequencing

There has been much work in characterising and grouping the oral microbiome with specific reference to periodontal disease, but less with reference to oral malodour. In their seminal paper, Socransky *et al.*, (1998) used whole DNA probes and checkerboard DNA-DNA hybridisation to generate a large dataset of microbial prevalence in 185 subjects. Using hierarchical clustering and correspondence analysis they split the taxa detected into five groups which they distinguished arbitrarily by colour. This grouping schema can be shown

in figure 4.2. Whilst limited in scope this grouping has remained the most common scheme for categorising periodontal pathogens. It is of interest to apply similar and enhanced techniques to nucleic based analysis, and to relate this to oral malodour.

Human Oral Microbe Identification Microarray (HOMIM), and Human Oral Microbe Identification using Next Generation Sequencing (HOMINGS) techniques are 16s rRNA gene sequencing methods for species identification of oral organisms. HOMIM analysis was introduced in 2008 and used an *in vitro* hybridization technique similar to DNA microarray technology to identify 293 predominant oral bacterial species (Paster and Dewhirst, 2009). The improved HOMINGS method was introduced in 2014 and relies on *in silico* hybridization to identify 597 species (Belstrøm *et al.*, 2016). The datasets produced by these methods allow powerful statistical techniques to be performed to analyse microbial ecology in the oral habitat. Some techniques similar to those used by Socransky, plus some novel techniques, will be discussed in this chapter.

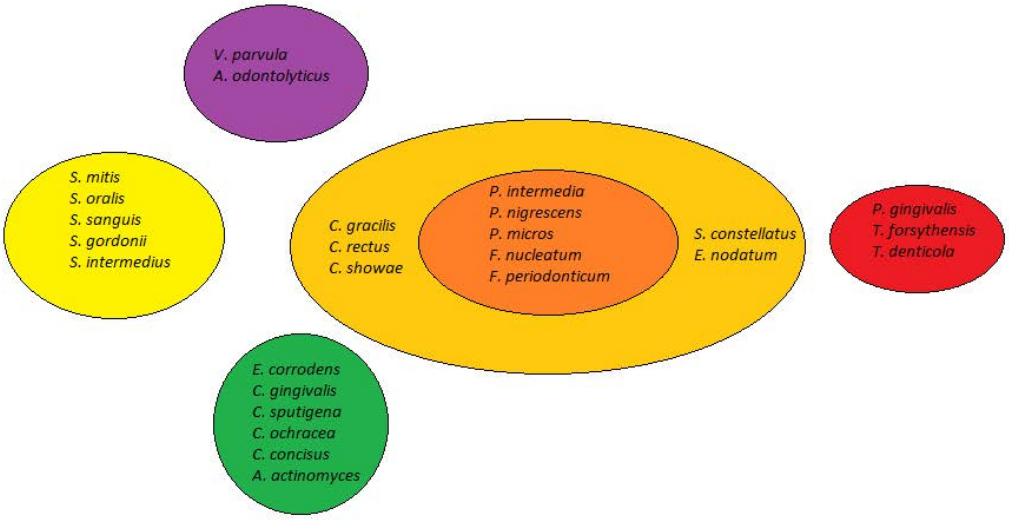

Figure 4.2 Subgingival microbial complex as described by Socransky *et al.,* 1998 (Reproduced with permission from John Wiley and Sons Inc.)

4.2 Materials and Methods

4.2.1 The volatilome *in vivo*

The volatilome of the human oral cavity was sampled by SIFT-MS as described in section 2.6.3. Short term changes were monitored in one subject over the course of the day and in another during a period of voluntary fasting. These were case studies of individuals and are presented as illustrations of the types of changes seen in the oral cavity, rather than exhaustive studies. Additionally, a number of volatile profiles of human volunteers examined by SIFT-MS were compared to the corresponding profiles obtained from *in vitro* biofilms as described below. All microbiological analysis was performed as described in section 2.2. Finally, the volatile profile of 39 subjects was compared with HOMIN analysis of the frequency of species seen in a tongue scrape sample. These methods are outlined in section 2.3. This volatile profile was compared with microbial composition before and after treatment.

4.2.2 The volatilome *in vitro*

In vitro biofilms were inoculated from samples as described in section 2.1. Gas sampling of the biofilm enclosure was performed as described in section 2.1.6 and in the previous chapter. With these techniques, the volatile profile of healthy individuals was compared with the profile obtained from biofilms inoculated from their tongue scrape

samples. Comparison of these profiles was performed by χ^2 analysis. pH of the biofilms was monitored in some cases, using the pHOptica optical device as described in section 3.2.

The effect of commercially available mouthwashes on the *in vitro* model was investigated using the methods described in section 2.1. Formulations tested were off the shelf samples of Listerine (Johnson & Johnson, New Jersey), Meridol (GABA, Germany), CB12 (Meda Pharmaceuticals Ltd., UK) and BreathRX (Phillips, UK). The active formulations were compared with sterile distilled water as a control. Pulses of 2ml of each treatment or control were applied to mature biofilms over a period of one minute and the effects on volatile production measured by SIFT-MS.

4.2.3 Species frequency analysis

Species frequency analysis was performed on tongue scrape samples from 40 individuals as described in section 2.3. The HOMIM data was analysed by a variety of statistical visualisation methods beginning with rank abundance plots and calculation of diversity indices. A novel technique, first presented here, is to plot heatmaps of organisms to better visualise the association between their frequency and malodour. Circos is a computer scripting language originally devised to visualise genomic data (Krzywinski, 2009), but it can be usefully employed to generate these type of heatmaps. The method is as follows; taxa are plotted radially around the a circular Circos plot and samples are ordered from low to high malodour score (by whatever measurement method has been used), starting at the centre of the plot. Points are coloured by heatmap ranging from pale to dark red based on the percentage frequency. This means that darker red at the outside of the

circular plot corresponds to the association of those organisms with malodour. Further analysis can be performed by analysing the skew coefficient for each organism 'spoke' of the circle. Positively skewed organisms are likely to be associated with malodour whereas negatively skewed organisms are likely to be more prevalent in low malodour individuals.

Another powerful statistical method that can be applied to these kinds of datasets is co-occurrence analysis. Assessing cooperation and competition in species has a long history, and the use of binary matrices has its roots in the "checkerboard" theory of Diamond (1975). The development of the ideas is well covered by Connor *et al.,* (2017). Nowadays probabilistic species co-occurrence modelling is best accomplished by computer algorithms (Veech, 2013) such as that implemented by Daniel Griffith in R-studio (Griffith, Veech and Marsh, 2016). These models are much more rapid than original techniques and avoid most Type I and II errors by avoiding data randomisation based comparative techniques. The matrix allocates 'positive', 'negative' or 'random' to each species pair combination based on whether the probability of the species pair occurring is greater than each species appearing with all the other species.

Multidimensional scaling (MDS) was also used to gain insight from the large dataset by analysing clustering before and after treatment. Not only can clustering in such plots indicate ecological associations between organisms, but the change in clustering before and after treatment can reveal the demographic action of a treatment.

4.3 Results

4.3.1 The oral volatilome

Figure 4.3 shows the progression in the profile of volatiles for a single subject over the course of a morning.

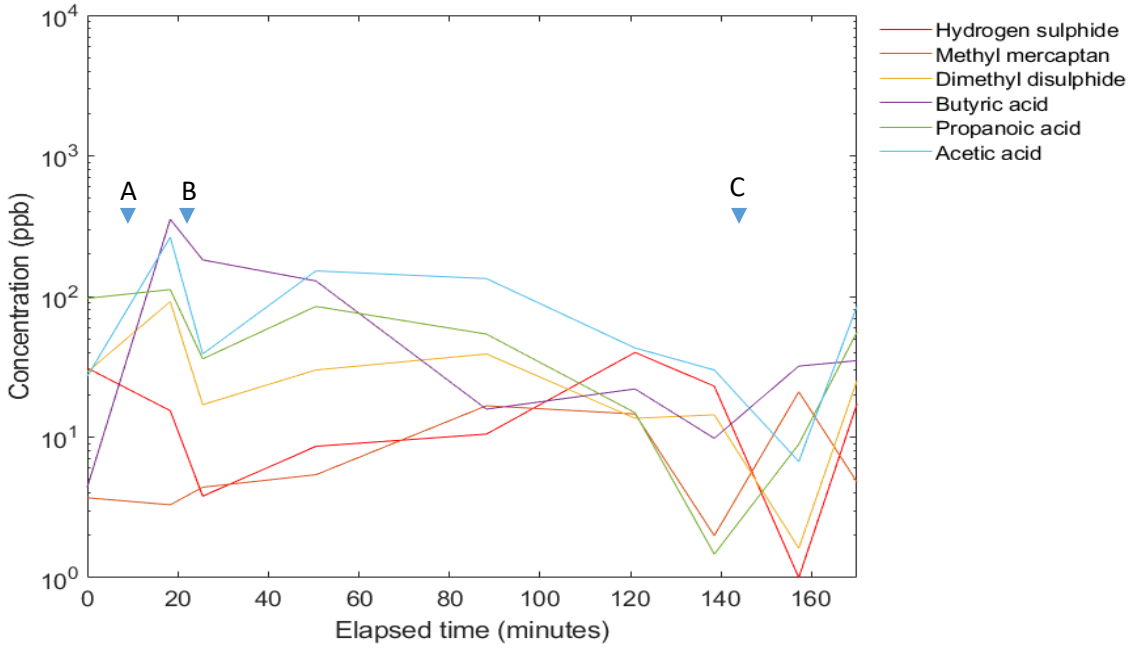

The subject drank coffee at t=10 minutes (A), ate a small snack at t=25 minutes (B) and lunch at 140 minutes (C)

Figure 4.3: Progression of the volatile profile in the oral cavity of a single subject.

The effect of variations in food intake by the human host is illustrated in another case study which involved monitoring of oral volatiles in a human subject during a period of voluntary fasting. As can been seen in figures 4.4 to 4.6 fasting had a dramatic effect on volatiles detected by SIFT-MS and the composition of the tongue biofilm. Anaerobic plate

counts were almost two orders of magnitude lower during the fasting period and the proportion of gram negative organisms twice as high. Production of sulphides was highest at the end of the fasting period with hydrogen sulphide production particularly pronounced. A further five days after recommencement of a normal diet, the profile of VOCs and composition of the biofilm had almost returned to the original state.

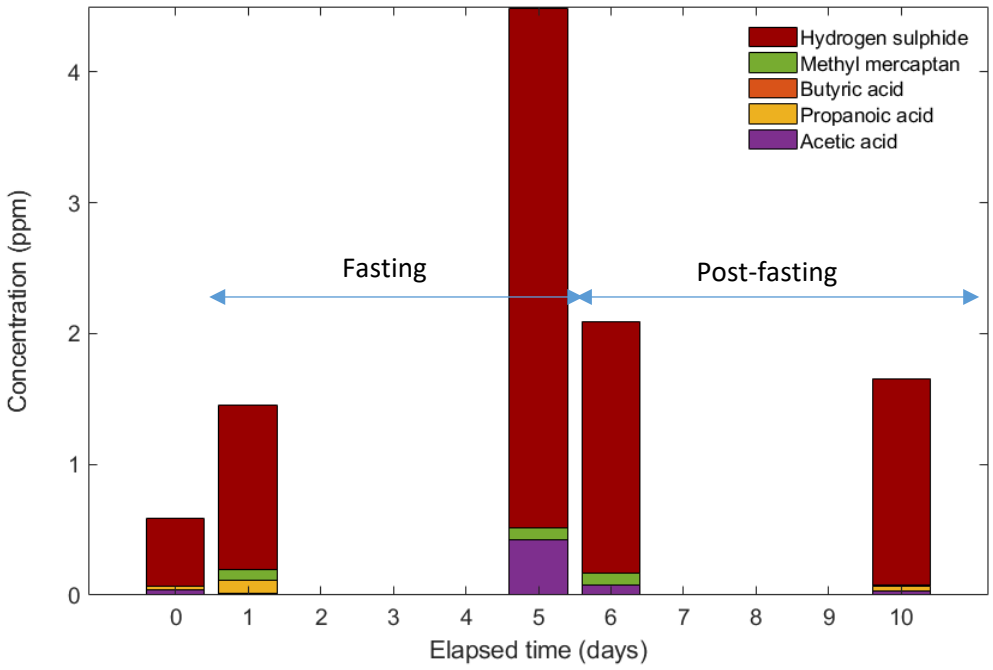

Figure 4.4: Changes in volatile profile before, during and after a period of fasting

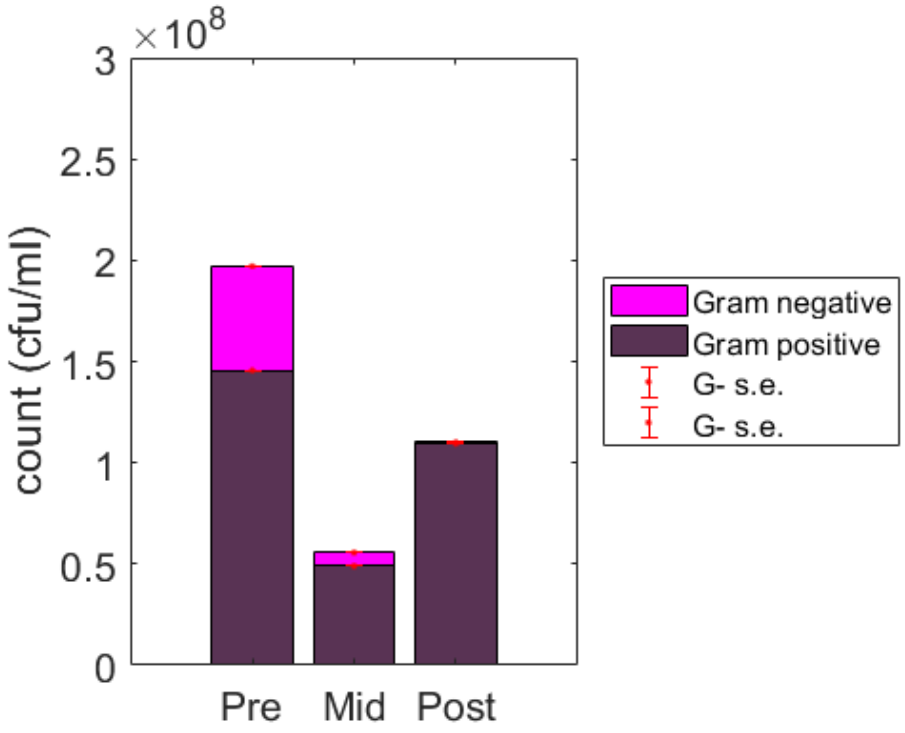

Figure 4.5: Microbiological changes before, during and after a period of fasting (Gram positive and negative organisms)

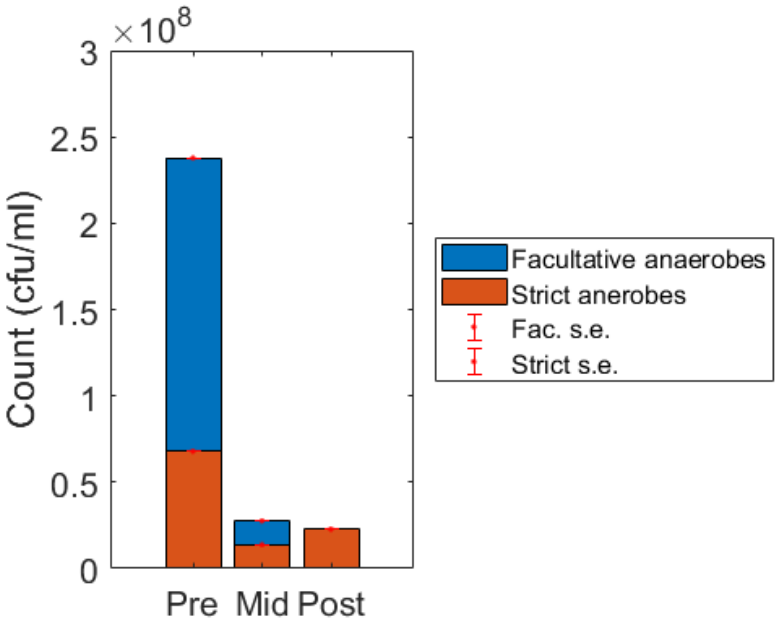

Figure 4.6: Microbiological changes before, during and after fasting (strict and facultative anaerobes)

4.3.2 Comparison of *in vivo* and *in vitro* biofilms by SIFT-MS

Figure 4.7 shows Profile3 SIFT-MS VOC profiles taken from the oral cavity of six volunteers, and their corresponding profiles from biofilms inoculated from their tongue scrape samples. In all cases where at least five compounds are seen in both samples, χ^2 analysis of the data shows the profiles to be indistinguishable (P = 0.9). In addition to validating the model, this data supports the hypothesis that bad breath, specifically in respect of volatile sulphide production, is a feature of the microcosm and the properties of the model reflect the different microcosms. Oral malodour is thus transplantable to the model. Whilst proportions of strict and facultative anaerobes and gram positive and negative organisms are similar *in vivo* and *in vitro* a far superior method for comparing the microbiological composition would be nucleic acid based techniques as discussed next.

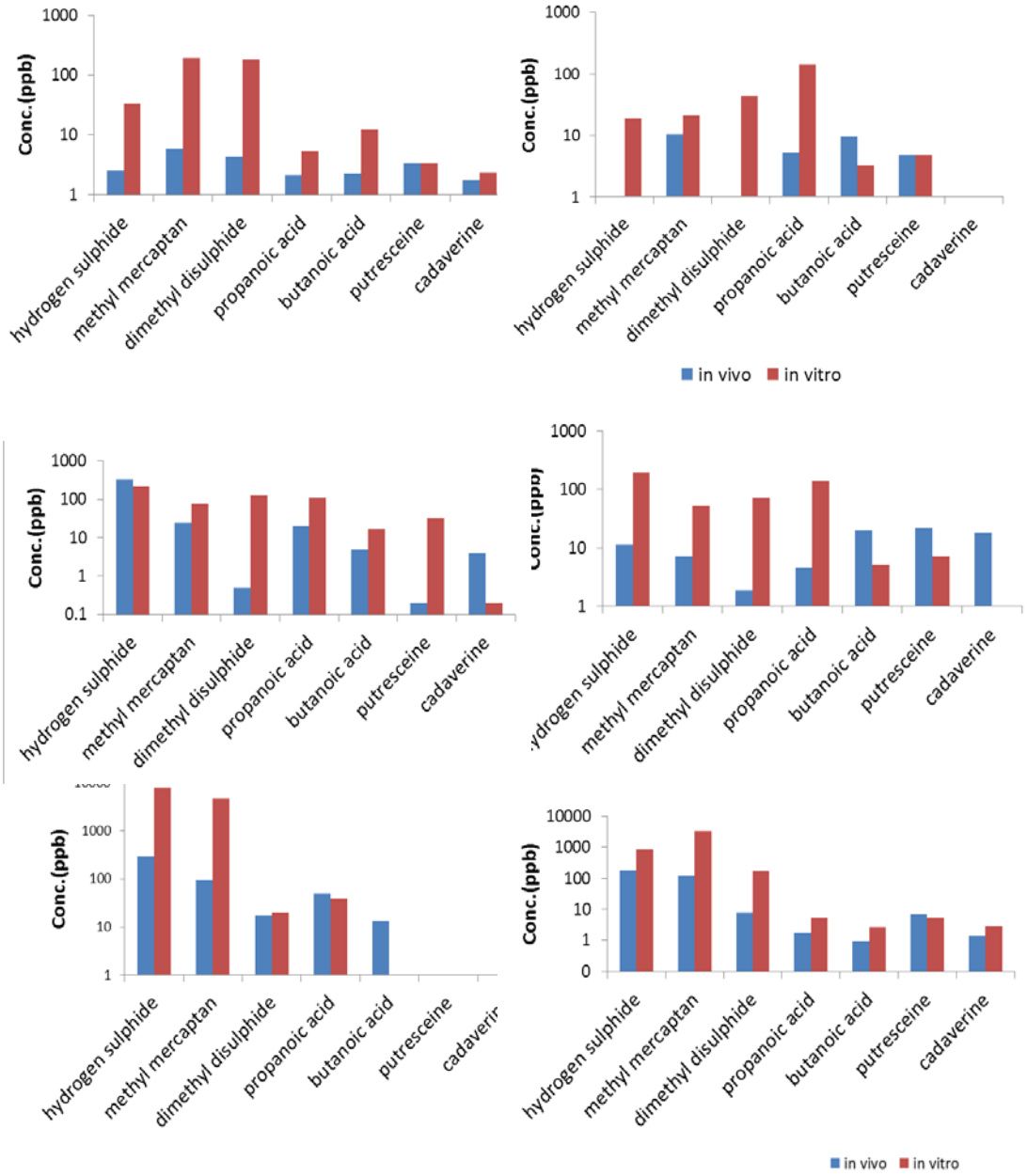

Figure 4.7: Comparison of VOC profiles from *in vivo* and *in vitro* biofilms from the same subjects

4.3.3 The effect of commercial mouthwashes on the *in vitro* biofilm

Figure 4.8 shows the effect on volatile profile by the application of commercial mothwashes to mature *in vitro* biofilms. Figure 4.9 shows the proportion of initial hydrogen sulphide production after treatment.

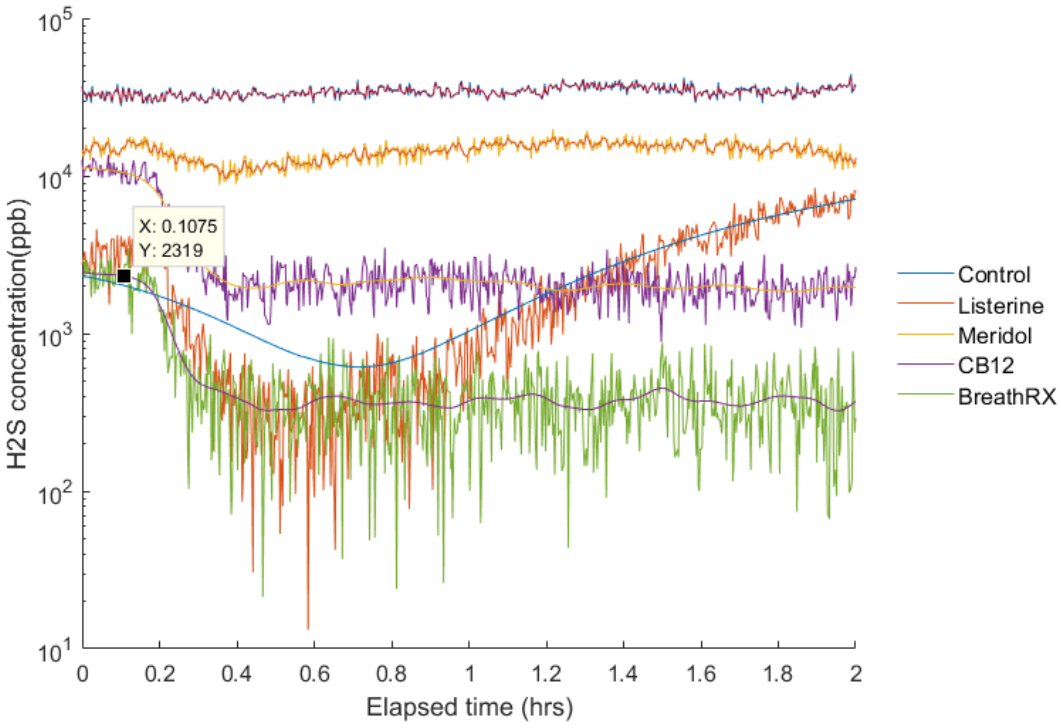

Figure 4.8: The effect of various commercial mouthwashes on the hydrogen sulphide production of six biofilms. Treatment occurred at t=0.

A useful comparison technique here, used again later, is to measure the total area under the response curve for each treatment. This is a useful measure as it takes into account both the initial reduction in volatile levels and the duration of that an effect. A bar chart showing the respective areas for each treatment is shown in 4.10.

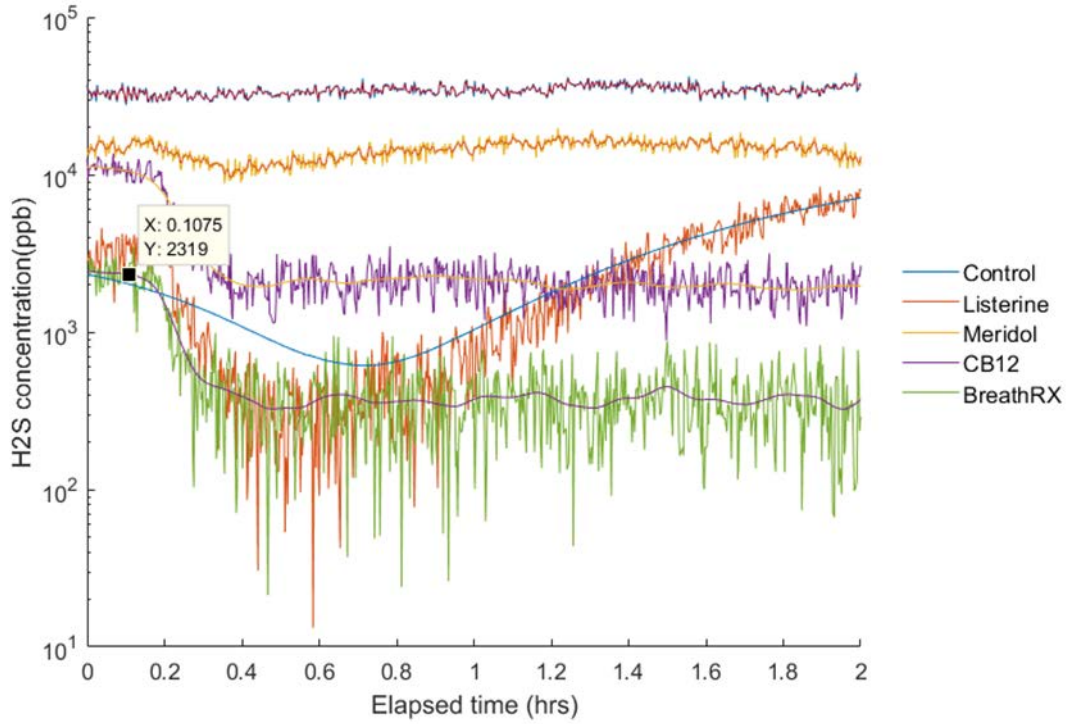

Figure 4.9: The effect of various commercial mouthwashes on the hydrogen sulphide production of six biofilms, shown as a proportion of the original level

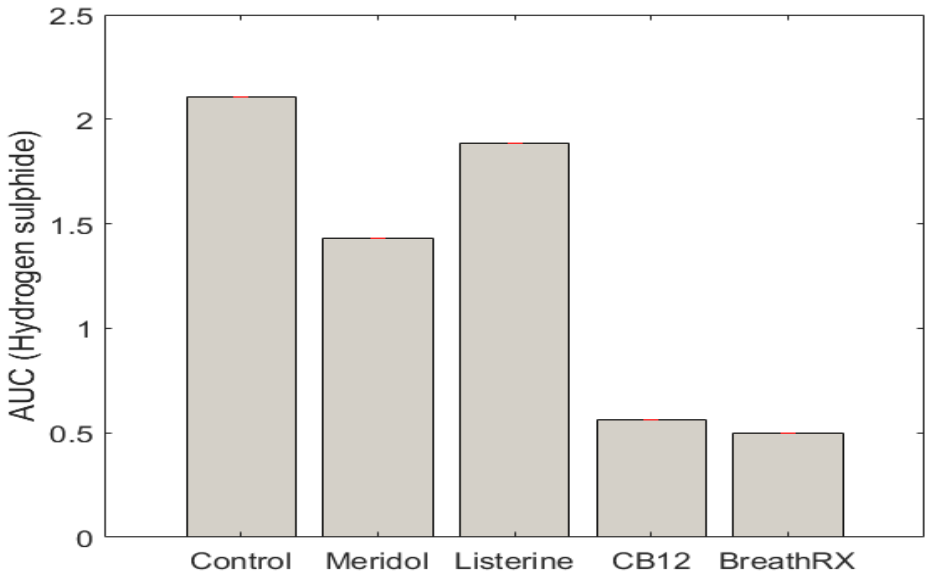

Figure 4.10: Area under the hydrogen sulphide curve for various commercial mouthwashes. Overall order of effectiveness is therefore BreathRX>>CB12>>Meridol>>Listerine>>Control.

4.3.4 Species frequency analysis

The dataset obtained from HOMIM analysis performed on 40 individuals before and after a treatment intervention consists of two 40 by 259 numerical arrays of non-integer values between 0 and 50. To represent this visually in ways that confer useful information is challenging. A common useful technique is to plot rank abundance charts. Because of the large number of organisms with low incidence, these charts have very long, flat tails, and it is more useful to plot only the most abundant organisms. The charts for the first forty organisms can be seen in figure 4.11. The shape of each of these charts would be reflected in the diversity indices calculated for each group. The Chao1 (Chao, 2016) index of overall species richness is not significantly different, but the Shannon diversity index (Shannon, 1948) is 3.07 for the first group and 2.90 for the second. This is a significant difference at the 95% level (P=0.0008). If the change in relative abundance of organisms before and after treatment is plotted for those with the highest change, it appears as in figure 4.12.

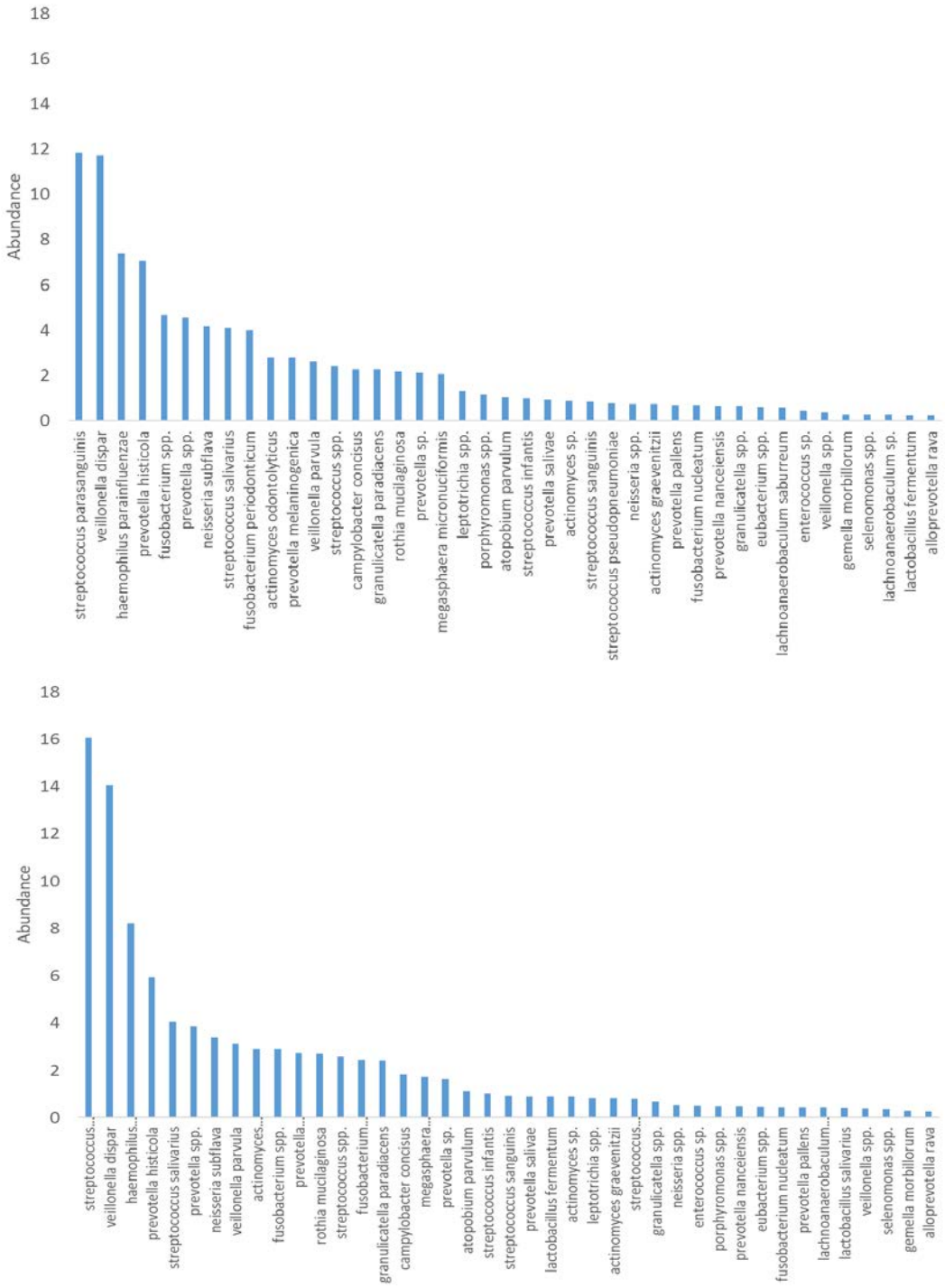

Figure 4.11: Rank abundance chart of organism frequency by 16s rRNA analysis of tongue scrapes from 40 individuals. Pprevalence is shown before (top) and after (bottom) treatment for the 40 most abundant organisms

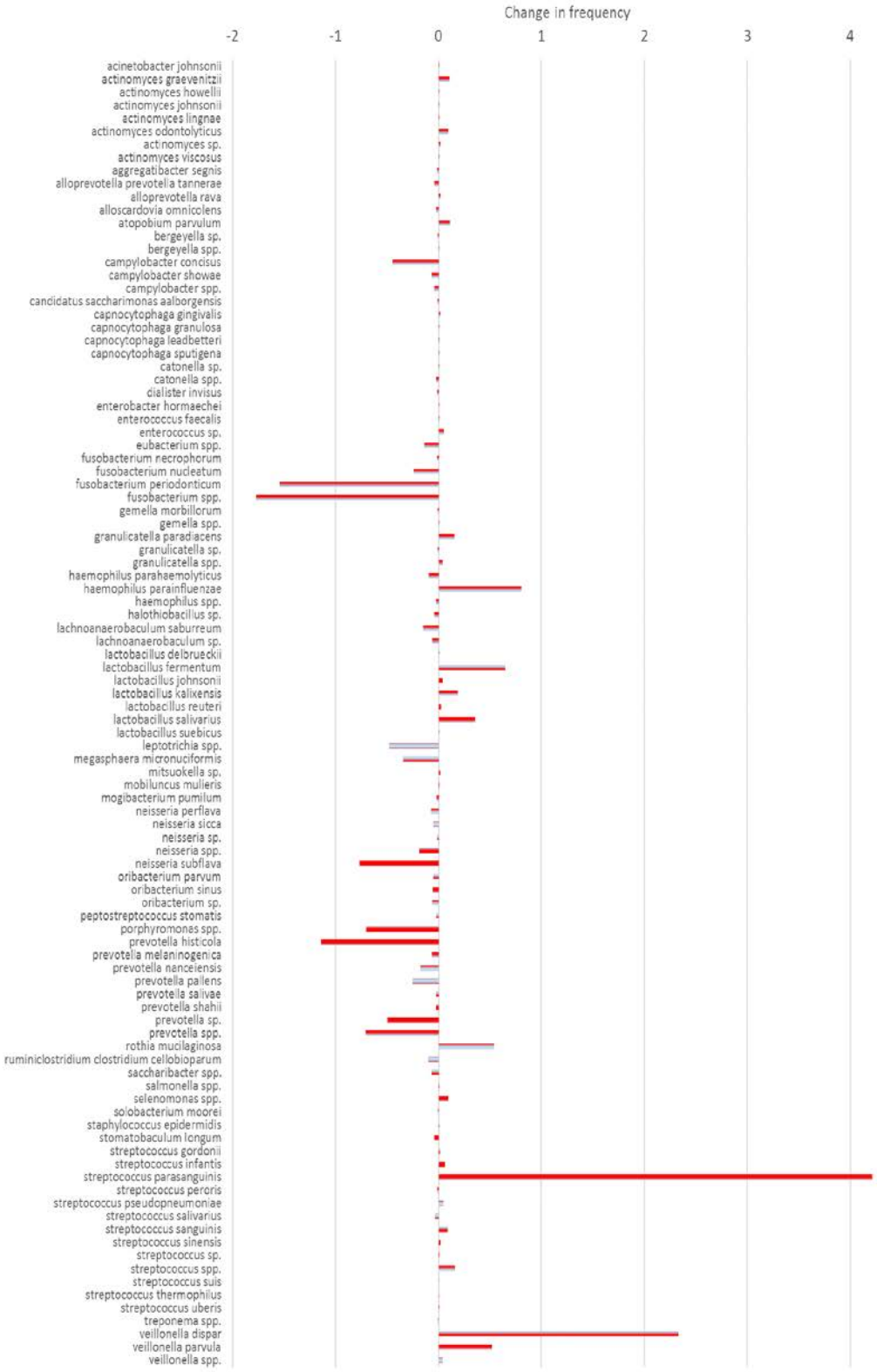

Figure 4.12: Change in relative abundance of fifty organism frequency by 16s rRNA analysis of tongue scrapes from 40 individuals. The species included showed the greatest positive or negative change after treatment with an antimalodour formulation.

A circus heatmap of the data, plotted as explained earlier, is shown in figure 4.13. Both Pearson's and Kelly's coefficient of skewness were calculated for each 'spoke' of the circle and the organisms showing the greatest skew are seen in figures 4.14 and 4.15.

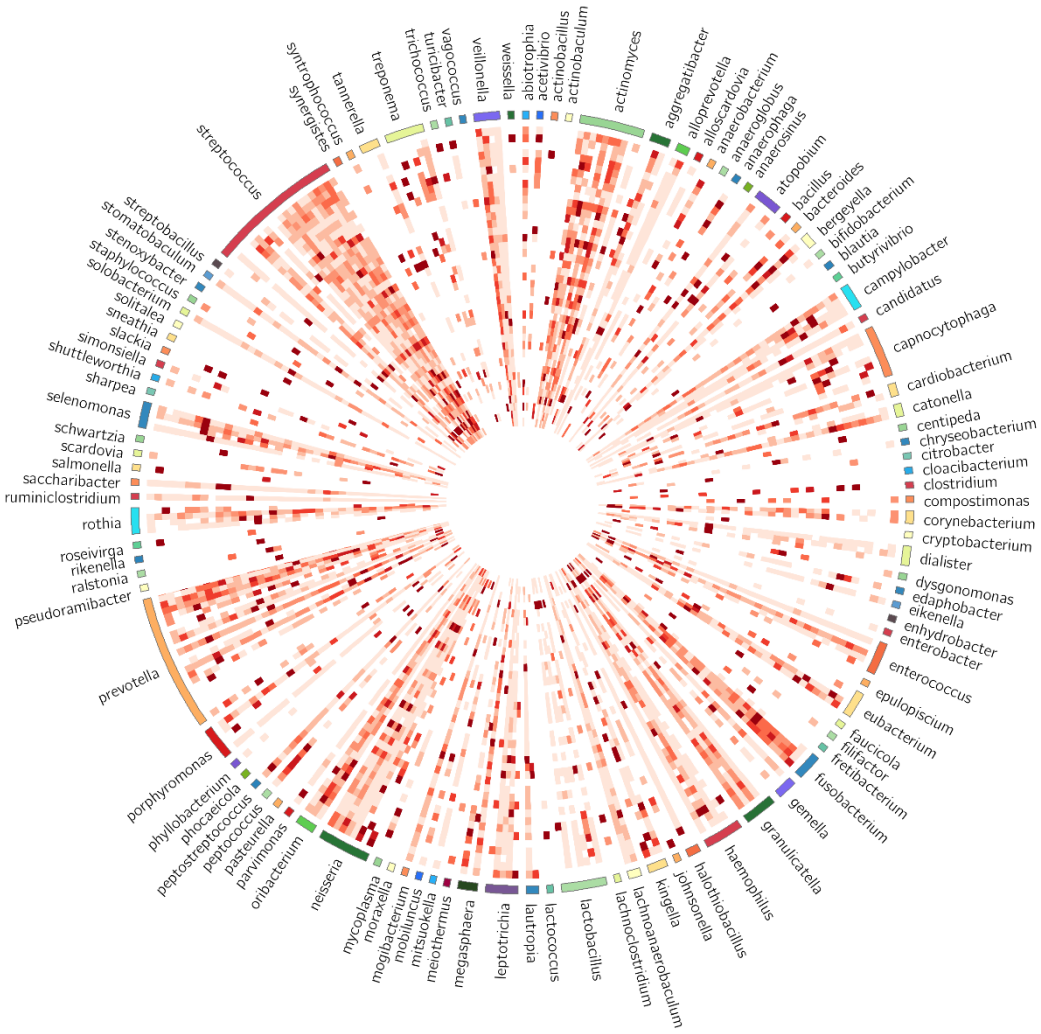

Figure 4.13: Heatmap of oral malodour and organism frequency by 16s rDNA analysis. Radial tracks represent individuals and spokes represent organisms. Higher relative frequency of each organism is represented by a darker red colour, and individuals are plotted radially outwards in order of measured malodour by SIFT-MS.

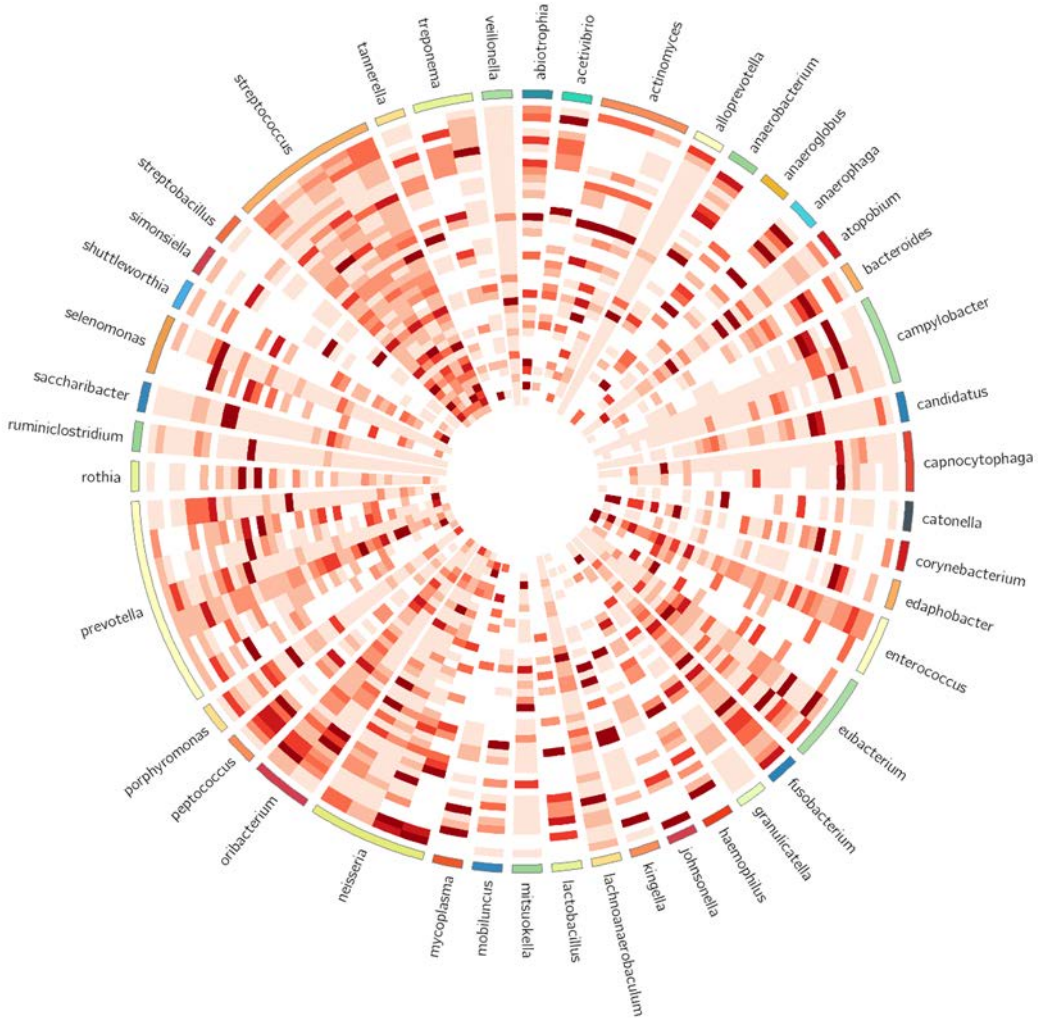

Figure 4.14: A select group of organisms showing positive skew by Pearson's coefficient previously identified by 16s rDNA analysis of 40 individuals. Radial tracks represent individuals and spokes represent organisms. Higher relative frequency of each organism is represented by a darker red colour, and individuals are plotted radially outwards in order of measured malodour by SIFT-MS.

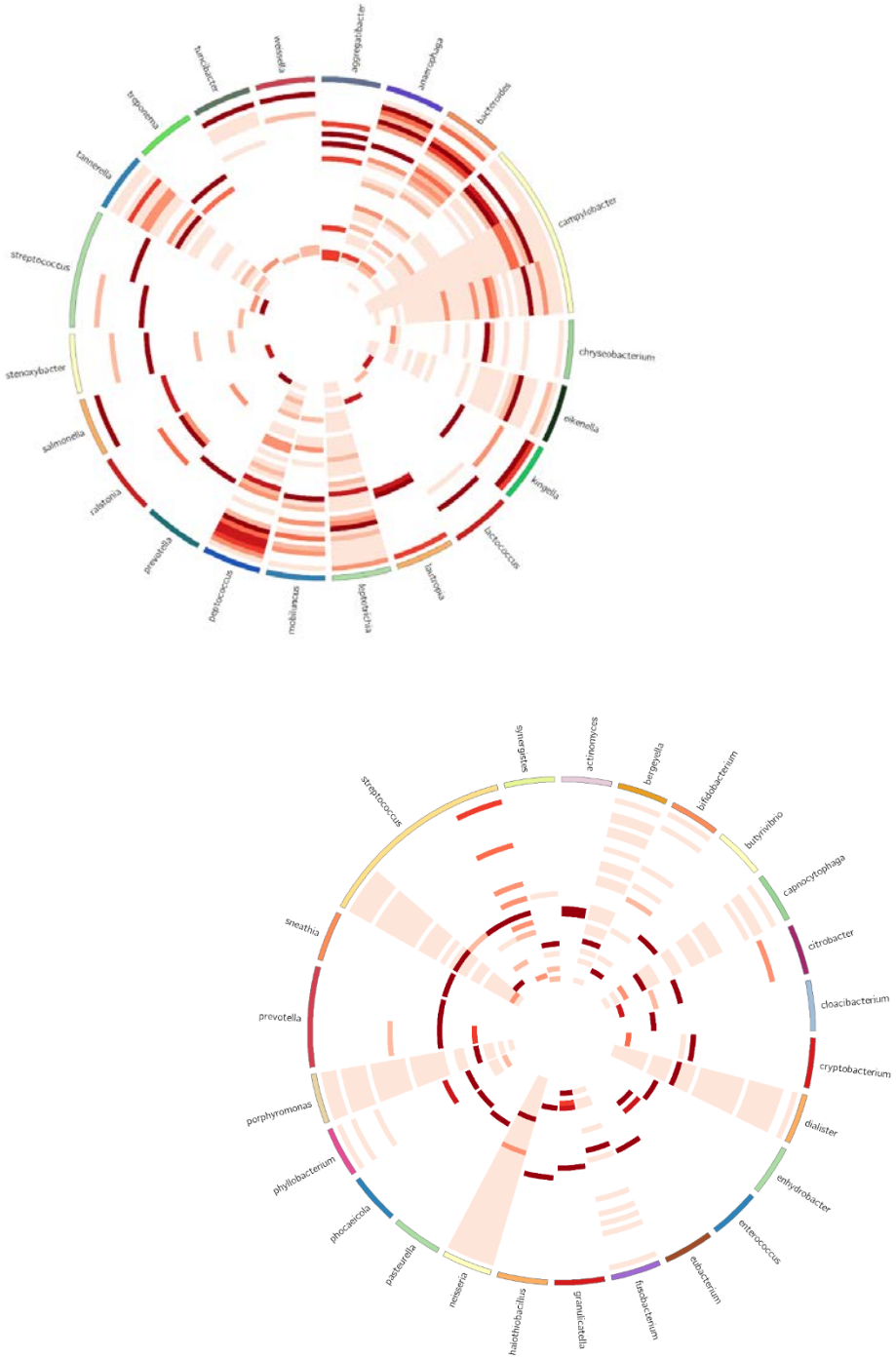

Figure 4.15: Positive skewed organisms (above) and negatively skewed (below) by Kelly's coefficient.These are a subset of organisms analyses by 16s rRNA analysis of tongue scrapes from 40 individuals. Radial tracks represent individuals and spokes represent organisms. Higher relative frequency of each organism is represented by a darker red colour, and individuals are plotted radially outwards in order of measured malodour by SIFT-MS.

A co-occurrence matrix of ‘positive’, ‘negative’ and ‘random’ associations between a subset of organisms can be seen in figure 4.16.

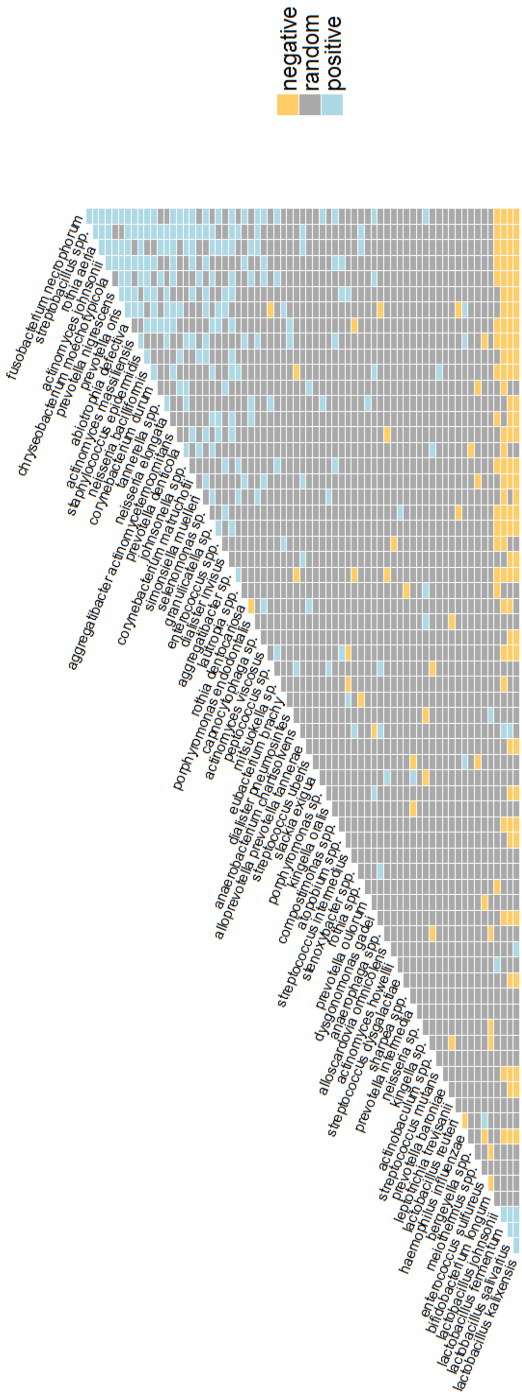

Figure 4.16: Co-occurrence matrix for a subset of the organisms identified in 40 samples by 16s rRNA analysis. Colour of the block at the intersection of the two organisms indicates if they are more (positive) or less (negative) likely to occur together

A number of MDS plots could be plotted from this data but an interesting one is presented here. The plot in figure 4.17 shows the distance distribution of the organisms before treatment and after treatment. Points are coloured according to Gram reaction. MDS plot a scaled transform of the Euclidean distances between points, thus a wider spread indicates more diversity.

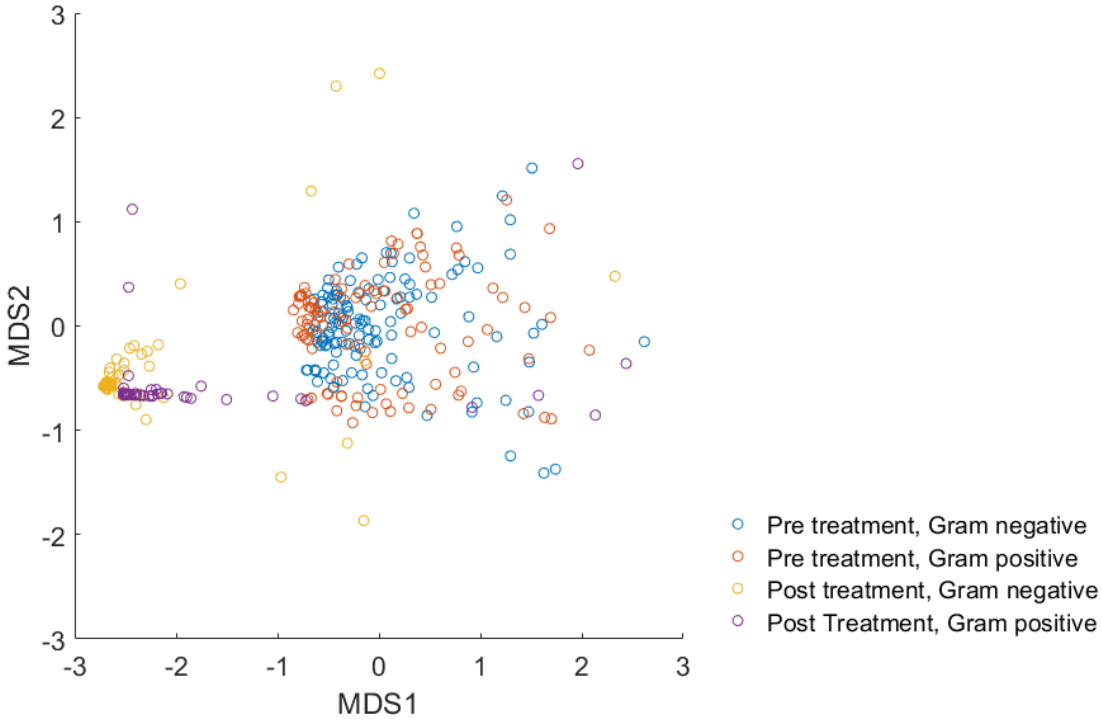

Figure 4.17: MDS analysis of species frequencies obtained by 16s RNA analysis of 40 subjects, with grouping based on Gram stain pre and post treatment.

K-means cluster analysis can also be performed on the Euclidean distance matrix in a similar way to that performed by Socransky with peridodontal organisms (1998). This leads to a grouping schema shown in figure 4.18 and the accompanying table 4.1. The number of clusters was chosen using within groups sum of squares method.

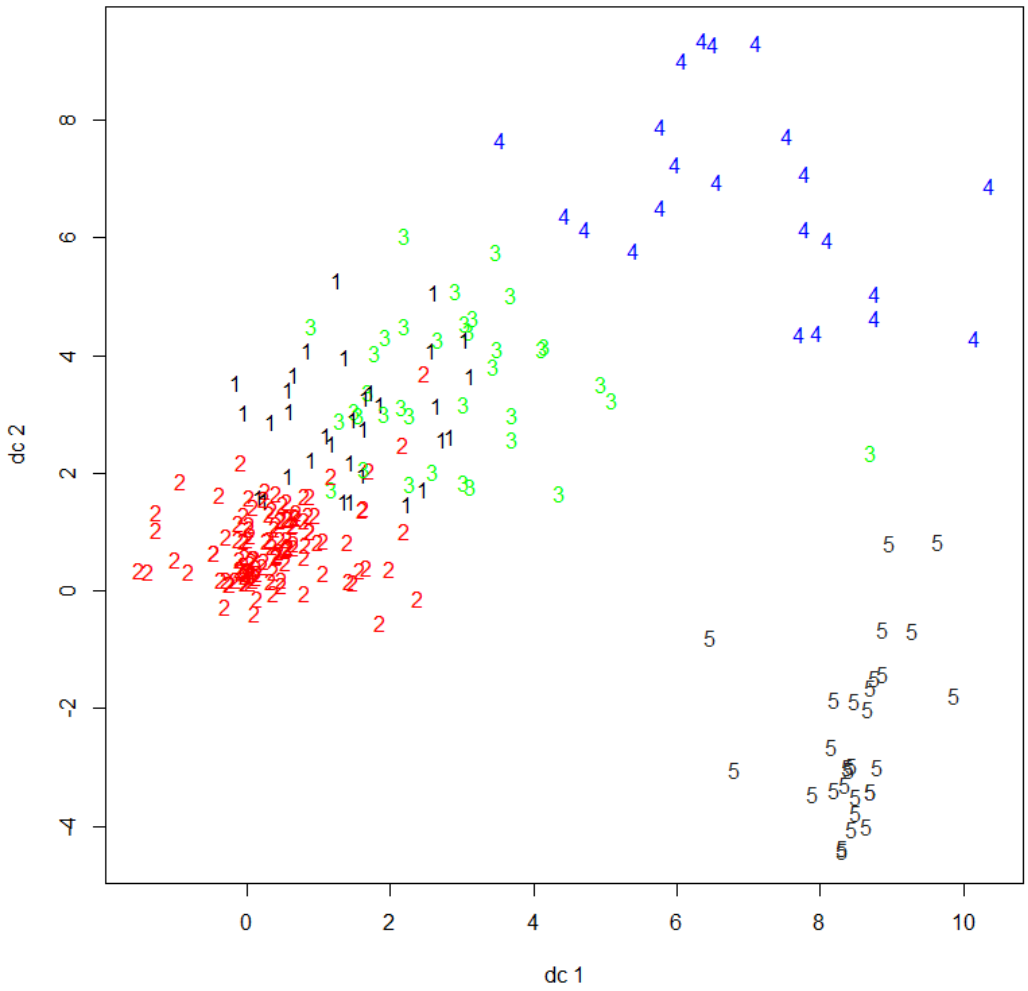

Figure 4.18 K-means cluster analysis of species frequencies obtained by 16s rRNA analysis of 40 subjects. The identity of the organisms in each cluster is given in Table 4.1

Table 4.1 Organisms grouped as in figure 4.18 (qv.)

Group		
1	*Acetivibrio* spp.	*Mycoplasma hyosynoviae*
	Anaerobacterium chartisolvens	*Neisseria elongata*
	Anaerophaga spp.	*Neisseria* sp.
	Bacteroides spp.	*Neisseria* spp.
	Bergeyella sp.	*Neisseria subflava*
	Capnocytophaga infantium	*Oribacterium parvum*
	Catonella spp.	*Peptococcus* sp.
	Clostridium intestinale	*Peptostreptococcus stomatis*
	Eubacterium sp.	*Porphyromonas* spp.
	Fusobacterium nucleatum	*Prevotella aurantiaca*
	Fusobacterium periodonticum	*Prevotella nanceiensis*
	Fusobacterium spp.	*Prevotella shahii*
	Haemophilus parainfluenzae	*Rothia* spp.
	Haemophilus sp.	*Streptococcus peroris*
	Kingella sp.	*Treponema socranskii*
	Lactobacillus helveticus	*Veillonella parvula*
	Megasphaera spp.	
Group		
2	*Actinobacillus succinogenes*	*Eikenella corrodens*
	Actinomyces spp.	*Enhydrobacter aerosaccus*
	Aggregatibacter sp.	*Enterobacter hormaechei*
	Alloprevotella prevotella tannerae	*Enterococcus gallinarum*
	Alloprevotella rava	*Enterococcus sulfureus*
	Alloscardovia omnicolens	*Eubacterium saphenum*
	Anaerosinus selenomonadaceae sb90	*Faucicola moraxellaceae bacterium*
	Atopobium rimae	*Fretibacterium fastidiosum*
	Atopobium sp.	*Fusobacterium necrophorum*
	Bergeyella spp.	*Gemella sanguinis*
	Bifidobacterium longum	*Haemophilus haemolyticus*
	Blautia sp.	*Halothiobacillus neapolitanus*
	Butyrivibrio sp.	*Halothiobacillus* sp.
	Campylobacter gracilis	*Johnsonella* spp.
	Campylobacter showae	*Kingella oralis*
	Campylobacter spp.	*Kingella* spp.
	Capnocytophaga gingivalis	*Lachnoanaerobaculum* sp.
	Capnocytophaga granulosa	*Lachnoclostridium clostridium symbiosum*
	Capnocytophaga haemolytica	*Lactobacillus fermentum*
	Capnocytophaga leadbetteri	*Lactobacillus johnsonii*
	Capnocytophaga sp.	*Lactobacillus kalixensis*
	Capnocytophaga spp.	*Lactobacillus reuteri*
	Capnocytophaga sputigena	*Lactobacillus salivarius*
	Cardiobacterium valvarum	*Lactobacillus suebicus*
	Catonella sp.	*Lactococcus lactis*
	Centipeda sp.	*Lautropia* sp.
	Chryseobacterium moechotypicola	*Lautropia* spp.
	Cloacibacterium spp.	*Leptotrichia goodfellowii*
	Compostimonas spp.	*Leptotrichia hofstadii*
	Cryptobacterium curtum	*Leptotrichia* sp.
	Dialister invisus	*Leptotrichia* spp.
	Dialister sp.	*Leptotrichia trevisanii*
	Edaphobacter spp.	*Megasphaera* sp.

Table 4.1 continued

Group		
2 (cont.)	*Meiothermus* spp.	*Selenomonas infelix*
	Mitsuokella sp.	*Selenomonas sputigena*
	Mobiluncus mulieris	*Sharpea* spp.
	Neisseria canis	*Simonsiella muelleri*
	Neisseria perflava	*Sneathia* spp.
	Neisseria sicca	*Solitalea* spp.
	Parvimonas micra	*Staphylococcus epidermidis*
	Pasteurella sp.	*Stenoxybacter* spp.
	Phocaeicola spp.	*Streptobacillus* spp.
	Phyllobacterium trifolii	*Streptococcus australis*
	Porphyromonas endodontalis	*Streptococcus constellatus*
	Porphyromonas genomsp. p3	*Streptococcus dysgalactiae*
	Porphyromonas gingivalis	*Streptococcus intermedius*
	Porphyromonas sp.	*Synergistes* spp.
	Prevotella baroniae	*Syntrophococcus sucromutans*
	Prevotella dentalis	*Tannerella forsythia*
	Prevotella enoeca	*Tannerella* sp.
	Prevotella intermedia	*Tannerella* spp.
	Prevotella marshii	*Treponema amylovorum*
	Prevotella oralis	*Treponema denticola*
	Prevotella oulorum	*Treponema lecithinolyticum*
	Pseudoramibacter alactolyticus	*Treponema* sp.
	Ralstonia solanacearum	*Treponema* spp.
	Rikenella spp.	*Trichococcus flocculiformis*
	Roseivirga sp.	*Turicibacter* spp.
	Rothia aeria	*Veillonella* sp.
	Ruminiclostridium clostridium cellobioparum	*Veillonella* spp.
	Salmonella spp.	*Weissella* spp.
	Schwartzia sp.	

Group		
3	*Actinomyces howellii*	*Mogibacterium pumilum*
	Actinomyces johnsonii	*Oribacterium* sp.
	Actinomyces massiliensis	*Prevotella denticola*
	Actinomyces viscosus	*Prevotella nigrescens*
	Aggregatibacter actinomycetemcomitans	*Prevotella oris*
	Aggregatibacter segnis	*Prevotella pallens*
	Anaeroglobus sp.	*Prevotella* sp.
	Atopobium parvulum	*Prevotella veroralis*
	Atopobium spp.	*Rothia dentocariosa*
	Campylobacter concisus	*Saccharibacter* spp.
	Candidatus saccharimonas aalborgensis	*Scardovia inopinata*
	Cardiobacterium hominis	*Selenomonas* sp.
	Corynebacterium durum	*Selenomonas* spp.
	Corynebacterium matruchotii	*Shuttleworthia satelles*
	Dialister pneumosintes	*Slackia exigua*
	Eubacterium brachy	*Solobacterium moorei*
	Eubacterium spp.	*Stomatobaculum longum*
	Lachnoanaerobaculum saburreum	*Streptococcus sinensis*

Table 4.1 continued

Group		
4	*Actinomyces cardiffensis*	*Prevotella melaninogenica*
	Actinomyces graevenitzii	*Prevotella salivae*
	Actinomyces lingnae	*Prevotella* spp.
	Actinomyces odontolyticus	*Rothia mucilaginosa*
	Actinomyces sp.	*Streptococcus gordonii*
	Enterococcus sp.	*Streptococcus salivarius*
	Granulicatella paradiacens	*Streptococcus* sp.
	Granulicatella spp.	*Streptococcus* spp.
	Megasphaera micronuciformis	*Streptococcus thermophilus*
	Oribacterium sinus	*Streptococcus uberis*
	Prevotella histicola	*Veillonella dispar*
Group		
5	*Abiotrophia defectiva*	*Haemophilus parahaemolyticus*
	Actinobaculum spp.	*Haemophilus* spp.
	Bacillus spp.	*Neisseria bacilliformis*
	Citrobacter spp.	*Prevotella micans*
	Dysgonomonas gadei	*Streptococcus dentirousetti*
	Enterococcus faecalis	*Streptococcus infantis*
	Enterococcus spp.	*Streptococcus mitis*
	Filifactor alocis	*Streptococcus mutans*
	Gemella morbillorum	*Streptococcus oralis*
	Gemella spp.	*Streptococcus parasanguinis*
	Granulicatella adiacens	*Streptococcus pseudopneumoniae*
	Granulicatella elegans	*Streptococcus sanguinis*
	Granulicatella sp.	*Streptococcus suis*
	Haemophilus influenzae	*Vagococcus* sp.

4.4 Discussion

4.4.1 The volatilome *in vitro* and *in vivo.*

The case studies of volatile profile with food intake give an indication of the link between short-term changes and the metabolism of the microbiome. Figure 4.2 shows the progression in the profile of volatiles for a single subject over the course of a morning. As can be seen, the first calorific intake of the day, in the form of a cup of coffee, causes a rapid increase in volatiles. Subsequent food intake causes an initial reduction in volatiles followed by an increase. The amount of dissolved hydrogen sulphide and methyl mercaptan in solution is highly pH dependant, whereas dimethyl disulphide is less so. This explains the dominance of these first two sulphides since acids are typically produced from food or saliva through microbial metabolism.

The effect of variations in food intake by the human host is illustrated in the second case study which involved monitoring of oral volatiles in a human subject during a period of voluntary fasting. As can been seen in figures 4.3 to 4.5 fasting had a dramatic effect on volatiles detected by SIFT-MS and the composition of the tongue biofilm. Anaerobic plate counts were almost two orders of magnitude lower during the fasting period and the proportion of Gram negative organisms twice as high. Production of sulphides was highest at the end of the fasting period with hydrogen sulphide production particularly pronounced. A further five days after recommencement of a normal diet, the profile of VOCs and composition of the biofilm had almost returned to the original state. Unfortunately oral pH was not monitored in this period although it is expected that it increased during the fasting period. Figure 4.6 shows that in the biofilm model, decrease in

pH was associated with decreased production of H_2S and CH_3SH and that this could be induced by a pulse of glucose.

Turning to the comparison of SIFT-MS profiles *in vivo* and *in vitro* (figure 4.7), the top row are low malodour individuals as scored by organoleptic judge, the second row medium malodour and the bottom row high malodour. It can be readily be seen that the VOC profiles are "transplantable" by using high, medium and low tongue scrape inoculum to generate the corresponding *in vitro* biofilm in the plate model. Absolute levels are significantly higher in the biofilm model, and in some cases this means that some compounds are seen only in the *in vitro* samples.

The commercial mouthwash experiment demonstrates that the biofilm model can be used to test the effects of antimicrobial interventions on the biofilm and the corresponding effect on volatile profile. Similar results are seen as in *in vivo* studies and the medium term effects of the treatments is visualised well by the area under the curve charts. This *in vitro* method is useful in this regard and is likely to become moreso as studies involving human participants become more difficult.

4.4.2 Species frequency analysis

Species frequency analysis in the study of the tongue biofilm and oral malodour has lagged behind similar studies in periodontal disease. Co-occurrence of *Bacteroides forsythus and gingivalis* were first noted (Gmür, Strub and Guggenheim, 1989) followed by *Treponema denticola* and *Porphyromonas gingivalis* (Simonson *et al*., 1992) and *Fusobacterium nucleatum* and *Prevotella intermedia* (Ali *et al.*, 1994). In 1998, Socransky

was the first to place sub-gingival organisms into groups referred to as 'complexes' (Socransky *et al.*, 1998) and this convention has been used widely since. These associations were mainly made by fairly simplistic methods such as contingency table analysis, and associations were not linked to other independently measureable variables such as volatile profile.

The visualisation techniques outlined here when taken as a whole demonstrate powerful methods for characterising microbial communities and their macroscopic effects. The Circos plots with accompanying skew analysis (figures 4.13 to 4.15) highlight organisms that may not have previously been associated with malodour. These organisms, such as *Edaphobacter* sp., *Oribacterium* sp. or *Anaerophagia* sp. may not directly produce volatiles themselves but their role in the microbial ecosystem may lead to their association with malodour. Whilst further work would obviously be required to evaluate cause and effect, there is obviously ample direction for further study. Similar techniques could be used in the field of periodontal disease, not only linking volatile profiles with microbial ones, but other contiguous clinical measures such as pocket depth.

Co-occurrence matrices can also reveal important interactions between organisms. Whilst the older contingency table methods were valid, modelling of complex chequerboard tables of numerous species is only possible now due to the ready availability increased computer processing power. Examination of figure 4.16 shows a number of well-known associations between groups of organisms, such as *Fusobacterium* sp., *Prevotella* sp., *Actinomyces* sp. and *Tannerella* sp. It is interesting, however, that *Lactobacillus fermentum, salivarius and kalixensis* are frequently seen together but are negatively associated with many known malodour producing organisms. It is tempting to suggest that such organisms may have the potential to have positive probiotic effect if administered

orally in combination with an antimicrobial mouthwash. This would be another area for further study.

Turning to effects seen before and after treatment, the rank abundance charts (figure 4.11) show different profiles, and the change in Shannon index but not Chao1 indicates that whilst overall richness is similar there is a loss of diversity which affects a smaller subpopulation. This is visually apparent in the difference in shapes of the primary rank abundance charts, the second chart appearing to have a sharper 'peak'. The subpopulation is likely to be of more common organisms rather than rare outliers. The change in abundance plot (figure 4.12) suggests that these organisms might be *Fusobacteria, Neisseria* and *Prevotallae,* whilst the frequency of *Veillonella dispar* and *Streptococcus parasanguinis* appears to have increased.

Multidimensional scaling relies on mapping the scaled Euclidian distance between points in variable space to gain insight into clustering and relational information. In this instance, the change in this two dimensional metric after treatment in of interest. Examining figure 4.17 shows that the shape of the overall species cluster has changed significantly after treatment with a narrowing in the y-direction that affects Gram positive organisms. This is likely to be a reflection of the relative selection towards organisms such as *S. parasanguinis* previously noted.

Comparison of k-means clustering of the organisms (figure 4.18) is interesting as parallels can be seen with groups proposed by Socransky for periodontal organisms. The so called 'Red Group' organisms are all seen in group 2, whilst the 'Orange Group' are split between this group and group 1. The 'Yellow Group' organisms are mainly seen in group 5. If the average skew score for malodour as previously described is taken into account, groups 1 and 2 are most associated with malodour.

4.5 Conclusions

The interplay between microbial ecology and physiology and the volatile profile that the community produces is complex and has many factors and influences. The flat plate perfusion system is an effective *in vitro* model for studying the behaviour of tongue-derived biofilms and how they respond to treatments. Further work is required to investigate more deeply the complex interplay between variables that occur in the tongue community. Additionally, these techniques could be applied to the human microbiome at other sites, both within the oral cavity and elsewhere. In the next chapter, the flat plate model will be applied to the study of both potential antimicrobial interventions and another device for analysing volatile profiles.

5. Comparison of a novel antimicrobial compound both *in vitro* and *in vivo*

5.1 Introduction

Most antimicrobial treatments commonly in use for the treatment of oral malodour rely on a combination of agents that target both the production of VSCs by microorganisms and their propensity to enter the gaseous phase once produced. Considering antimicrobial substances, attention quickly focussed on membrane-active cationic compounds such as chlorhexidine, alexidine, cetyl pyridinium chloride and hexetidin (Roberts and Addy, 1981). Of these, chlorhexidine (CHX) has become the most commonly used by the dental profession for treating caries, gingivitis and periodontal disease as well as oral malodour (Jones, 1997). The second method of reducing VSC in breath has focussed on the use of metal salts. Ions of transition metals such as Hg^{2+}, Cd^{2+}, Cu^{2+}, Zn^{2+} and Sn^{2+} all have a high affinity for sulphides, and their binding to VSC precursors prevents the malodourous compounds from being released (Young *et al.,* 2001). Whilst many salts of these metal ions have been tested *in vitro* only salts of copper, tin or zinc are considered safe enough for use clinically. Of these, zinc (II) salts show the best balance of efficiency and safety. When combined with chlorhexidine, zinc salts have an effective synergistic effect on oral malodour and this combination is very successfully used in leading commercial mouthwashes (Thrane *et al.,* 2007).

CMD is the codename given to a novel compound which had previously shown a positive synergistic effect with chlorhexidine against *Staphylococcus aureus.* The purpose of this study was to test the effects of this compound in concert with both chlorhexidine

and zinc acetate against oral biofilms both *in vitro* and *in vivo.* The three compounds were combined in three formulations containing between 0.1 and 0.3% of the active ingredients and compared with two positive and a negative controls as described below.

5.2 Materials and Methods

Five active treatments and a negative control consisting of distilled water were selected. Three of these treatments contained a combination of CMD, chlorhexidine acetate and zinc acetate in varying proportions as outlined in Table 5.1: Products used in the *in vitro* and *in vivo* Investigation of a novel antimicrobial.. Treatment 4 was a commercial mouthwash that also incorporated zinc acetate and chlorhexidine diacetate plus sodium fluoride (proportions shown in table 5.1). Treatment 5 contained only chlorhexidine digluconate as an active ingredient at a concentration of 0.2%.

Selection of volunteers for the study was performed by Dr. Saliha Saad of UWE (CRIB, Oral Malodour group). The sample group was a subset of a larger group of 120 volunteers used in previous studies. The majority demographic was those working or studying at the University, but were of varied gender, age and ethnic background. Preliminary organoleptic investigations were undertaken by judge and instrument. Eligibility and exclusion criteria used to select the final 39 participants are given in figure 2.2. In order to maintain anonymity all volunteer data was coded and randomised before being allocated a treatment. These procedures were scrutinised and approved by the University's Ethics Committee and are covered by UWE NRES Ref: North-West Haydock 15/NW/0316.

Trials were performed by crossover design. Before and between each treatment a one week washout period was performed using a proprietary toothpaste and a standard brush (see Table 5.1). Microbiological analysis was performed on tongue scrape samples before and after treatment as described

in section 2.2. These were taken using a standardised sterile toothbrush from a 1cm^2 area of the tongue dorsum. Samples were inoculated directly into degassed brain heart infusion and vortexed. Relevant dilutions were plated on fastidious anaerobe agar (LabM, Bury, UK) with and without vancomycin (2.5 mgl^{-1}; Sigma-Aldrich, UK) and incubated anaerobically for seven days. Plate counts were performed for strict and facultative anaerobes as well as total viable organisms. A random anonymous portion of one of these tongue scrape samples was used to inoculate the biofilms for the *in vitro* arm of the study. The six biofilms were monitored sequentially by Profile3 SIFT-MS using the PEEK multivalve system set to a switching time of 50 seconds. Monitoring took place over a 48hr period and three repeat pulses of each product were introduced, giving four in total. Please refer to general methods chapter for more detail if required.

5.2.1. *In vivo* sampling of the oral cavity

VOC sampling occurred before treatment, 1 hour afterwards and again at 3 and 6 hrs afterward. Sampling was by trained organoleptic judge, OralChroma and Profile3 SIFT-MS as described in section 2.5. Tongue scrape samples were taken before treatment and at 3 and 6 hrs. Plate counts were performed as for the *in vitro* study.

5.2.2. Trained Organoleptic Judge

Organoleptic scoring by a trained judge was used to assess malodour. The mouth was kept closed for two minutes to allow formation of headspace equilibrium in the oral cavity, then the head was inclined backwards and the mouth opened to allow assessment by judge. Malodour was categorised from 0-5 where 0 = no odour, 1 = barely noticeable, 2 = slight odour, 3 = moderate odour, 4 = strong odour and 5 = very strong odour.

5.2.3. The OralChroma

Samples were collected from the human volunteers as recommended by Abilit corporation. A 2 ml volume of air from the oral cavity was collected by gas syringe (B. Braun Medical Ltd, Sheffield, UK) and injected into the injection port of the gas chromatograph (OralChroma^{TM} AbilitCorporation, Japan). The area under the peaks was used to calculate levels of hydrogen sulphide and combined volatile sulphur compounds (VSC) concentrations from a previously generated calibration curve.

5.2.4. SIFT-MS

The Profile3 instrument was used for sampling set up as described in section 2.6.3. It was necessary to modify the sampling inlet of the SIFT-MS to measure VOC levels in the oral cavity. The rear port of the sampling head was connected to a mini diaphragm pump. The front inlet was adapted to hold a disposable straw that could be introduced into the oral cavity. Air was thus drawn from the oral cavity and this stream was then subsampled by the SIFT-MS. Dynamic calibration was performed by flow rate as recommended.

Table 5.1: Products used in the *in vitro* and *in vivo* Investigation of a novel antimicrobial.

Test Product 1:

Reference label	CMD01
Active compounds	
Chlorhexidine diacetate	0.01%
CMD	0.01%
Zinc acetate	0.07%

Test Product 2:

Reference label	CMD02
Active compounds	
Chlorhexidine diacetate	0.03%
CMD	0.03%
Zinc acetate	0.07%

Test Product 3:

Reference label	CMD03
Active compounds	
Chlorhexidine diacetate	0.03%
CMD	0.03%
Zinc acetate	0.30%

Test Product 4:

Name of product	Positive control A
Reference label	CB12
Name of manufacturer	MEDA OTC AB, Solna, Sweden
Active compounds	
Chlorhexidine diacetate	0.025%
Zinc acetate	0.30%
Sodium flouride	0.05%

Table 5.1 continued

Test Product 5:

Name of product	Positive control B Chlorhexidine digluconate
Reference label	CHX
Name of manufacturer	GSK
Active compounds	
Chlorhexidine digluconate	0.20%

Test Product 6

Name of product	Negative control sterile distilled water
Reference label	Control
Name of manufacturer	N/A
Active compounds	
None	

Toothpaste (for wash-in and wash-out phase)

Name of product	Colgate Cavity protection
Name of manufacturer	Colgate-Palmolive
Active compounds	
Sodium Monofluorophosphate,	(1400 ppm F-)
Sodium fluoride	(450 ppm F-)
Other ingredients (qualitative)	Dicalcium Phosphate Dihydrate, Aqua, Glycerin, Sodium Lauryl Sulphate, Cellulose Gum, Aroma, Sodium monofluorophosphate, Tetrasodium Pyrophosphate, Sodium Saccharin, Sodium Fluoride, Calcium Glycerophosphate, Limonene.

5.3 Results

5.3.1. *In vitro* study

Treatments occurred at 1hr, 8hrs, 24hrs and 32hrs. The levels of hydrogen sulphide produced during this period can be seen in Figure 5.1

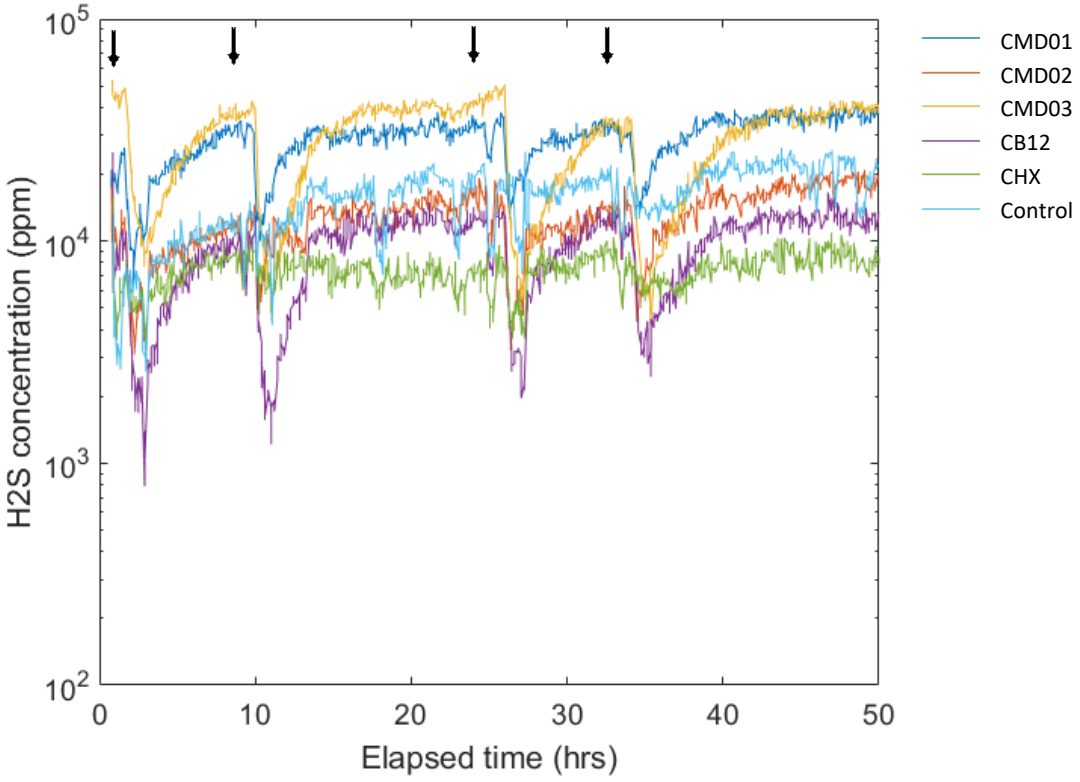

Figure 5.1: Hydrogen sulphide levels produced by biofilms during repeated challenge with various test formulations and negative water control as described in Table 5.1. Arrows indicate the time points at which treatments occurred.

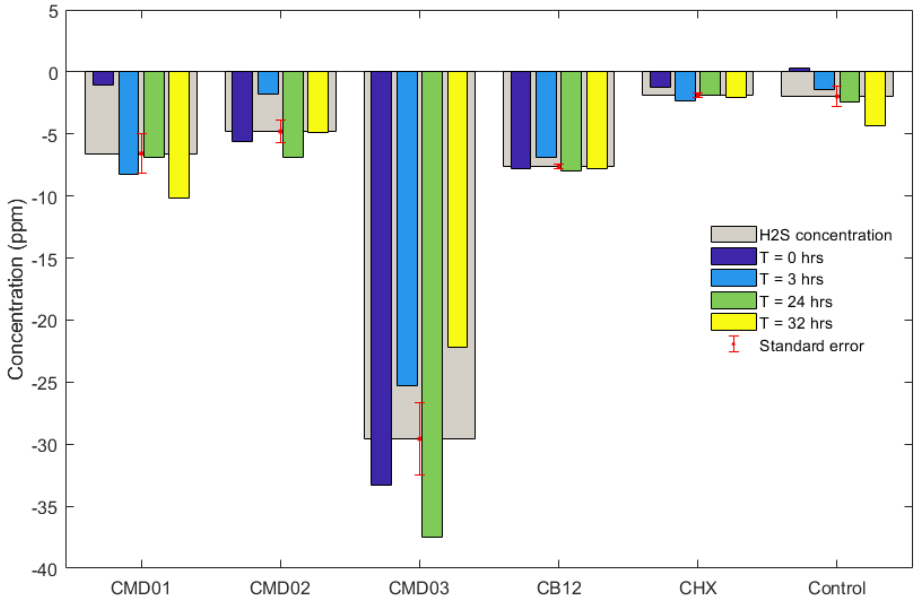

Figure 5.2: Reduction in H2S levels for each product at each time point. Mean concentration drop of n=4 timepoints is shown by grey bar.

The difference in hydrogen sulphide levels before and after each treatment (i.e. the reduction in concentration due to the inhibitory activity of the treatments) was plotted as a bar chart in figure 5.2. Also, each curve was normalised to a common baseline and the area under the curve for each product calculated. This is a useful metric, as described in section 3, as it gives a result in which the initial drop and the length of effect are both taken into account. This is shown in figure 5.3, with smaller bars thus indicating smaller area under the curve and therefore greater effect. Similar bar charts were produced for total VSC (hydrogen sulphide, methyl mercaptan and dimethyl-disulphide) and total VOC (total VSC plus indole, skatole, propanoic acid, butyric acid, trimethylamine, putresceine and cadaverine).

Order of effectiveness is CMD03>>CB12>>CMD02>>CMD01>>CHX>>Control.

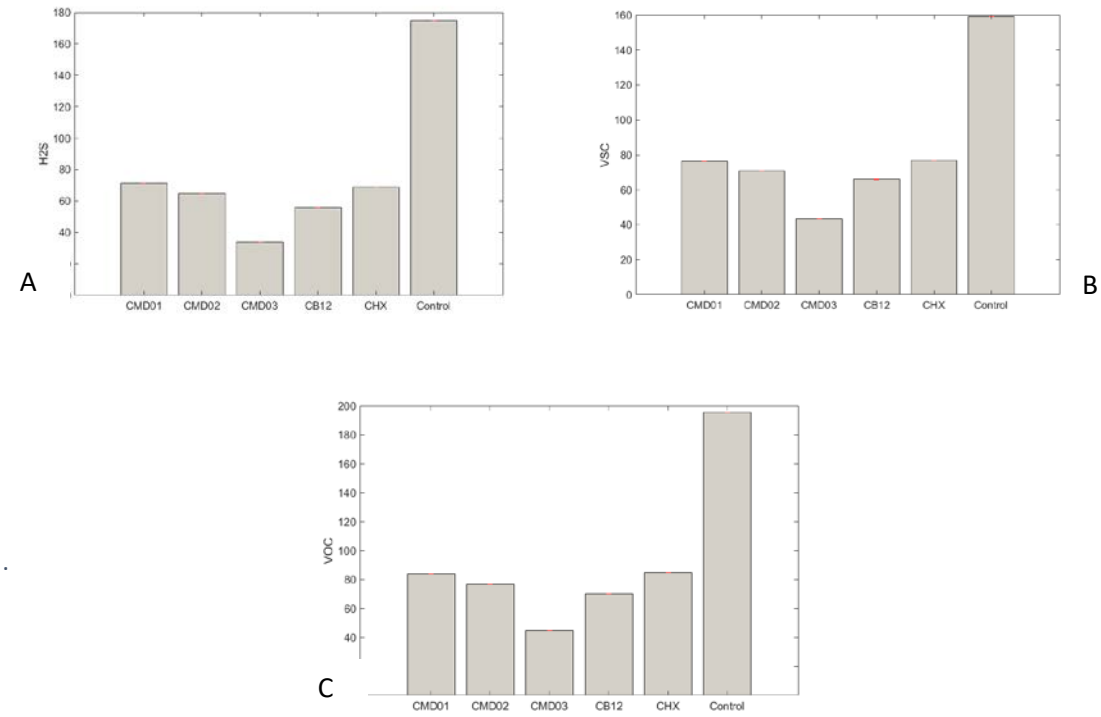

Figure 5.3: Bar charts showing the effect of the six formulations on (A) hydrogen sulphide (B) VSCs and (C) VOCs, as measured by area under the SIFT-MS trace over 48hrs

Plate counts were performed on 1ml of eluate from the biofilm before and after each treatment. The area under the curve method for can be used here also, and this is shown in figure 5.4. Again, smaller bars show a greater effect on numbers of organisms (both facultative and strict anaerobes). The order of effectiveness is CHX>>CMD03>>CB12>>CMD01>>CMD02>>Control for facultative anaerobes and CHX>>CMD02>>CB12>>Control>>CMD01>>CMD03 for strict anaerobes.

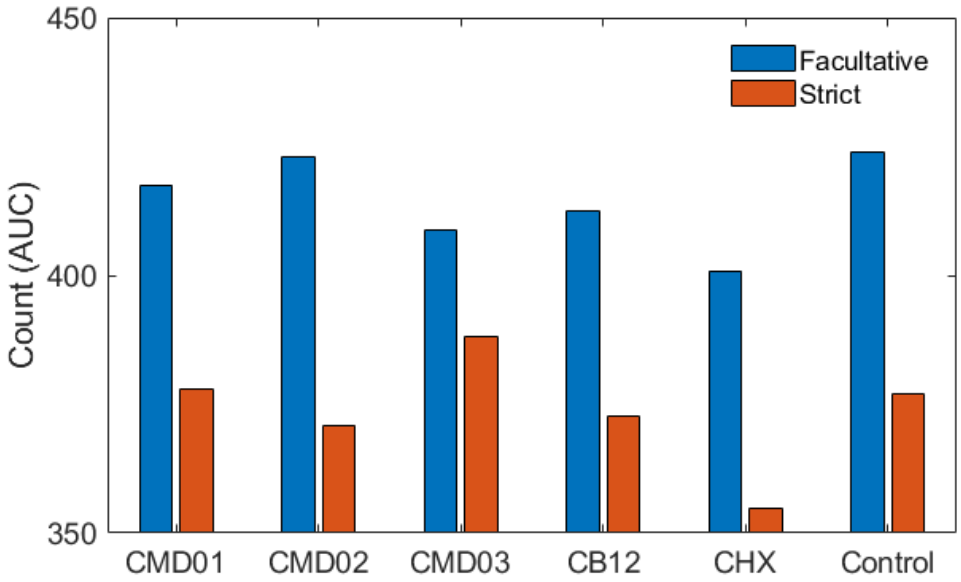

Figure 5.4: Microbiology results showing effect of the six formulations on facultative and strict anaerobes on eluate from the biofilms

5.3.2. *In vivo* study

All of the treatments showed a greater effect than the distilled water control, with an initial reduction in malodour levels followed by a recovery rate following the treatment period. The results for organoleptic score can be seen in figure 5.5. As with the *in vitro* study, this data can be better represented using bar charts of the area under each curve. More effective treatments therefore show smaller bars. This can be seen for the organoleptic data shown, and the other measurements by instruments, in figures 5.6-5.11. Direct comparison of the effects of the treatment between the *in vivo* and *in vitro* arms can be seen in figures 5.1 and 5.4. The area under the curve graphs further allow comaprison of the full cumalitive effect of the treatments in each arm of the trial.

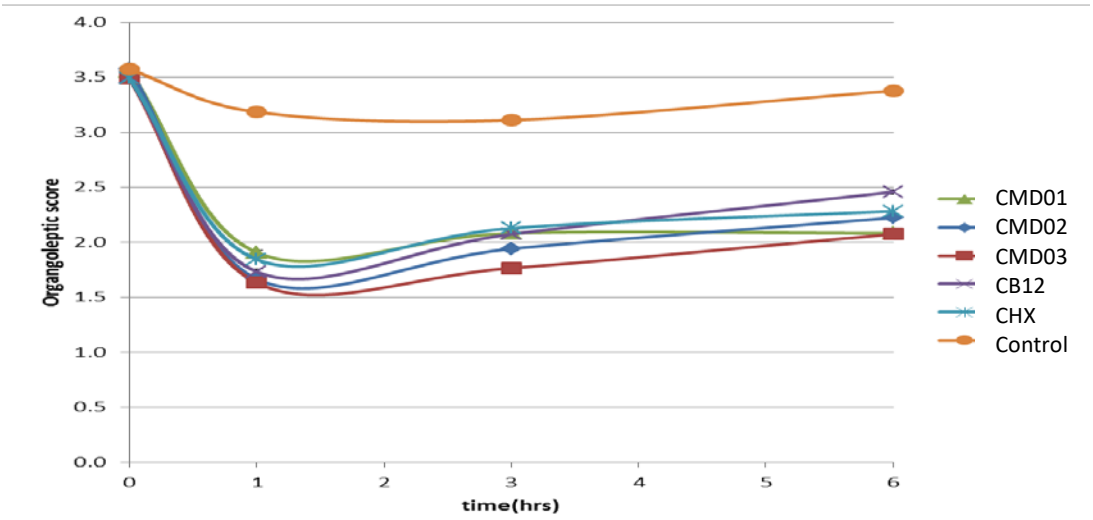

Figure 5.5: Effect on organoleptic score over time for the six formulations.

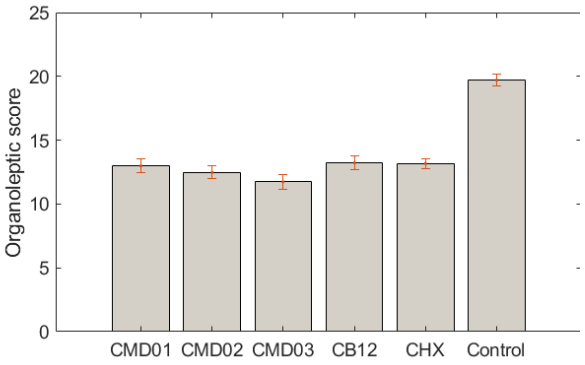

Figure 5.6: Effect of six formulations on organoleptic score. Area under the curve is shown as a histogram with smaller bars representing larger effect.

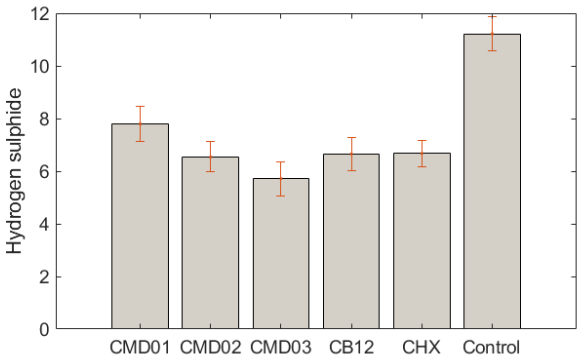

Figure 5.7: Effect of six formulations on OralChroma H_2S. Area under the curve is shown as a histogram with smaller bars representing larger effect.

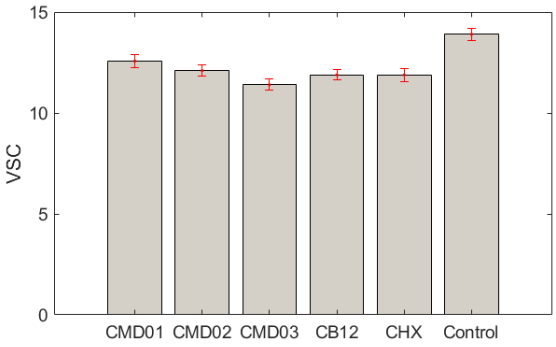

Figure 5.8: Effect of six formulations on OralChroma VSC. Area under the curve is shown as a histogram with smaller bars representing larger effect.

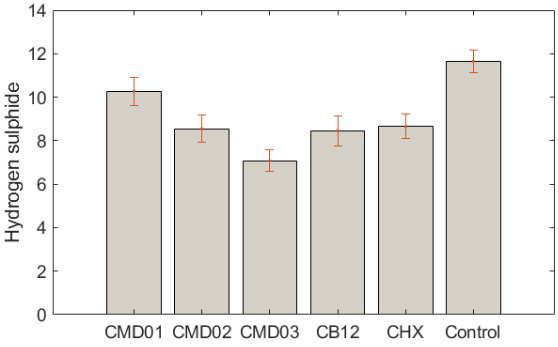

Figure 5.9: Effect of six formulations on H_2S by SIFT-MS. Area under the curve is shown as a histogram with smaller bars representing larger effect.

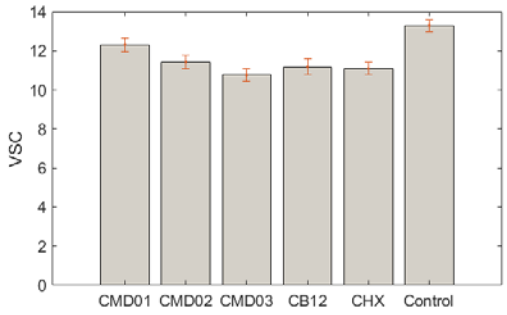

Figure 5.10: Effect of six formulations on VSCs by SIFT-MS. Area under the curve is shown as a histogram with smaller bars representing larger effect.

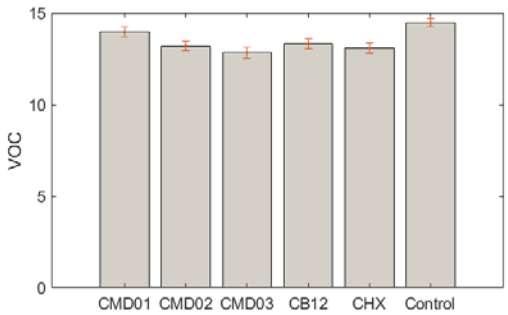

Figure 5.11: Effect of six formulations on VOCs by SIFT-MS. Area under the curve is shown as a histogram with smaller bars representing larger effect.

As with the *in vitro* trial, microbiology for total viable count and strict and facultative anaerobes were performed. Area under the curve bar charts can be seen below. In this case order of effectiveness is CHX>>CMD02>>CMD01>>CB12>>CMD03>>Control for both categories of anaerobes.

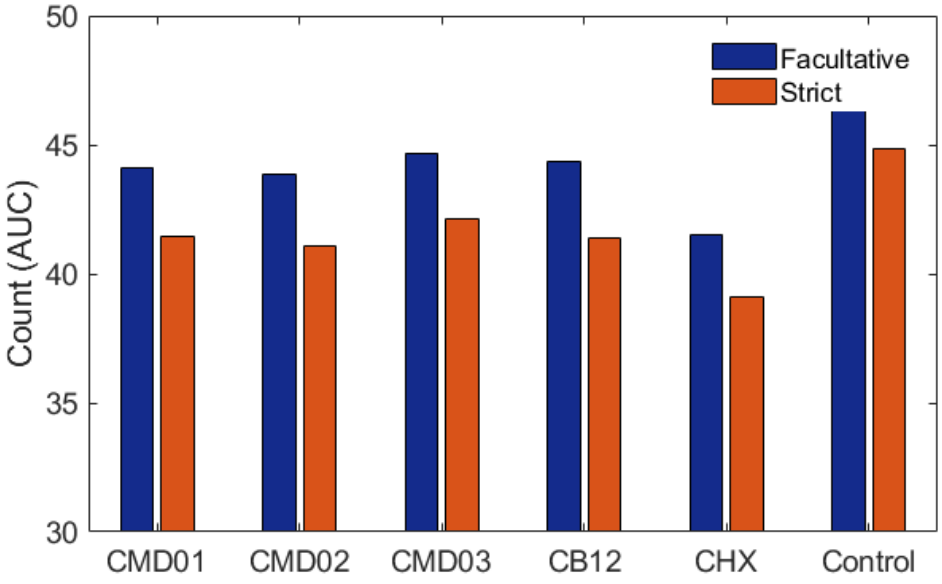

Figure 5.12: Microbiology of *in vivo* data. Smaller bars indicate greater effect on microbiological counts.

Statistical comparison of the data shows that all treatments show significantly more effect than the control at the $P < 0.05$ level for organoleptic score and levels of volatiles measured by OralChroma and SIFT-MS. CMD01 showed less effect than the other active treatments by SIFT-MS. All of the compounds also showed significantly more effect on all microbial counts than the control ($P < 0.05$). Chlorhexidine alone was the only compound that outperformed the others in reducing microbial load at the same significance level. Very similar results were seen in the study of biofilm hydrogen sulphide production, with all products showing significantly more effect that water. However in the *in vitro* study, CMD03 showed significantly more reduction of VOC than the other active compounds ($P<0.05$).

Table 5.2: Results summary and comparison (all data is area under curve)

	in vitro				***in vivo***			
	H_2S	**TVC**	**Facultative**	**Strict**	**H_2S**	**TVC**	**Facultative**	**Strict**
CMD01	4.0	424.4	417.5	378.0	10.3	45.0	44.1	41.5
CMD02	3.6	426.4	423.1	371.0	8.5	44.7	43.8	41.1
CMD03	1.8	424.9	408.7	388.1	7.1	45.6	44.7	42.1
CB12	3.1	418.1	412.6	372.7	8.5	45.2	44.4	41.4
CHX	3.9	405.5	400.9	354.7	8.7	42.5	41.5	39.1
Control	11.9	428.2	423.9	377.1	11.7	48.2	47.2	44.9

5.4 Discussion

Chlorhexidine ((1,6-di(4-chlorophenyl-diguanido)hexane) is a membrane-active cationic bisbiguanide antimicrobial agent. It has a wide spectrum of activity which is efficacious against Gram-positive and Gram-negative bacteria as well as some yeasts, dermatophytes and lipophilic viruses (Denton, 1991). Structurally it contains ten nitrogen atoms separated by a hexamethylene bridge and it is the positive charge distributed over these atoms which gives it affinity for negatively charged surfaces. This bicationic nature gives it the ability to bind to bacterial cell walls (Davies, 1973) and surfaces in the oral cavity (Rølla *et al.,* 1971), potentially simultaneously. It has a bacteriostatic effect in low concentrations but becomes bacteriocidal as concentrations rise. It affects non-multiplying cells and persists in the oral cavity for considerable time (Jenkins *et al.,* 1988). These antimicrobial effects are due to binding to the cytoplasmic membrane leading first to increased permeability and then precipitation of cytoplasmic components. These effects do not show an increase in ATPase inhibition suggesting only a direct effect on the membrane (Kuyyakanond and Quesnel, 1992). It is for these reasons that chlorhexidine is still considered the gold standard oral antimicrobial (Jones, 1997).

CMD is a novel compound which has shown broad spectrum activity and has been effective against methicillin sensitive and resistant *Staph. aureus.* It is also anionic lipophilic and membrane-active, appearing to act on the phosphatidylglycerol containing fraction of the cytoplasmic membrane.

When compared with chlorhexidine it shows similar but differing effects on natural and model membranes of *Staph. aureus.* Zinc salts however operate by providing ions that form sulphides of low solubility with precursors of VSC such as HS^-, $S2^-$ and CH_3S^-. It has also been suggested that zinc may directly inhibit cysteine desulphydrase or other sulphur metabolising enzymes (Greenman 1999).

Examination of the results of both the *in vitro* and *in vivo* arms of the current study shows the effects of the combination of these three compounds in combination in three formulations. The compound most effective at combating malodour, as measured by the smallest area under curve for VSC both *in vitro* and *in vivo* was test product 3, CMD03. It outperformed the industry leading oral malodour formulation even though it contained similar levels of chlorhexidine and zinc, and no sodium fluoride. It is interesting that this novel compound shows activity in these circumstances since *in vitro* models with their greater bacterial loads, larger volume of EPS and higher VSC production would tend to be less sensitive to the effects of membrane active compounds (Hope and Wilson 2004). This appears to support the view suggested by Hubbard *et al.,* (2017) that chlorhexidine and CMD act in synergy by affecting different parts of the cytoplasmic membrane. However, it is interesting that CMD02, with a lower concentration of zinc, did not perform as well even though it contained the same amounts of CMD and chlorhexidine. This suggests that increased permeability of the membrane allows zinc ions better access to VSC precursors or enzymes before they can produce volatile malodour compounds. The finding that only the high concentration chlorhexidine formulation

acted with significant and lasting antimicrobial effect, as shown by the microbiology results, is not surprising. Concentrations in this range are known to be the most effective bacteriocides (Cumming and Loe, 1973). However, the side effects of chlorhexidine at this concentration, such as staining of dental enamel, prevent formulations such as this from being used on a regular basis as prophylaxis against malodour (Flötra *et al.,* 1971).

5.5 Conclusions

Comparison of *in vitro* and *in vivo* showed that for hydrogen sulphide levels as measured by SIFT-MS the order of effectiveness of the formulations was identical. This was, in order of decreasing efficacy; CMD03>>CB12>>CMD02>>CHX>>CMD01>>Water. CMD03 showed the greatest effect on volatiles by all measurement methods. In terms of antimicrobial effects, the results were more mixed, with the highest concentration of chlorhexidine showing the highest bacteriocidal effect. The difference in formulation of nutrients in the two systems meant that the *in vitro* model produced much higher transformation rates of VSC and VOC. Despite this, the effectiveness of the synergy between the inhibitory compounds against the oral biofilm was still readily apparent.

CMD shows high potential as a broad spectrum antimicrobial agent against complex multispecies biofilms both *in vitro* and *in vivo.* There are also indications that it may improve the ability of zinc compounds to remove VSC precursors from the malodour generation pathway.

Further work is needed to investigate this, and to examine the effects of these combinations of treatments on specific groups of organisms in the biofilm, for example by use of 16s rRNA analysis (Dewhirst et al., 2010). If the proportion of all oral organisms were profiled before and after various combinations of treatments, it would be possible to assess the effect of each component on different organisms within the oral microbiome. By further examination of key organisms, accompanied by membrane modelling experiments, the mode of action of these compounds could be further elucidated. Parallel experiments with metal salts such as zinc acetate may provide further information on direct effects of clinical formulations on volatile production in the oral cavity.

6 The effect of D-amino acids on the tongue biofilm *in vitro*.

6.1 D-amino acids as potential biofilm dispersal agents

It is now commonly agreed that the most likely reason for homochirality in nature is that circularly polarised infrared light in the early universe preferentially degraded one chiral form (Bonner 1991; Bailey *et al.,* 1998). In the majority of the animal kingdom, therefore, amino acids are utilised in their left-handed or L-enantiomeric form, with a few exceptions in the form of opioid peptides (Broccardo *et al.,* 1981), neurotransmitters (Santos *et al.,* 1995) and neurotoxins (Jimenéz *et al.,* 1996). The situation is different with prokaryotic organisms, the majority of which utilise the D, or right handed forms in their cell walls (Weidel *et al.,* 1960; Osborn 1969). The periplasmic space in Gram negative organisms and the extra-cytoplasmic space in Gram positives is maintained by peptidoglycan (PG) layers in which the glycan strands are separated by short peptides that incorporate D-amino acids (Vollmer *et al.,* 2008). These non-canonical d-amino acids (NCDAA) are generally produced by the action of racemases. Whilst D-Ala and D-Glu are the most common, D-methionine (Met), D-valine (Val), D-tyrosine (Tyr), D-threonine (Thr), D-tryptophan (Trp), D-phenylalanine (Phe), D-leucine (Leu) and D-Isoleucine (Ile) have all been found in bacterial structures (Lam *et al.,* 2009). In 2010, Kolodkin-Gal *et al.,* published a high profile paper describing disassembly of *Bacillus subtilis* biofilms exposed to a combination of D-Leu, D-Met, D-Tyr, and D-Trp. They further showed prevention of biofilm formation in *Staph. aureus* and *Ps. aeruginosa* by D-amino acids. Hochbaum *et al.,* (2011) went on to show the enantiomers did not prevent initial binding, but seemed to block the development of larger assemblies of cells by interfering

with the protein component of the matrix. It has been further shown that D-amino acids incorporated into polyurethane scaffolds can reduce biofilm formation *in vitro* in contaminated femoral defects (Sanchez *et al.,* 2013). Work with wastewater biofilms found that D-tyrosine in particular interfered with biofilm formation and that D-Tyr impregnated membranes resisted biofilm formation. This was also shown to be due to inhibition of cellular communication and EPS production (Xu and Liu 2011a, 2011b).

Many foodstuffs we consume contain D forms of amino acids that are created by alkali and heat treatments in food processing (Friedman 1999). This racemisation can reduce the nutritional value by impairing digestion, but actual toxicity appears low. Only D-serine, D-cysteine and D-proline have shown renal toxicity in mice, and this was when relatively high concentrations were administered (Kaltenbach *et al.,* 1979; Carone *et al.,* 1985; Friedman and Gumbmann 1988; Kampel *et al.,* 1990). Furthermore, human saliva has been seen to contain relatively high concentrations of D-amino acids naturally (Nagata *et al.,* 2006) suggesting their potential safe use in a mouthwash formulation.

The aims of this chapter were to investigate the effects of D-amino acids on multispecies oral biofilms but comparing the development of biofilms exposed to them during maturation with control biofilms exposed to the L-forms or standard media.

6.2 Materials and methods

Tongue scrape samples were obtained from a single subject with ethical approval as previously described (section 2.4). After anaerobic pre-incubation these were transferred to biofilm enclosures. Biofilms were fed either standard media or media containing amino acids

in either the D or L form at a concentration of 10mM (Sigma-Aldrich, UK). All media was equalised to pH 7.4.

Analysis of the VOC profile of the biofilms was by Profile3 SIFT-MS (section 2.3). A value of total VOCs created from the measured levels of hydrogen sulphide, methyl mercaptan, dimethyl disulphide, indole, skatole, cadaverine, putrecine, trimethylamine, propanoic acid, butyric acid and hexanoic acid.

EPS extraction was based on the preferred method of Liu and Fang (2002) following their comparative work on extraction from sludges and is outlined in section 2.4.

Following extraction, EPS solutions were assayed for polysaccharides and proteins by the DuBois (DuBois *et al.,* 1956) and modified Lowry (Redmile-Gordon *et al.,* 2013) methods. To gauge further differences in EPS polysaccharide composition the extracts were assayed with Congo Red and absorbance was measured at 540/620nm (Fluostar spectrophotometer). β-glucan from barley was used to generate a calibration curve.

Total viable counts along with counts for strict and facultative anaerobes were performed as described in section 2.1. Colonies were distinguished by morphology and Gram strain to gauge shifts in population. Dry weights were calculated by filtering portions of suspension onto accurately pre-dried and weighed filter paper. These were then dried again in an oven for 2hrs at 110°C and reweighed.

Confocal Laser Scanning Microscopy was performed on portions of biofilm by the method outlined in section 2.5. A number of stains were used with varying degrees of success. The best images were obtained using Horsch 33258 stain for intracellular DNA, SYPRO^{TM} Orange for proteins and Congo Red for polysaccharides and amyloids fibres. See section 6.7 and 6.8 for further details.

6.3 Results

In a preliminary experiment undertaken as a part of this thesis, biofilms were grown in the presence of five D-amino acids (D-Glu, D-Asp, D-Met, D-Cys, and D-Trp) compared to those grown in standard media. Stark differences were observed (Figure 6.1).

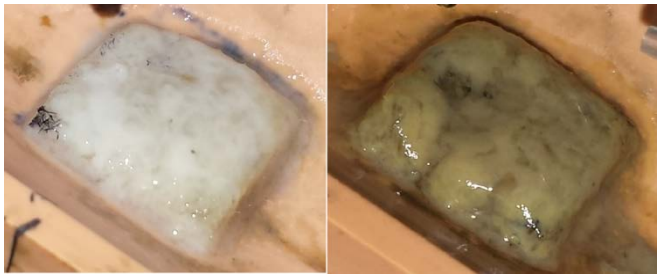

Figure 6.1: Oral biofilms grown (A) in the presence of D-amino acids and (B) with standard media. Microbiological cell counts were not significantly different in each case.

The next experiments with single D-amino acids showed no visible effect compared to controls. The simplest combination of D-amino acids seen to have an effect was a combination of D-Glu and D-Asp, and all further experiments tested the effects of this combination.

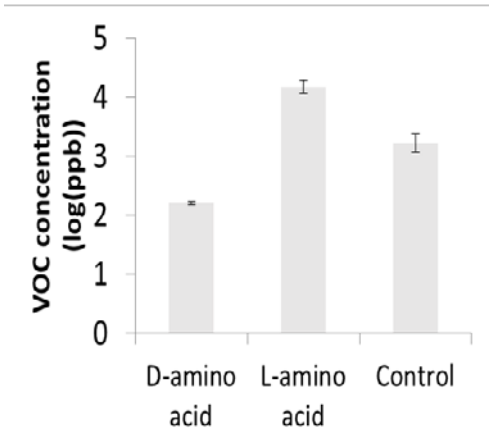

Figure 6.2: Volatile profile of combined VOCs produced by n=18 biofilms exposed to D-Asp and D-Glu, L-Asp and L-Glu and standard media. Error bars represent standard error.

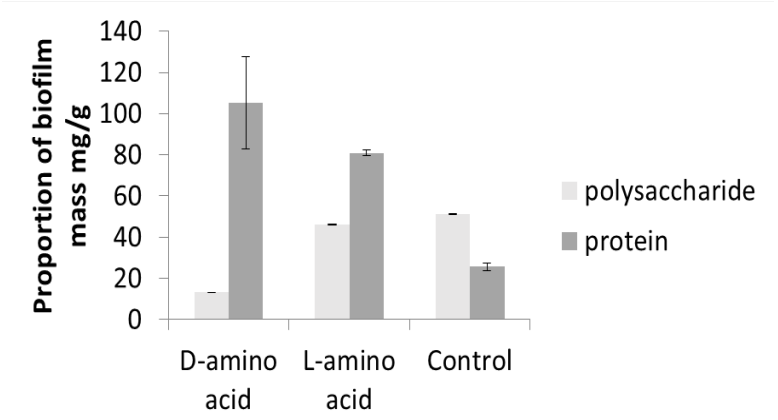

Figure 6.3: Proportion of proteins and polysaccharides in EPS extract from n=18 biofilms exposed to D and L forms of Glu and Asp amino acids, plus standard media. Error bars represent standard error.

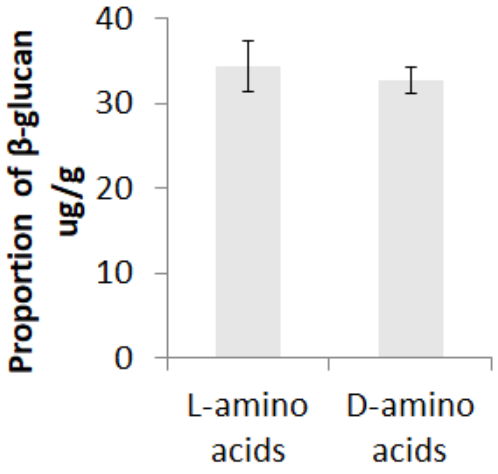

Figure 6.4: Congo red assay for β-glucan polysaccharides in EPS of amino acids exposed biofilms. (n=12). Error bars represent standard error.

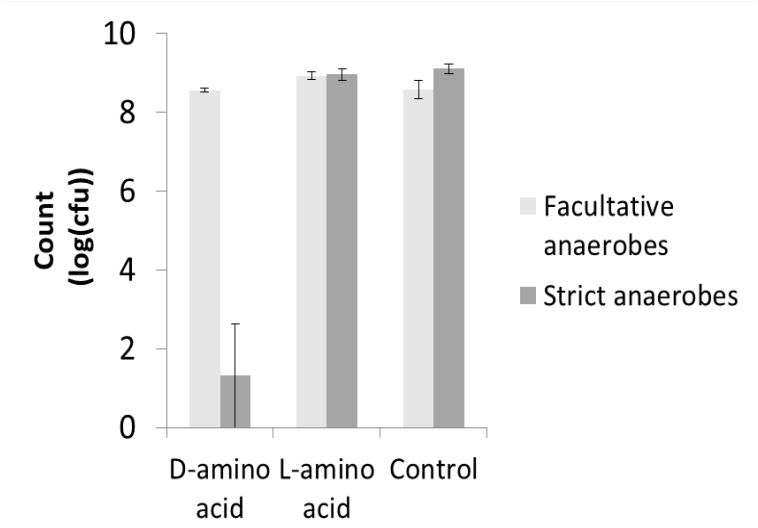

Figure 6.5: Proportion of facultative and strict anaerobes in D and L amino acid exposed biofilms compared with controls fed standard media. (n=14). Error bars represent standard error.

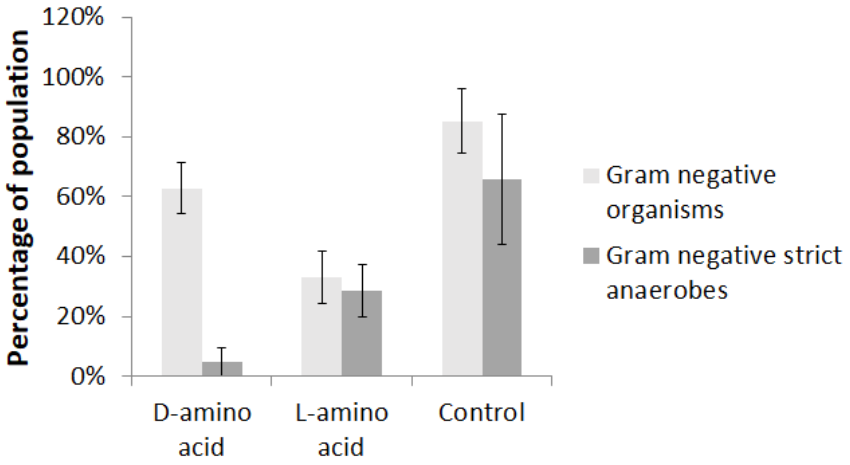

Figure 6.6: Proportion of Gram negative organisms in D and L amino acid exposed biofilms compared with controls. (n=14). Error bars represent standard error.

One way ANOVA with Bonferroni's Multiple Comparison Test shows that the D-amino acid exposed biofilms show significant differences ($p < 0.01$) from L-amino acid exposed biofilms for VOC, EPS polysaccharides, and strict anaerobes, and significant differences from control biofilms for VOC, EPS polysaccharides, EPS proteins and strict anaerobes.

CLSM images of biofilms treated with D-amino acids and control are shown in figure 6.7 and 6.8.

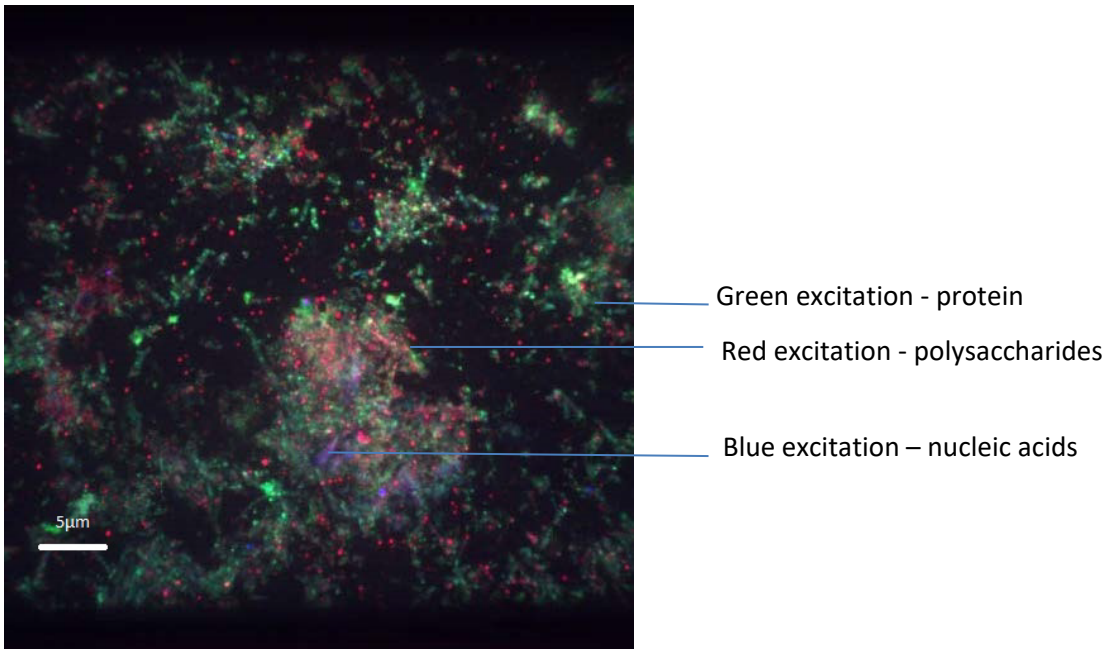

Figure 6.7: CLSM images of a D-amino acid exposed biofilm showing diffuse distribution of proteins and polysaccharides

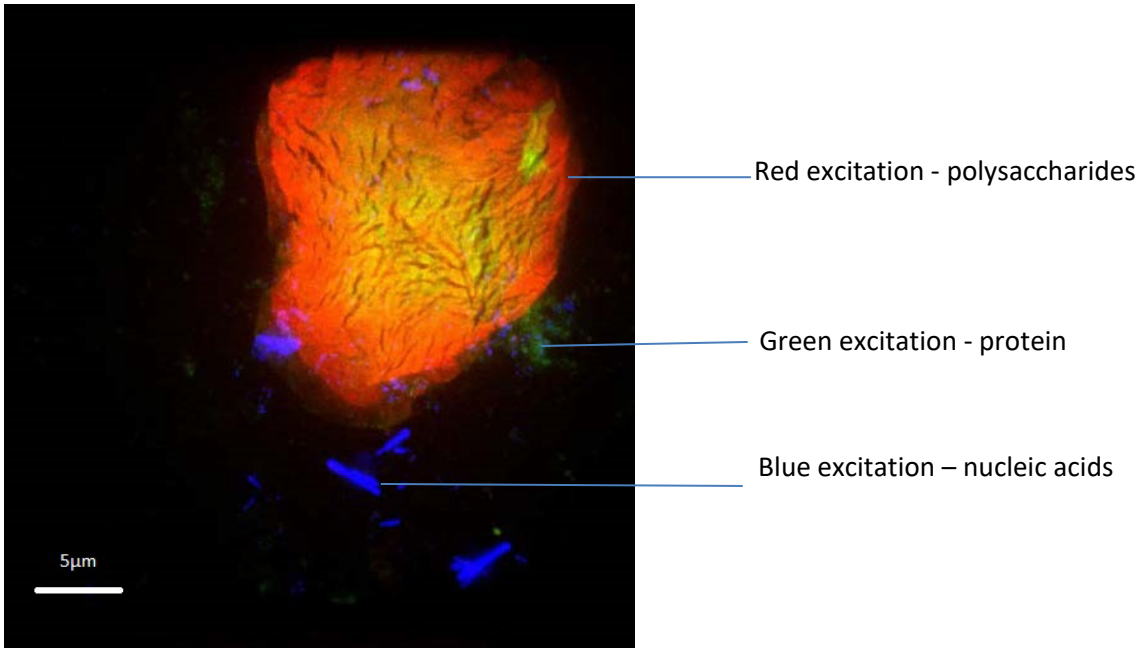

Figure 6.8: CLSM image of a control biofilm showing structured area that appears to be made up of proteins and polysaccharides

6.4 Discussion

For as long as it has been known that D-amino acids exist in the PG layer of the bacterial cell wall, it has also been known that prokaryotes also incorporate them into antimicrobial substances that they produce (Bodanszky and Perlman 1969). In some cases the D-amino acid moiety itself appears to be directly involved in binding to cell wall PG and subsequent lysis (Lark *et al.,* 1963; Tsuruoka *et al.*,1985). More recent work has indicated that some bacteria may release D-amino acids in the stationary phase, and this causes morphological changes in the cell wall via the PG layer (Lam *et al.,* 2009). It has been shown that in several organisms D-amino acids can be incorporated into the PG layer with both positive and negative consequences. This incorporation is independent of whether the amino acids are exogeneously or endogeneously produced (Cava, *et al.,* 2011). It is the studies specifically on biofilm formation that are of interest here, of which there are unfortunately few. Kolodkin-Gal *et al.,* (2010) used radioactive labelling to show that D-tyrosine was incorporated into the cell wall, and that the presence of D-alanine prevented this. They proposed that incorporation of NCDAAs into the cell wall interferes with the anchoring of TasA amyloid fibres thus disrupting the extracellular matrix. An earlier study by Tsuruoka *et al.,* (1984) suggested that the binding of D-Met and D-Cys inhibited lipoprotein binding to PG in *E. coli.* Cava and Lam (2011) have gone on to suggest that in mixed biofilms NDAAs my act as a paracrine signal which controls the architecture of the community. Nevertheless, this is merely conjecture since there have been no studies performed on mixed species biofilms.

This work shows significant differences in mixed oral biofilms grown in a flat plate perfusion model when exposed to D-amino acids as opposed to the L forms or standard media. The effects affect Gram negative organisms more than positives, and strict anaerobes

more than facultatives. L-amino acid exposed biofilms produce higher levels of volatile compounds compared to controls, and this might be expected due to them having an extra source of carbon energy. The D-amino acid exposed biofilms however show much lower production of VOCs compared to controls. It is known that many gram negative strict anaerobes are associated with malodour (see section 1.2) and the VOC results combined with the microbiology results would seem to indicate that gram negative strict anaerobes are affected more by the D-amino acids and that this in turn leads to lower production of VOCs. CLSM images of biofilms treated with D-amino acids and control are shown in 6.7 and 6.8. The staining procedure shows the distribution of red-orange staining polysaccharide, which were commonly observed in control biofilms, but much less so in biofilms treated exposed to D-amino acids. The distribution of stained protein (shown as green colour) is also different; the control does not take up as much green stain, suggesting that proteins are cryptic by being covered or fully bound to EPS. However, in the biofilm treated by D-amino acids, the cell-wall proteins are much more exposed to staining. The nucleic acid (blue) staining is again different, showing entire bacterial cells in the control biofilm, but a "background smear" of stained but fuzzy material distributed more evenly across the film. The change in EPS which is visible both macro- and microscopically is also evident in the analysis of the extracts. The D-amino acid exposed biofilms have proportionally lower levels of polysaccharides but much higher levels of proteins by mass (figure 6.3). This may not be supportive of the hypothesis that it is the anchoring of lipo- and glyco-proteins to the PG membrane that is most affected by the D-amino acids. Morphological changes in the cell wall seen in previous studies usually occur during the stationary phase (Kolodkin-Gal *et al.,* 2010), indicating that D-amino acids should have an effect on mature biofilms as well as ones in the growth phase, although so far this has not been shown in this model. Also, whilst D-Glu is present in the PG layer, D-Asp has not been previously reported as interfering with membrane synthesis, and has not been shown to affect biofilm formation when present in extracellular supernatant (Lam et al.,

2009). It is interesting to hypothesise as to alternative modes by which the biofilm is being affected.

NCCDAs may be acting on multispecies biofilms either directly, through mechanisms such as incorporation or disruption of cellular membranes, or indirectly by affecting EPS production by all bacterial cells. Any effects could apply to individual species, groups of species or the biofilm as a whole. The complex interplay between species in such a microbial ecosystem means that teasing apart cause and effect is very challenging. It can be hard to assess whether an overall effect on EPS favours certain strains, or the absence of strains due to an effect on another system or structure. An alternative theory to PG involvement is that a combination of D-Asp and D-Glu in particular interfere with the C-di-GMP based mediation of the EPS matrix. Aspartic and glutamic acids are notably present in the GDDEF domains of diguanine cyclase, and it has been shown that it is these residues that bind to the N1 and N2 molecules of the Watson-Crick edge of C-di-GMP (Chou and Galperin 2016). Whilst the PG hypothesis for NCCDA effects on biofilms is strong, this alternative is attractive as downregulation of C-di-GMP is known to affect biofilms in the ways observed within this study (see section 1.1.5). C-di-GMP levels in biofilms in response to D-amino acids, or indeed other interventions, have not been extensively studied, and in the case of mixed species biofilms not at all.

Quantifying intracellular levels of C-di-GMP is problematic. The gold standard method is HPLS-MS/MS (Spangler *et al.,* 2010), but apart from cost and complexity of this method, bacterial cells must be lysed to release the compound for assay. Thiazole orange has been used to assay C-di-GMP fluorescently (Nakayama *et al.,* 2011) but so far this also relies on lysed cells. However, given that thiazole orange is frequently used in CLSM then staining of viable cells may be possible. This could potentially give a powerful technique to probe the C-di-GMP signalling network. Another method of interest involves the use of a fluorescent

reporter strain of *Ps. aeruginosa* engineered in Denmark (Rybtke *et al.,* 2012). The advantage of this would be real time quantification of C-di-GMP levels by fluorescence measurement. Unfortunately, the major limitation is that only single species biofilms of *Ps. aeruginosa* can be studied.

6.5 Conclusions

It has been shown by this work that complex mixed species oral biofilms are significantly affected by D-amino acids in the growth phase. The mechanisms are unclear but affect both the microbiology of the biofilm and the production and composition of the EPS. This coupled with their demonstrated low toxicity in both humans and animal models suggests that further work in the development of a D-amino acid containing mouthwash formulation may be fruitful.

7 Assessment of a novel SPR based biosensor for the quantitative detection of oral malodour

7.1 Introduction

Surface Plasmon Resonance (SPR) has been used to investigate the properties and binding of thin biological films to surfaces for nearly forty years. Surface plasmons are coherent oscillations of electrons at the barrier between two materials of different relative permittivity, first theorised by R.H. Richie in 1957. In the case of thin depositions of metals such as gold or silver on a glass prism, photons travelling through the prism and striking the inside metal layer cause resonance of the plasmons via the evanescent wave. This resonance condition is given by equation 1, where n_c and n_s are the refractive indices of the prism and sensing layer respectively, θ is the incident angle and ε_{mr} is the real part of the metal dielectric constant (Dwivedi *et al.,* 2008).

$$K_0 n_c \sin\theta = K_0 \left(\frac{\varepsilon_{mr} n_s^2}{\varepsilon_{mr} + n_s^2}\right)^{\frac{1}{2}}; K_0 = \frac{2\pi}{\lambda}$$

Equation 7.1: SPR resonance condition

If the permittivity of the layer changes due to, for example, binding of additional molecules from within the fluid layer, then changes in the resonant condition cause changes in the reflectivity at a given angle (figure 7.1). This was first described by Beaglehole in March

of 1970 (Beaglehole, 1970) and further developed practically by Kretschmann, (1971). Liedberg and Nylander(1983) were the first to demonstrate that SPR could be used to investigate the binding of biological materials in a liquid medium to the metal surface above the prism. Their work with Pharmacia and later Pharmacia Biosensor led to the development of the BIAcore and BIAlite in 1990 and 1994. These devices used the SPR technique to facilitate real time analysis of binding interactions (Jönsson *et al*., 1991; Liedberg *et al*., 1995). Resulting kinetic association and disassociation curves can be used to calculate binding constants and other thermodynamic parameters. Miniaturisation of prism based SPR techniques was further accomplished by groups such as Foster *et al.* (1994) and Cahill *et al.* (1997). Pharmacia continued to develop the technique and became Biacore AB Corporation in 1996, releasing increasingly advanced SPR based devices into the next decade. SPR biosensors have since been used in food analysis, immunogenicity, proteomics and drug discovery (Karlsson 2004).

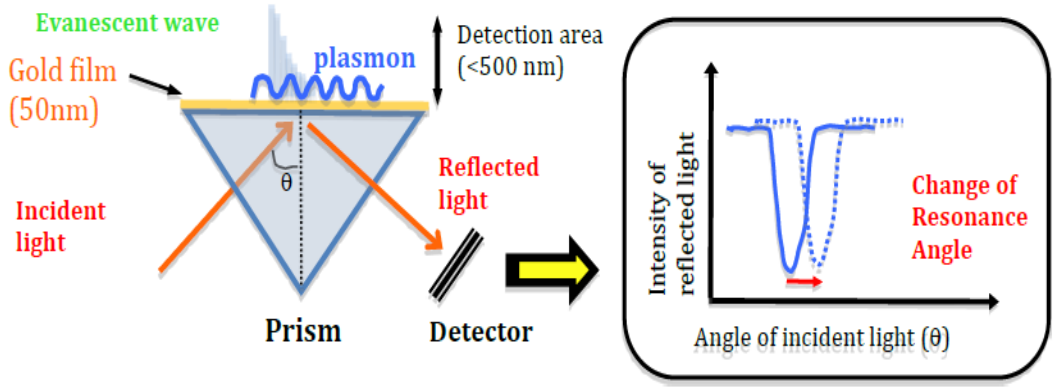

Figure 7.1: The principle of surface plasmon resonance.

Aryballe Technologies were founded in 2014 and are developing a SPR based biosensor to detect and quantify volatile compounds in gaseous phase from a variety of sources. Gaseous volatiles interact with both surface bound biologically active molecules and

the metallic surface itself. This causes a measureable change in the reflectance of incident LED light.

It was the purpose of this study to evaluate the potential application of the instrument (the NeOse) to the assessment of oral malodour. In order to assess the ability of the instrument to detect and quantify oral malodour it was compared to both a trained organoleptic judge and gas analysis by SIFT-MS.

7.2 Materials and Methods

7.2.1 In vitro study

Tongue scrape samples were obtained from two individuals with high and low organoleptic score. Two biofilms were inoculated with each sample as described in section 2.1. Sequential sampling was performed as described in section 3.2.

7.2.2 In vivo study

7.2.2.1 Selection of participants

Participants in the study were selected from a group of volunteers from the University of the West of England. They were of good oral hygiene and dental health and possessed a minimum of 20 original adult teeth. Exclusion criteria were; smoking; medical history of infectious diseases; active severe caries, gingivitis or periodontitis; antibiotic medication within one month prior to attendance; consumption of sweets or other products known to contain antimicrobial substances; history of diabetes mellitus, bronchitis, tonsillitis, sinusitis or any other conditions known to affect oral malodour. Subjects were instructed to perform their usual oral hygiene routine until the evening before sampling, but abstain on the day of

attendance. They were also instructed not to consume odorous foodstuffs such as garlic, spices or alcohol on the day before sampling, and any food on the attendance day. Subjects were permitted to drink water whenever desired when not in the laboratory.

7.2.2.2 Sampling of the oral cavity

Subjects were assessed and scored for oral malodour by organoleptic judge and Voice200 SIFT-MS as described previously in sections 1.5.1 and 1.5.4 respectively. Additionally, they were assessed using the NeOse instrument. As with the other methods, the mouth was kept closed for two minutes to allow headspace equilibrium to be reached. The inlet of the NeOse was modified to enable a disposable straw to be inserted into the oral cavity of the subject (figure 7.2). The instrument was set to take 10 seconds of background followed by 30 seconds of static signal measurement. After the first ten seconds the subject placed the straw in their mouths so that the opening was held near the dorsal part of the tongue. Sampling was performed for ten to fifteen seconds then the straw was removed for the remaining seconds.

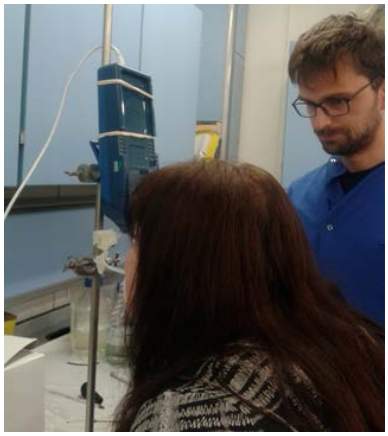

Figure 7.2: Sampling from a human subject by NeOse

In order to facilitate co-sampling with both instruments, a T-junction was introduced upstream of the disposable straw allowing both the NeOse and the SIFT-MS to draw gases

from the oral cavity and to subsample from the side branch. Sampling was performed as above.

7.2.3 Statistical Analysis

Multidimensional Scaling (MDS) were performed using R studio (Boston, USA) and plotted with MATLAB (MathWorks Inc., Massachusetts, USA). Correlation between SPR signal and SIFT-MS results was performed by the following method. Difference between plateau and baseline was calculated for each sample. These values were compared with the SIFT-MS values given for hydrogen sulphide, VSCs, total VOCs, amines, acids and indoles. The R^2 correlation values were plotted on three-dimensional surface and contour plots to reveal biosensor spots most accurately responding to VOC concentration.

7.3 Results

A typical signal obtained from a single biosensor following exposure to biofilm headspace is shown in figure 7.3. MDS analysis of the low and high VOC producing biofilms showed good separation of the two groups. Figure 7.4 shows the distance plot, with hydrogen sulphide concentration by SIFT-MS shown on the Z axis. Figures 7.5 and 7.6 show correlation plots generated as described previously. Higher bars in the Z direction correspond to regions of the biosensor matrix that have responded in a more accurate way with respect of the concentration of the corresponding group of compounds. A relatively lower response was observed with the *in vitro* experiments and this is thought to be due to high concentrations of sulphides blocking the surface of the biosensor. It can be seen, however, that the general pattern of response is the same in each group.

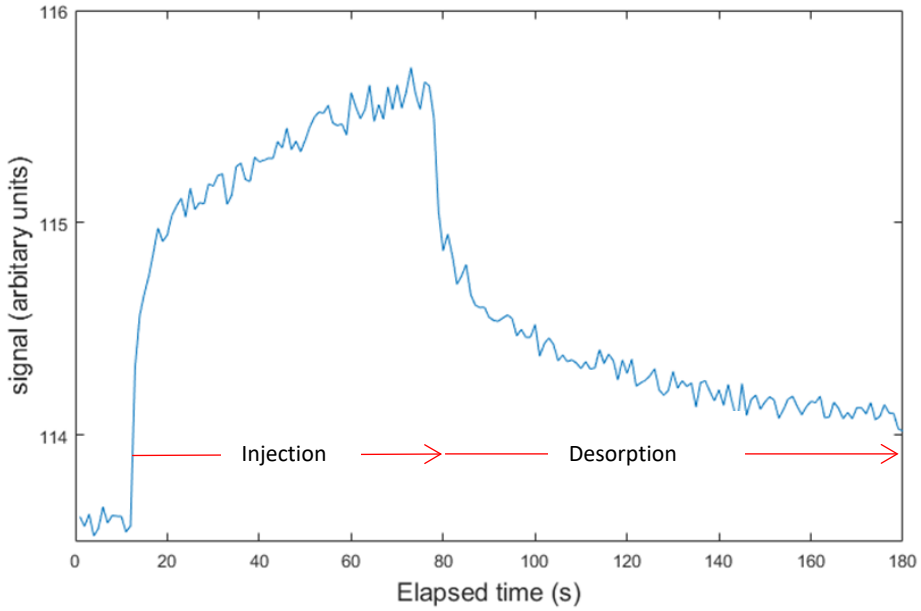

Figure 7.3: Typical response to signal by a single biosensor spot.

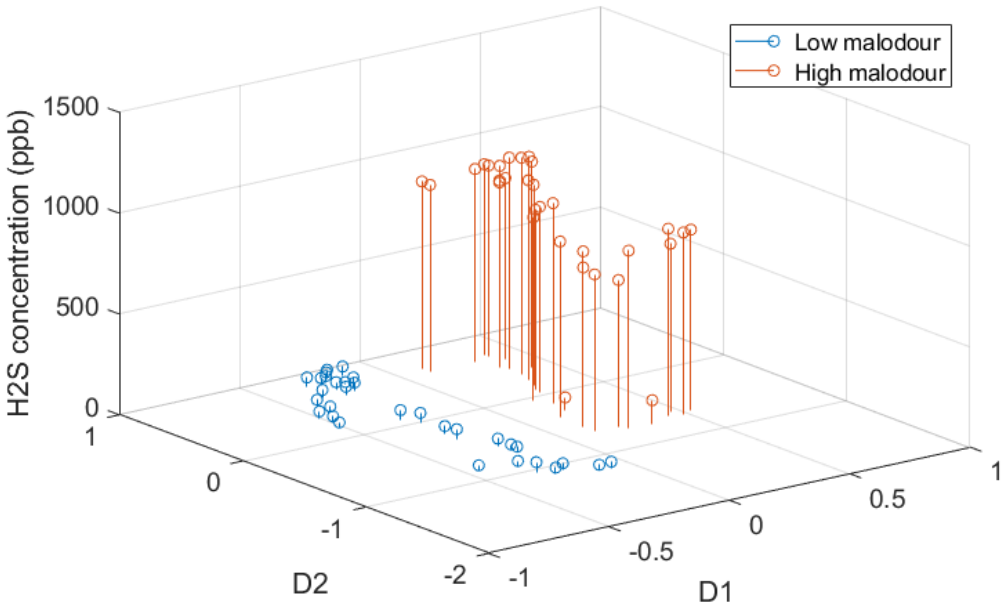

Figure 7.4: MDS analysis of *in vitro* biosensor data showing high and low VOC producing biofilms. X and Y-axes show Euclidean multidimensional spacing of biosensor data and the Z-axis shows hydrogen sulphide concentration as measured by SIFT-MS.

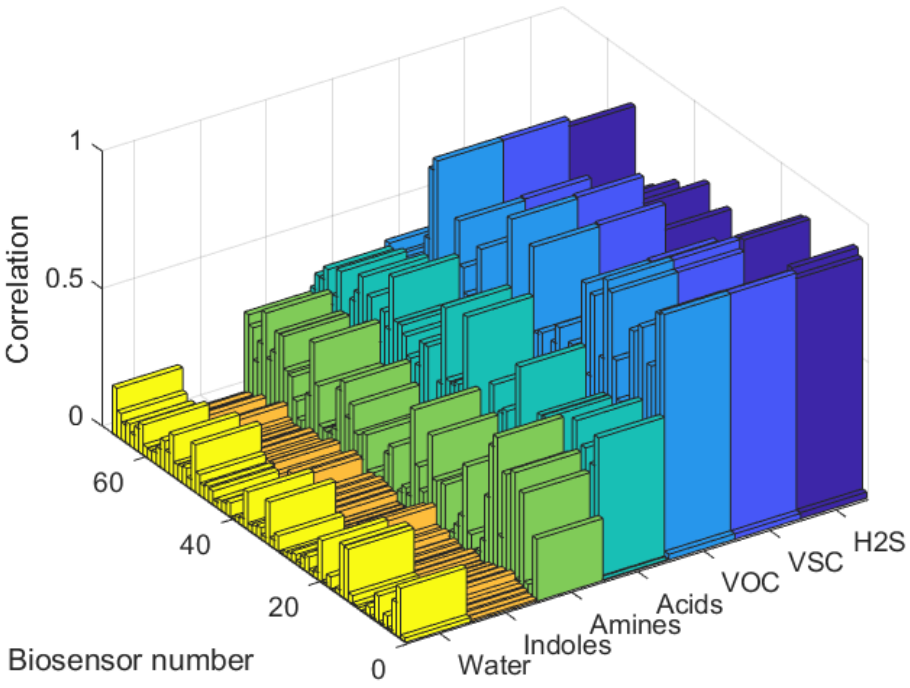

Figure 7.5: Biosensor correlation plot (in vitro). High bars indicate better response to that group of compounds. Grouping is described in Table 7.1.

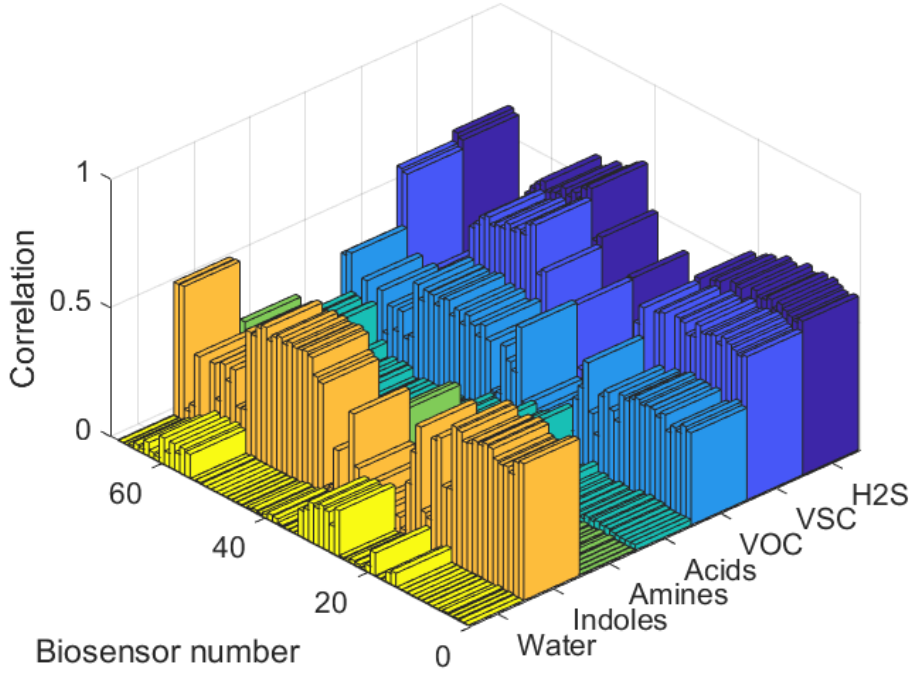

Figure 7.6: Biosensor correlation plot (in vivo). High bars indicate better response to that group of compounds. Grouping is described in Table 7.1.

Following these experiments with high VOC producing biofilms, the response observed by the prism was reduced. A fresh prism was installed for the *in vivo* experiments and a significant increase in response was seen. This response can be seen in figure 7.6.

The biosensor that responded in the most appropriate way to sulphides in the oral cavity was number 42. The correlation between this spot and the SIFT-MS data can be seen figure 7.7. MDS analysis of *in vivo* NeOse data, are shown in figure 7.8, with hydrogen sulphide concentrations as measured by SIFT-MS shown on the Z-axis. Table 7.1 shows a summary of the human volunteer data for all subjects.

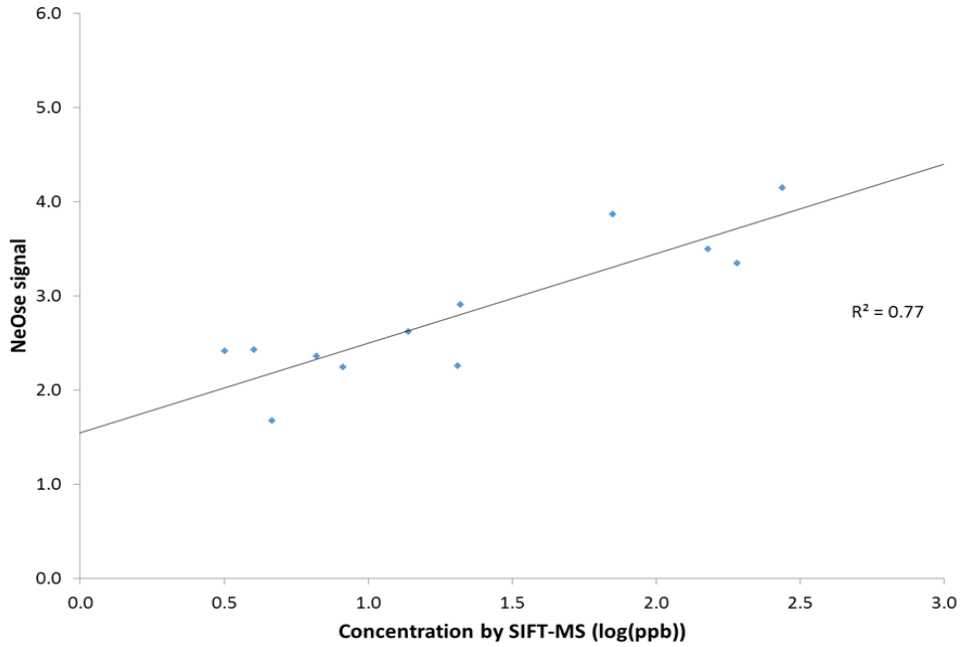

Figure 7.7: NeOse biosensor 42 response to hydrogen sulphide

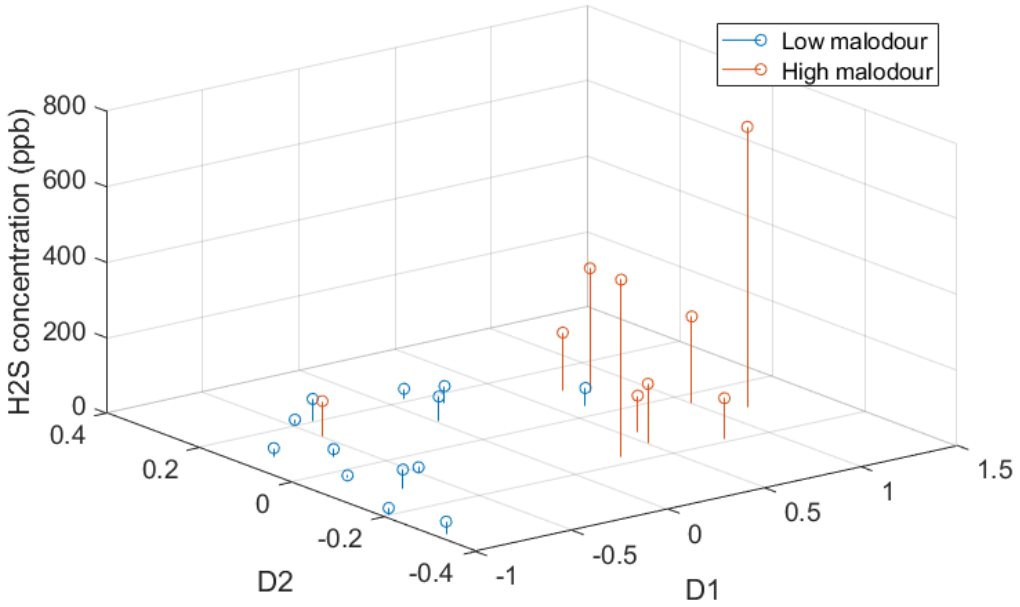

Figure 7.8: MDS analysis of *in vivo* data. X and Y-axes show Euclidean multidimensional spacing of biosensor data and the Z-axis shows hydrogen sulphide concentration as measured by SIFT-MS.

Table 7.1: Human volunteer data obtained from SIFT-MS analysis and NeOse breath measurements.

				SIFT-MS				NeOSe	Organoleptic
	H2S	VSC	VOC	Acids	Amines	Indoles	Water	Signal	Judge
P01	3.99	25.49	799.63	7.16	3.72	0.31	1277.57	2.43	2
P02	4.62	15.29	403.37	10.78	7.53	0.28	1361.44	1.67	3.25
P03	6.61	17.47	721.50	9.64	4.37	0.34	1341.62	2.36	1.5
P04	8.15	36.80	698.01	9.41	6.30	0.42	1287.78	2.24	2.5
P05	190.57	313.43	1437.39	14.62	8.09	1.28	1515.56	3.35	4
P06	70.52	102.61	898.13	8.43	4.98	0.70	1349.54	3.87	2
P07	20.41	75.29	1191.66	8.97	4.39	0.66	1454.83	2.26	N/A
P08	3.18	18.97	841.34	8.64	4.02	0.27	1687.80	2.41	2.5
P09	272.99	486.55	1151.38	12.83	7.23	1.27	1324.22	4.15	3.5
P10	20.82	55.40	730.30	10.47	4.55	0.25	1378.73	2.91	3.5
P11	151.25	241.77	1369.40	7.03	4.40	1.79	1354.64	3.50	4
P12	13.73	41.28	1412.18	12.34	3.19	0.54	1525.83	2.62	5

VSC = H_2S + CH_3SH + $(CH_3)_2S$; VOC = sum of all detectable VOC compounds; Acids = acetic + propionic + butyric + valeric and isovaleric acids; Amines = putrescine + cadaverine + trimethylamine; Indoles = indole + skatole; NeOse signal = response (Biosensor 42)

7.4 Discussion

The *in vitro* and *in vivo* studies both show that the SPR based biosensor responds to a mixture of volatile compounds. Furthermore the biosensor spots respond differentially, meaning that both qualitative and quantitative discrimination can be made between different compounds present in breath. The surface and contour plots show that the biosensors in the region 0-15 and 40-55 respond most accurately to sulphides and possibly to a lesser extent, indoles. There is a less accurate response to indoles and amines, although the response is better in a prism that has previously been exposed to high levels of sulphides, suggesting that blocking of the prism occurs preferentially in certain sites. The binding of sulphides to gold surfaces is well understood and known to be difficult to reverse and so the blocking of the biosensor by high levels of sulphides is predicted. This cannot be the full picture, though, and further work is required.

However, in the human oral cavity sulphide levels are much lower than those found in the *in vitro* biofilm model and discrimination of high and low malodour human subjects is reliable and reproducible. Good clustering by high malodour individuals is seen in the MDS plots and it is likely that unknown samples could be well categorised. By incorporating a flushing and cleaning stage this behaviour should be reproducible as long as very high (ppm) levels of VSCs do not contaminate the prism.

7.5 Conclusions

The multiple spot SPR based biosensor has demonstrated sensitivity in the detection of VSCs in the human oral cavity with a limit of detection below 10 ppb. It has also shown the ability to reliably discriminate between low and high malodour individuals in a sample group. Specific areas of the biosensor surface can be seen to be responding preferentially to subjects with a higher relative malodour.

The approach used could also be used to assess the very many other potential applications for this SPR based technology. By comparing the response of the biosensor to results obtained by SIFT-MS, machine-learning algorithms can inform current and further sensor development.

8 General Discussion and Further Work

8.1 General Discussion

At the beginning of this work the flat plat perfusion biofilm model was at an early stage of development and only preliminary work had been done towards adapting the system to modelling the oral biofilm. In order to fulfil the potential of the technique, a number of significant technical challenges had to be overcome (Chapter 3). By installing each biofilm enclosure in a separate mini-incubator and routing all connections through the door, the stability of physiological conditions of the biofilm was much more readily maintained. It also facilitated the creation of a bank of six incubators that could be set up in parallel and sampled sequentially. A software controlled PEEK bodied solenoid valve allowed this process to be automated so that volatile profiles of six biofilms could be monitored for extended periods. Redesign of the slope allowed contamination of the interior of the enclosure to be minimised, and allowed a window to be installed under the biofilm. This allowed a fibre optic pH sensor to be installed to allow pH to be measured in real time. A modification to the lid of the enclosures allowed the installation of LED illumination and the ability to test photodynamic interventions on the oral biofilm. An accompanying window cut in the top of one of the incubators allowed timelapse recording of the biofilm, and the ability to use engineered bioluminescent organisms to monitor metabolic processes and their relationship to volatile production. The combination of all these modifications has resulted in a versatile model for the study of biofilms *in vitro.* Whilst the remainder of this work has focussed on human tongue dorsum derived biofilms, the model could be applied to the *in vitro* study of many other biofilms of mammalian or environmental origin.

Turning to the scientific aims, the primary goal of this study was to validate the flat plate perfusion model as a method of studying tongue-derived biofilms, to examine the effects of various interventions on biofilm growth, physiology and metabolism, and to compare this with similar interventions performed *in vivo.* It has been shown that biofilms derived from the tongue biota of individuals is transplantable to the model (chapter 4) and that the volatilome of the biofilm is conserved. It has further been shown that the physiology of the biofilm and it's response to interventions is similar to that expected, both by theory and *in vivo* experiment. In the course of this investigation, new methods of analysing and visually representing the oral microbiome have been devised.

Whilst the effects of a number of different antimicrobials were investigated, including photodynamic therapy and several commercial mouthwashes, attention has focussed on two areas. One was a novel compound shown to act in synergy with chlorhexidine in disrupting cell membranes (chapter 5), and the second was a combination of D-amino acids that was also shown disrupt biofilms in a way that did not occur with the L-forms or with standard media (chapter 6). The mechanism by which this occurs is currently unconfirmed. These two main studies have given insight into the way multispecies biofilms develop and mature, and have indicated novel ways in which interventions can influence their growth and characteristics. These valuable techniques have the potential to investigate many types of chemical and physical interventions on diverse types of microbial biofilm, as well as those of human oral origin. As the metabolism and physiology of complex, mixed species biofilms is still relatively poorly understood techniques which allow this kind of study are important. The methods could lead to valuable new formulations to treat oral malodour or other conditions caused or influenced by microbial biofilms. As issues of cost, ethical approval and legislature continue to plague *in vitro* studies, *in vitro* modelling is likely to become more important as a tool. Additionally, multisampling of replicate innocula allows statistically significant results to now be obtained relatively rapidly.

The flat plate perfusion model has also been shown to be a very useful method for assessing the performance of other sensors for volatile compounds. The NeOse device described in chapter 7 is a SPR based sensor that incorporates almost one hundred different biosensors into one device. Whilst this gives the device enormous potential for detection of many volatile compounds, characterisation of each individual biosensor on the prism is challenging. The ability of the flat plate model to generate complex profiles of volatiles that are similar to those found *in vivo,* and the abiilty to quantify these volatiles in real time by SIFT-MS, gives an invaluable technique for assessing the response of the biosensors to the gases. By using techniques such as MDS and correlating individual biosensors with volatiles as measured by SIFT-MS, the performance of the device can be assessed, and prisms can therefore be tailored to the specific application. By learning in this way, accompanied by algorithmic MDS techniques, the NeOse device has the potential to become an extremely sensitive and discriminatory biosensor for multiple compounds and with multiple applications.

8.2 Further Work

Whilst it has been shown that the flat plate perfusion model satisfactory it would be extremely interesting to undertake a large rRNA based study of oral biofilms *in vivo* and the corresponding biofilms transplanted into the *in vitro* model. A combination of cost and commercial sensitivity of data has so far meant that this has been impossible. Combined with the techniques outlined in chapter 4, rRNA analysis of the model biofilms has the potential to investigate changes to the transplanted microbiome and volatilome in many important ways. For example, shifts in volatile production away from those gases considered objectionable can be linked not only to those organisms which are directly responsible, but

by cooccurence analysis other organisms which may not have been previously identified as important. This kind of study is also extremely important in the respect of the interventions investigated in chapters 5 and 6. Any potential intervention will influence different species in different ways, and knowing the exact nature of these factors allows now only tailoring of treatments to specific key organisms, but also scientific advancement through knowledge gained about mechanisms and pathways of antimicrobial resistance and sensitivity. As it becomes increasingly obvious that multispecies biofilms are the norm rather than the exception in nature, techniques which allow us to investigate the interaction and interplay between species within them is of paramount importance.

Turning specifically to the effects of D-amino acids, investigation of processes within biofilms exposed to NCDAAs, by performing 16s rDNA analysis of biofilms exposed to the different enantiomers and controls, it may be possible to learn which species are affected most and least, and thus gain information on the mode of action. The effect of the enantiomers on single species biofilms grown from key species could then be investigated. By what method NCDAAs act, and whether or not c-di-GMP is involved, this area of study is still very important in it's own right. As knowledge of GGDEF domain expression in oral bacteria is incomplete, more work to investigate the presence of these domains is needed.

If C-di-GMP is implicated, either in the effect of NCDAAs or in other biofilm disrupting agents, an assay of intracellular C-di-GMP would be a powerful tool given that the importance of this signalling network is now apparent. Various types of staining and assay techniques, both destructive and non-destructive have been suggested and could be investigated. Cloning of bioluminescent reporter genes has been achieved with *Ps. aeriginosa* and whilst single of multispecies biofilms incorporating this organism might be interesting, more relevant organisms might be more useful. Cloning bioluminescent report genes into anaerobic organisms is problematic as the technique can only be used with facultative or

microaerophilic organisms due to the involvement of oxygen. If bioluminescent clones of oral organisms were developed, the flat plate perfusion model as described would be extremely well suited to such work.

Whatever the process by which NCDAAs act, their potential as biofilm disruptors is obvious, and synergistic effects between them and other antimicrobials (e.g CHX), anti-malodour components (e.g. zinc compounds) and disrupting agents (e.g. CMD) should be investigated.

Another technique that has showed promise in this work, but requires much more development in this specific application is CLSM. The ability to image living biofilms in three dimensions is extremely powerful, but there are two main hurdles to overcome. The first is to do with issues of sample preparation and presentation to the microscope. In this model, biofilms grow on a perfusable cellulose matrix, and this is one of the reasons the model is a good representation of *in vivo* conditions. However cellulose autofluoresces and must be excluded from the CLSM preparation. There are two possible solutions to this problem. Firstly, another matrix could be used that does not fluoresce. Some other biofilm subtrates were tested very early on in the course of this thesis but did not adequately model the conditions of the oral biofilm. It is possible that other perfusable materials could be found that would be non-fluorescing and able to be mounted on the stage of a confocal microscope. Such a material would have to be thin enough and light permeable enough to allow sufficient illumination of the biofilm for microscopy. If such material could be found, and there are plenty of candidates, then it is possible that a laminated biofilm substrate could be constructed from layers of the material, allowing the biofilm to be pulled apart and imaged at varying depths.

The second way to develop confocal techniques is development of the method described in chapter 2, whereby a removable glass coverslip is placed under the biofilm

matrix during maturation and growth. It did however prove difficult to ensure that enough biofilm material adhered to the glass surface, and that it was a true representation of the structure of the main biofilm. Chemically or biologically treating the glass surface in different ways may improve adhesion, and this could be explored.

Development of the NeOse is expected to continue apace and the biofilm model will continue to play a role in this. More data needs to be gathered from human subjects to improve the power of the device in discriminating between low, medium and high malodour individuals. Using data gathered from further *in vitro* studies it should become possible tailor the device to discriminate between specific classes of compounds from the oral cavity. The device has great potential in other areas of interest, and the ability to diagnose other types of microbial infections or colonisations will be investigated. As with studies of antimicrobial agents, the *in vitro* model should prove very useful in identifying which areas are most promising before time or money is committed to specific *in vivo* projects involving humans or animals.

9 References

Adams, N.G. and Smith, D., 1976. The selected ion flow tube (SIFT); A technique for studying ion-neutral reactions. *International Journal of Mass Spectrometry and Ion Physics*, 21 (3), 349–359.

Addy, M., 1986. Chlorhexidine compared with other locally delivered antimicrobials. A short review. *Journal of Clinical periodontology,* 13 (10), 957-964.

Agladze, K., Wang, X., and Romeo, T., 2005. Spatial periodicity of Eschenchia coli K-12 biofilm microstructure initiates during a reversible, polar attachment phase of development and requires the polysaccharide adhesin PGA. *Journal of Bacteriology*, 187 (24), 8237–8246.

Ali, R.W., Skaug, N., Nilsen, R. and Bakken, V., 1994 Microbial Associations of 4 Putative Periodontal Pathogens in Sudanese Adult Periodontitis Patients Determined by DNA Probe Analysis. J*ournal of Periodontology*. 65 (11), pp. 1053–1057.

Allesen-Holm, M., Barken, K.B., Yang, L., Klausen, M., Webb, J.S., Kjelleberg, S., Molin, S., Givskov, M., and Tolker-Nielsen, T., 2006. A characterization of DNA release in Pseudomonas aeruginosa cultures and biofilms. *Molecular Microbiology*, 59 (4), 1114–1128.

Allison, D.G., Ruiz, B., Sanjose, C., Jaspe, A., and Gilbert, P., 1998. Extracellular products as mediators of the formation and detachment of Pseudomonas fluorescens biofilms. *FEMS Microbiology Letters*, 167 (2), 179–184.

Allison, V.C. and Katz, S.H., 1919. An investigation of stenches and odors for industrial purposes. *Industrial and Engineering Chemistry*, 11 (4), 336–338.

Amikam, D. and Galperin, M.Y., 2006. PilZ domain is part of the bacterial c-di-GMP binding protein. *Bioinformatics*, 22 (1), 3–6.

Anicich, V.G., 2003. An index of the literature for bimolecular gas phase cation-molecule reaction kinetics. *JPL-Publication-03-19*, (November), 1194.

Arweiler, N.B., Netuschil, L., and Reich, E., 2001. Alcohol-free mouthrinse solutions to reduce supragingival plaque regrowth and vitality. A controlled clinical study. *Journal of Clinical periodontology,* 28 (2), 168–174.

ASTM Committee E-18 on Sensory Evaluation of Materials and Products, 1968. *Manual on sensory testing methods*. Philadelphia: American Society for Testing and Materials.

Backman, E.L., 1917. The strength of odorous substances and their solubility in water and in oil. *Journal de Physiologie et de Pathologie Generale*, 17, 1–4.

Bailey, J., Chrysostomou, A., Hough, J.H., Gledhill, T.M., McCall, A., Clark, S., Ménard, F., and Tamura, M., 1998. Circular Polarization in Star- Formation Regions: Implications for Biomolecular Homochirality. *Science*, 281 (5377), 672 LP-674.

Beaglehole, D., 1970. Optical Excitation of Surface Plasmons. *IEEE Transactions on Electron Devices*, ED-17 (3), 240–244.

Beard, S.J., Salibury, V., Lewis, R.J., Sharpe, J.A., and Macgowan, A.P., 2002. Expression of lux Genes in a Clinical Isolate of Streptococcus pneumoniae: Using Bioluminescence To Monitor Gemifloxacin Activity. *Antimicrobial Agents and Chemotherapy*, 46 (2), 538–542.

Beech, I.B., 1996. The potential use of atomic force microscopy for studying corrosion of metals in the presence of bacterial biofilms — an overview. *International Biodeterioration &*

Biodegradation, 37 (3–4), 141–149.

Beighton, D., Smith, K. and Hayday, H., 1986, The growth of bacteria and the production of exoglycosidic enzymes in the dental plaque of macaque monkeys. *Archives of Oral Biology.* 31 (12), pp. 829–835.

Belstrøm, D., Paster, B.J., Fiehn, N.E., Bardow, A., and Holmstrup, P., 2016. Salivary bacterial fingerprints of established oral disease revealed by the Human Oral Microbe Identification using Next Generation Sequencing (HOMINGS) technique. *Journal of Oral Microbiology*, 8 (1).

Ben-Hur, E., & Horowitz, B. 1995. Advances in Photochemical Approaches for Blood Sterilization. *Photochemistry and Photobiology*, *62*(3), 383–388.

Berglund, B., Berglund, U., Lindvall, T., and Svensson, L.T., 1973. A quantitative principle of perceived intensity summation in odor mixtures. *Journal of Experimental Psychology*, 100 (1), 29–38.

Bian, J., Liu, X., Cheng, Y.Q., and Li, C., 2013. Inactivation of cyclic di-GMP binding protein TDE0214 affects the motility, biofilm formation, and virulence of Treponema denticola. *Journal of Bacteriology*, 195 (17), 3897–3905.

Biasioli, F., Yeretzian, C., Märk, T.D., Dewulf, J., and Van Langenhove, H., 2011. Direct-injection mass spectrometry adds the time dimension to (B)VOC analysis. *TrAC - Trends in Analytical Chemistry*, 30 (7), 1003–1017.

Blake, R.S., Monks, P.S., and Ellis, A.M., 2009. Proton-Transfer Reaction Mass Spectrometry. *Chemical Reviews*, 109 (3), 861–896.

Bodanszky, M. and Perlman, D., 1969. Peptide Antibiotics. *Science*, 163 (3865), 352–358.

Bolepalli, A., Munireddy, C., Peruka, S., Polepalle, T., Alluri, L.C. and Mishaeel, S. 2015, Determining the association between oral malodor and periodontal disease: A case control study. *Journal of International Society of Preventive and Community Dentistry.* 5 (5), page. 413.

Bonner, W.A., 1991. The origin and amplification of biomolecular chirality. *Origins of Life and Evolution of the Biosphere*, 21 (2), 59–111.

Boring, E.G., 1942. *Sensation and perception in the history of experimental psychology.* Appleton-Century.

Bosy, A., Kulkarni, G. V, Rosenberg, M., and McCulloch, C.A.G., 1994. Relationship of Oral Malodor to Periodontitis: Evidence of Independence in Discrete Subpopulations. *Journal of Periodontology*, 65 (1), 37–46.

Bowen, W.H., Amsbaugh, S.M., Monell-Torrens, S., Brunelle, J., Kuzmiak-Jones, H., and Cole, M.F., 1980. A method to assess cariogenic potential of foodstuffs. *The Journal of the American Dental Association*, 100 (5), 677–681.

Bradshaw, D.J., McKee, A.S., and Marsh, P.D., 1989. Effects of Carbohydrate Pulses and pH on Population Shifts within Oral Microbial Communities in vitro. *Journal of Dental Research*, 68 (9), 1298–1302.

Brambilla, E., 2001. Fluoride – Is It Capable of Fighting Old and New Dental Diseases? *Caries Research*, 35(suppl 1 (Suppl. 1), 6–9.

Broccardo, M., Erspamer, V., Falconieri, G., Improta, G., Linari, G., Melchiorri, P., and Montecucchi, P.C., 1981. Pharmacological data on dermorphins, a new class of potent opioid peptides from amphibian skin. *British journal of pharmacology*, 73 (3), 625–631.

Bryers, J.D., 1987. Biologically Active Surfaces: Processes Governing the Formation and Persistence of Biofilms. *Biotechnology Progress*, 3 (2), 57–68.

Cahill, C.P., Johnston, K.S., and Yee, S.S., 1997. A surface plasmon resonance sensor probe based on retro-reflection. *Sensors and Actuators B: Chemical*, 45 (2), 161–166.

Cappellin, L., Probst, M., Limtrakul, J., Biasioli, F., Schuhfried, E., Soukoulis, C., Märk, T.D., and Gasperi, F., 2010. Proton transfer reaction rate coefficients between H3O+ and some sulphur compounds. *International Journal of Mass Spectrometry*, 295 (1–2), 43–48.

Carone, F.A., Nakamura, S., and Goldman, B., 1985. Urinary loss of glucose, phosphate, and protein by diffusion into proximal straight tubules injured by D-serine and maleic acid. *Laboratory investigation; a journal of technical methods and pathology,* 52 (6), 605—610.

ten Cate, J.M., 2006. Biofilms, a new approach to the microbiology of dental plaque. *Odontology*, 94 (1), 1–9.

Cava, F., Lam, H., De Pedro, M.A., and Waldor, M.K., 2011. Emerging knowledge of regulatory roles of d-amino acids in bacteria. *Cellular and Molecular Life Sciences*, 68 (5), 817–831.

Cava, F., De Pedro, M.A., Lam, H., Davis, B.M., and Waldor, M.K., 2011. Distinct pathways for modification of the bacterial cell wall by non-canonical D-amino acids. *EMBO Journal*, 30 (16), 3442–3453.

Chao, A., 2016. Estimating the Population Size for Capture-Recapture Data with Unequal Catchability. *Biometrics*, 43 (4), 783–791.

Characklis, W.G. and Wilderer, P.A., 1989. *Structure and function of biofilms : report of the Dahlem Workshop on Structure and Function of Biofilms*. Chichester ; New York: Wiley.

Chaudhuri, S., Pratap, S., Paromov, V., Li, Z., Mantri, C.K., and Xie, H., 2014. Identification of a diguanylate cyclase and its role in Porphyromonas gingivalis virulence. *Infection and Immunity*, 82 (7), 2728–2735.

Cherepin, V.T., 1992. Cryoscanning electron microscopy of microbial extracellular polysaccharides and their association with minerals Secondary Ion Mass Spectroscopy of Solid Surfaces, VNU Science Press, Utrecht. *Scanning*, 14 (November), 360–364.

Chou, S.H. and Galperin, M.Y., 2016. Diversity of cyclic di-GMP-binding proteins and mechanisms. *Journal of Bacteriology*, 198 (1), 32–46.

Christen, M., Christen, B., Allan, M.G., Folcher, M., Jenö, P., Grzesiek, S., and Jenal, U., 2007. DgrA is a member of a new family of cyclic diguanosine monophosphate receptors and controls flagellar motor function in Caulobacter crescentus. *Proceedings of the National Academy of Sciences*, 104 (10), 4112–4117.

Christensen, L.D., Gennip, M. van, Rybtke, M.T., Wu, H., Chiang, W.C., Alhede, M., Høiby, N., Nielsen, T.E., Givskov, M., and Tolker-Nielsena, T., 2013. Clearance of pseudomonas aeruginosa foreign-body biofilm infections through reduction of the cyclic di-gmp level in the bacteria. *Infection and Immunity*, 81 (8), 2705–2713.

Collado, M.C., Cernada, M., Baüerl, C., Vento, M., and Pérez-Martínez, G., 2012. Microbial ecology and host-microbiota interactions during early life stages. *Gut Microbes*, 3 (4).

Colwell, R.R. and Grimes, D.J., 2000. *Nonculturable microorganisms in the environment.* ASM press.

Connor, E. F., Collins, M. D. and Simberloff, D. 2013. The checkered history of checkerboard distributions. *Ecology*, 94: 2403-2414.

Consortium, T.H.M.P., 2013. Structure, Function and Diversity of the Healthy Human Microbiome. *Nature*, 486 (7402), 207–214.

Cooke, V., Petropolou, K., Mandel, J.D., Ellison, S.A., Falcetti, J., and Trieger, N., 1982. Plaque in tube-fed persons. *IADR Program and Abstracts*, 61 (646).

Costello, E.K., Stagaman, K., Dethlefsen, L., Bohannan, B.J.M., and Relman, D.A., 2012. The Application of Ecological Theory Toward an Understanding of the Human Microbiome. *Science*, 336 (6086), 1255 LP-1262.

Costerton, J.W. and Irvin, R.T., 1981. The Bacterial Glycocalyx in Nature and Disease. *Annals of Reviews in Microbiology*, 35, 299–324.

Costerton, J.W., Irvin, R.T., Cheng, K.-J., and Sutherland, I.W., 1981. The Role of Bacterial Surface Structures in Pathogenesis. *CRC Critical Reviews in Microbiology*, 8 (4), 303–338.

Cucarella, C., Solano, C., and Valle, J., 2001. Bap, a *Staphylococcus aureus* surface protein involved in biofilm formation. *Journal of Bacteriology,* 183 (9), 2888–2896.

Cumming, B.R. and Loe, H., 1973. Optimal dosage and method for delivering chlorhexidine solutions for the inhibition of dental plaque. *Journal of Peridontal Research*, 8, 57–62.

Danese, P.N., Pratt, L.A., and Kolter, R., 2000. Exopolysaccharide production is required for development of *Escherichia coli* K-12 biofilm architecture. *Journal of Bacteriology*, 182 (12), 3593–3596.

David, L.A., Materna, A.C., Friedman, J., Campos-Baptista, M.I., Blackburn, M.C., Perrotta, A., Erdman, S.E., and Alm, E.J., 2015. Host lifestyle affects human microbiota on daily timescales. *Genome Biology*, 15 (7), 1–15.

Davies, A., 1973. The mode of action of chlorhexidine. *Journal of Periodontal Research*.

Diamond, J.M., 1975, Assembly of species communities. In: *Ecology and evolution of communities*. Harvard University Press, 342–444.

Van Dellen, K.L., Houot, L., and Watnick, P.I., 2008. Genetic analysis of Vibrio cholerae monolayer formation reveals a key role for in the transition to permanent attachment. *Journal of Bacteriology*, 190 (24), 8185–8196.

Denton, G.W., 1991. Chlorhexidine. *Disinfection, sterilization and preservation. 4th ed. Philadelphia: Lea and Febiger*, 274–289.

Dewhirst, F.E., Chen, T., Izard, J., Paster, B.J., Tanner, A.C.R., Yu, W.H., Lakshmanan, A., and Wade, W.G., 2010. The human oral microbiome. *Journal of Bacteriology*, 192 (19), 5002–5017.

Diamond, J.M., 1975. Assembly of species communities. *Ecology and evolution of communities*, 342–444.

Dobell, C. and Leeuwenhoek, A. van, 1960. *Antony van Leeuwenhoek and his 'Little animals' : being some account of the father of protozoology and bacteriology and his multifarious discoveries in these disciplines*. New York: Dover Publications.

Donaldson, A.C., McKenzie, D., Riggio, M.P., Hodge, P.J., Rolph, H., Flanagan, A., and Bagg, J., 2005. Microbiological culture analysis of the tongue anaerobic microflora in subjects with and without halitosis. *Oral Diseases*, 11 (SUPPL. 1), 61–63.

DuBois, M., Gilles, K. a., Hamilton, J.K., Rebers, P. a., and Smith, F., 1956. Colorimetric method for determination of sugars and related substances. *Analytical Chemistry*, 28 (3), 350–356.

Dwivedi, Y.S., Sharma, A.K., and Gupta, B.D., 2008. Influence of design parameters on the performance of a surface plasmon sensor based fiber optic sensor. *Plasmonics*, 3 (2–3), 79–86.

Ellison, S.A., Cooke, V., Mandel, I.D., Trieger, N., and Falcetti, J., 1982. Plaque in tube-fed persons II. *IADR Programs and Abstracts*, 61 (647).

Flötra, L., Gjermo, p e r, Rölla, G., and Waerhaug, J., 1971. Side effects of chlorhexidine mouth washes. *European Journal of Oral Sciences*, 79 (2), 119–125.

Foster, M.W., Ferrell, D.J., and Lieberman, R.A., 1994. Surface plasmon resonance biosensor miniaturization. *Chemical, Biochemical, and Environmental Fiber Sensors VI,* 2210–2293.

Franklin, M.J. and Ohman, D.E., 1996. Identification of algI and algJ in the Pseudomonas aeruginosa alginate biosynthetic gene cluster which are required for alginate O Alginate Biosynthetic Gene Cluster Which Are Required for Alginate O Acetylation. *Journal of Bacteriology*, 178 (8), 2186–2195.

Freedman, J.C., Rogers, E.A., Kostick, J.L., Zhang, H., Iyer, R., Schwartz, I., and Marconi, R.T., 2010. Identification and molecular characterization of a cyclic-di-GMP effector protein, PlzA additional evidence for the existence of a functional cyclic-di-GMPin Borrelia burgdorferi. *FEMS Immunology and Medical Microbiology*, 58 (2), 285–294.

Friedman, M., 1999. Chemistry, Nutrition, and Microbiology of D-Amino Acids. *Journal of Agricultural and Food Chemistry,* 47 (9), 3457–3479.

Friedman, M. and Gumbmann, M.R., 1988. Nutritional Value and Safety of Methionine Derivatives, Isomeric Dipeptides and Hydroxy Analogs in Mice. *The Journal of Nutrition*, 118 (3), 388–397.

Galperin, M.Y., Nikolskaya, a N., and Koonin, E. V, 2001. Novel domains of the prokaryotic two-component signal transduction systems. *FEMS Microbiology Letters*, 203 (1), 11–21.

Gjermansen, M., Ragas, P., and Tolker-Nielsen, T., 2006. Proteins with GGDEF and EAL domains regulate Pseudomonas putida biofilm formation and dispersal. *FEMS Microbiology Letters*, 265 (2), 215–224.

Gmür, R., Strub, J.R. and Guggenheim, B. (1989) Prevalence of Bacteroides forsythus and Bacteroides gingivalis in subgingival plaque of prosthodontically treated patients on short recall. *Journal of Periodontal Research*. 24 (2), pp. 113–120.

Gould, R.G., 1959. The LASER, light amplification by stimulated emission of radiation. *In*: *The Ann Arbor conference on optical pumping, the University of Michigan*. 128.

Greenman, J., 1999. *In: Dental plaque revisited; oral biofilms in health and disease*. Bioline.

Greenman, J., Duffield, J., Spencer, P., Rosenberg, M., Corry, D., Saad, S., Lenton, P., Majerus, G., and Nachnani, S., 2004. Study on the Organoleptic Intensity Scale for Measuring Oral Malodour. *Journal of dental research*, 83 (1), 81–85.

Greenman, J., Duffield, J., Spencer, P., Rosenberg, M., Corry, D., Saad, S., Lenton, P., Majerus, G., Nachnani, S., and El-Maaytah, M., 2004. Study on the Organoleptic Intensity Scale for Measuring Oral Malodor. *Journal of Dental Research*, 83 (1), 81–85.

Griffith, D.M., Veech, J.A., and Marsh, C.J., 2016. **cooccur** : Probabilistic Species Co-Occurrence Analysis in *R*. *Journal of Statistical Software*, 69 (Code Snippet 2), 1–17.

Haldi, J., Wynn, W., Shaw, J.H., and Sognnaes, R.F., 1953. The Relative Cariogenicity of Sucrose When Ingested in the Solid form and in Solution by the Albino Rat. *The Journal of Nutrition*, 49 (2), 295–306.

Hamblin, M. R., & Newman, E. L. (1994). Photosensitizer targeting in photodynamic therapy I. Conjugates of haematoporphyrin with albumin and transferrin. *Journal of Photochemistry and Photobiology B: Biology*, 26(1), 45–56.

Hanada, M., Koda, H., Onaga, K., Tanaka, K., Okabayashi, T., Itoh, T., and Miyazaki, H., 2003. Portable oral malodor analyzer using highly sensitive In2O3 gas sensor combined with a simple gas chromatography system. *Analytica Chimica Acta*, 475 (1–2), 27–35.

Hannan, S., Ready, D., Jasni, A.S., Rogers, M., Pratten, J., and Roberts, A.P., 2010. Transfer of antibiotic resistance by transformation with eDNA within oral biofilms. *FEMS Immunology and Medical Microbiology*, 59 (3), 345–349.

Haraszthy, V.I., Gerber, D., Clark, B., Moses, P., Parker, C., Sreenivasan, P.K., and Zambon, J.J., 2008. Characterization and prevalence of Solobacterium moorei associated with oral halitosis. *Journal of Breath Research*, 2 (1).

Haraszthy, V.I., Zambon, J.J., Sreenivasan, P.K., Zambon, M.M., Gerber, D., Rego, R., and Parker, C., 2007. Identification of oral bacterial species associated with halitosis. *Journal of the American Dental Association*, 138 (8), 1113–1120.

Hartley, M., El-Maaytah, M., McKenzie, C., and Greenman, J., 1996a. Assessment of impressed toothbrush as a method of sampling tongue microbiota. *Bad breath: a multidisciplinary approach.* Leuven University Press: Leuven, Belgium, 123–133.

Hartley, M.G., El-Maaytah, M. a., McKenzie, C., and Greenman, J., 1996b. The Tongue Microbiota of Low Odour and Malodorous Individuals. *Microbial Ecology in Health and Disease*, 9 (5), 215–223.

Hendrick, W.A., Orr, M.W., Murray, S.R., Lee, V.T., and Melville, S.B., 2017. Cyclic di-GMP binding by an assembly ATPase (PilB2) and control of type IV pilin polymerization in the Gram-positive pathogen Clostridium perfringens. *Journal of Bacteriology*, 199 (10), 1–17.

Hentzer, M., Teitzel, G.M., Balzer, G.J., Molin, S., Givskov, M., Matthew, R., Heydorn, A., and Parsek, M.R., 2001. Alginate Overproduction Affects Pseudomonas aeruginosa Biofilm Structure and Function. *Journal of bacteriology*, 183 (18), 5395–5401.

Hess, J., Greenman, J., and Duffield, J., 2008. Modelling oral malodour from a tongue biofilm. *Journal of Breath Research*, 2 (1), 17003.

Hochbaum, A.I., Kolodkin-Gal, I., Foulston, L., Kolter, R., Aizenberg, J., and Losick, R., 2011. Inhibitory effects of D-amino acids on staphylococcus aureus biofilm development. *Journal of Bacteriology*, 193 (20), 5616–5622.

Van der Hoeven, J.S. and Camp, P.J.M., 1991, Synergistic Degradation of Mucin by Streptococcus oralis and Streptococcus sanguis in Mixed Chemostat Cultures. *Journal of Dental Research*. 70 (7), pp. 1041–1044.

Hope, C.K., Bakht, K., Burnside, G., Martin, G.C., Burnett, G., de Josselin de Jong, E., and Higham, S.M., 2012. Reducing the variability between constant-depth film fermenter experiments when modelling oral biofilm. *Journal of Applied Microbiology*, 113 (3), 601–608.

Hope, C.K. and Wilson, M., 2004. Analysis of the Effects of Chlorhexidine on Oral Biofilm Vitality and Structure Based on Viability Profiling and an Indicator of Membrane Integrity. *Antimicrobial Agents and Chemotherapy*, 48 (5), 1461–1468.

Hubbard, A.T.M., Barker, R., Rehal, R., Vandera, K.-K.A., Harvey, R.D., and Coates, A.R.M., 2017. Mechanism of Action of a Membrane-Active Quinoline-Based Antimicrobial on Natural and

Model Bacterial Membranes. *Biochemistry*, 56 (8), 1163–1174.

Huntress, W.T., 1974. A Review of Jovian Ionospheric Chemistry. *In*: D.R. Bates and B.B.T.-A. in A. and M.P. Bederson, eds. *Advances in Atomic and Molecular Physics*. Academic Press, 295–340.

Imfeld, T. and Lutz, F., 1980. Intraplaque acid formation assessed in vivo in children and young adults. *Pediatric Dentistry*, 2 (2).

Inoué, S., 2006. Foundations of confocal scanned imaging in light microscopy. *Handbook of Biological Confocal Microscopy: Third Edition*, 1–19.

Jacques, M. and Gottschalk, M., 1997. Use of monoclonal antibodies to visualize capsular material of bacterial pathogens by conventional electron microscopy. *Microscopy And Microanalysis*, 3 (3), 234–238.

Jenkins, S., Addy, M., and Wade, W., 1988. The mechanism of action of chlorhexidine: A study of plaque growth on enamel inserts in vivo. *Journal of Clinical Periodontology*, 15 (7), 415–424.

Jimenéz, E.C., Olivera, B.M., Gray, W.R., and Cruz, L.J., 1996. Contryphan is a D-tryptophan-containing Conus peptide. *Journal of Biological Chemistry*, 271 (45), 28002–28005.

Jones, C.G., 1997. Chlorhexidine: is it still the gold standard? *Periodontology 2000*, 15, 55–62.

Jones, F.N., 1958a. Subjective Scales of Intensity for the Three Odors. *The American Journal of Psychology*, 71 (2), 423–425.

Jones, F.N., 1958b. Scales of Subjective Intensity for Odors of Diverse Chemical Nature. *The American Journal of Psychology*, 71 (1), 305–310.

Jones, F.N. and Marcus, M.J., 1961. The subject effect in judgments of subjective magnitude. *Journal of Experimental Psychology*, 61 (1), 40.

Jones, F.N. and Woskow, M.H., 1963. On the Intensity of Odor Mixtures. *Annals of the New York Academy of Sciences*, 116 (2), 484–494.

Jönsson, U., Fägerstam, L., Ivarsson, B., Johnsson, B., Karlsson, R., Lundh, K., Löfås, S., Persson, B., Roos, H., and Rönnberg, I., 1991. Real-time biospecific interaction analysis using surface plasmon resonance and a sensor chip technology. *BioTechniques*, 11 (5), 620—627.

Jordan, A., Haidacher, S., Hanel, G., Hartungen, E., Herbig, J., Märk, L., Schottkowsky, R., Seehauser, H., Sulzer, P., and Märk, T.D., 2009. An online ultra-high sensitivity Proton-transfer-reaction mass-spectrometer combined with switchable reagent ion capability (PTR + SRI - MS). *International Journal of Mass Spectrometry*, 286 (1), 32–38.

Kaeberlein, T., Lewis, K., and Epstein, S.S., 2002. Isolating 'Uncultivable' Microorganisms in Pure Culture in a Simulated Natural Environment. *Science*, 296 (5570), 1127 LP-1129.

Karlsson, R., 2004. SPR for molecular interaction analysis: A review of emerging application areas. *Journal of Molecular Recognition*, 17 (3), 151–161.

Kaltenbach, J.P., Ganote, C.E., and Carone, F.A., 1979. Renal tubular necrosis induced by compounds structurally related to d-serine. *Experimental and Molecular Pathology,* 30 (2), 209–214

Kampel, D., Kupferschmidt, R., and Lubec, G., 1990. Toxicity of D-proline BT - *In: Amino Acids: Chemistry, Biology and Medicine.* G. Lubec and G.A. Rosenthal, eds. Dordrecht: Springer Netherlands, 1164–1171.

Kilian, M., Chapple, I.L.C., Hannig, M., Marsh, P.D., Meuric, V., Pedersen, A.M.L., Tonetti, M.S., Wade, W.G., and Zaura, E., 2016. The oral microbiome – an update for oral healthcare professionals.

British Dental Journal, 221 (10), 657–666.

Kinniment, S.L., Wimpenny, J.W.T., Adams, D., and Marsh, P.D., 1996. The effect of chlorhexidine on defined, mixed culture oral biofilms grown in a novel model system. *Journal of Applied Bacteriology*, 81 (2), 120–125.

Klausen, M., Heydorn, A., Ragas, P., Lambertsen, L., Aaes-Jørgensen, A., Molin, S., and Tolker-Nielsen, T., 2003. Biofilm formation by Pseudomonas aeruginosa wild type, flagella and type IV pili mutants. *Molecular Microbiology*, 48 (6), 1511–1524.

Klemm, P., Hjerrild, L., Gjermansen, M., and Schembri, M.A., 2004. Structure-function analysis of the self-recognizing Antigen 43 autotransporter protein from Escherichia coli. *Molecular Microbiology*, 51 (1), 283–296.

Koga, K., Harada, T., Shimizu, H., and Tanaka, K., 2005. Bacterial luciferase activity and the intracellular redox pool in Escherichia coli. *Molecular Genetics and Genomics*, 274 (2), 180–188.

Kolenbrander, P.E. and London, J., 1993. Adhere today, here tomorrow: Oral bacterial adherence. *Journal of Bacteriology*, 175 (11), 3247–3252.

Kolodkin-Gal, I., Romeroa, D., Cao, S., Clardy, J., Kolter, R., and Losick, R., 2010. D-Amino Acids Trigger Biofilm Disassembly. *Science*, 328 (30 April), 627–629.

Kretschmann, E., 1971. Die bestimmungen optischer Konstanten von Metallen durch Anregung van Oberflächen plasma-schwingungen. *Zeitschrift für Physik*, 241, 313–324.

Krzywinski, M. et al, 2009. Circos: an Information Aesthetic for Comparative Genomics. *Genome Research*, 19 (604), 1639–1645.

Kuramitsu, H.K., He, X., Lux, R., Anderson, M.H., and Shi, W., 2007. Interspecies interactions within oral microbial communities. *Microbiology and molecular biology reviews*, 71 (4), 653–670.

Kuyyakanond, T. and Quesnel, L.B., 1992. The mechanism of action of chlorhexidine. *FEMS Microbiology Letters*, 100 (1–3), 211–215.

Labbate, M., Queck, S.Y., Koh, K.S., Rice, S.A., Givskov, M., and Kjelleberg, S., 2004. Quorum Sensing-Controlled Biofilm Development in Serratia liquefaciens MG1. *Journal of Bacteriology*, 186 (3), 692–698.

Lam, H., Oh, D.-C., Cava, Felipe, Takacs, C.N., Jon, C., de Pedro, M. a., and Waldor, M.K., 2009. D-Amino Acids Govern Stationary Phase. *Science*, 325 (September), 1552–1555.

Lark, C., Bradley, D., and Lark, K.G., 1963. Further Studies on the Incorporation of D-Methionine Into the Bacterial Cell Wall; Its Incorporation Into the R-Layer and the Structural Consequences. *Biochimica et biophysica acta*, 78, 278–88.

Lawrence, J.R., Neu, T.R., and Swerhone, G.D.W., 1998. Application of multiple parameter imaging for the quantification of algal, bacterial and exopolymer components of microbial biofilms. *Journal of Microbiological Methods*, 32 (3), 253–261.

Lee, E.R., Baker, J.L., Weinberg, Z., Sudarsan, N., and Breaker, R.R., 2010. An Allosteric Self-Splicing Ribozyme Triggered by a Bacterial Second Messenger. *Science*, 329 (5993), 845 LP-848.

Lemos, J.A.C., Abranches, J., and Burne, R.A., 2005. Responses of cariogenic streptococci to environmental stresses. *Current Issues in Molecular Biology*, 7 (1), 95–108.

Lewis, R. J., Baldwin, A., O'Neill, T., Alloush, H. A., Nelson, S. M., Dowman, T., & Salisbury, V. (2006). Use of Salmonella enterica serovar Typhimurium DT104 expressing lux genes to assess, in real

time and in situ, heat inactivation and recovery on a range of contaminated food surfaces. *Journal of Food Engineering*, *76*(1), 41–48.

Lewis, K., Epstein, S., D'Onofrio, A., and Ling, L.L., 2010. Uncultured microorganisms as a source of secondary metabolites. *The Journal of Antibiotics*, 63 (June), 468–476.

Li, G., Smith, C.S., Brun, Y. V, Jay, X., and Tang, J.X., 2005. The Elastic Properties of the Caulobacter crescentus Adhesive Holdfast Are Dependent on Oligomers of N The Elastic Properties of the Caulobacter crescentus Adhesive Holdfast Are Dependent on Oligomers of N - Acetylglucosamine. *Journal of bacteriology*, 187 (1), 257–265.

Liedberg, B., Nylander, C., and Lundström, I., 1995. Biosensing with surface plasmon resonance - how it all started. *Biosensors and Bioelectronics*, 10 (8).

Liedberg, B., Nylander, C., and Lunström, I., 1983. Surface plasmon resonance for gas detection and biosensing. *Sensors and Actuators*, 4, 299–304.

Littleton, N.W., Carter, C.H., and Kelley, R.T., 1967. Studies of oral health in persons nourished by stomach tube I. Changes in the pH of plaque material after the addition of sucrose. *The Journal of the American Dental Association*, 74 (1), 119–123.

Liu, H. and Fang, H.H.P., 2002. Extraction of extracellular polymeric substances (EPS) of sludges. *Journal of Biotechnology*, 95 (3), 249–256.

Loesche, W.J. and Kazor, C., 2002. Microbiology and treatment of halitosis. *Periodontology 2000*, 28, 256–279.

Van Loosdrecht, M.C.M., Heijnen, J.J., Eberl, H., Kreft, J., and Picioreanu, C., 2002. Mathematical modelling of biofilm structures. *Antonie van Leeuwenhoek, International Journal of General and Molecular Microbiology*, 81 (1–4), 245–256.

Loveren, C. Van, 1990. The Antimicrobial Action of Fluoride and its Role in Caries Inhibition. *Journal of Dental Research*, 69 (2_suppl), 676–681.

Ma, Q., Yang, Z., Pu, M., Peti, W., and Wood, T.K., 2011. Engineering a novel c-di-GMP-binding protein for biofilm dispersal. *Environmental Microbiology*, 13 (3), 631–642.

Magasanik, B., 1961. Catabolite Repression. *Cold Spring Harbor Symposia on Quantitative Biology* , 26, 249–256.

Marsh, P.D., 1989. Host defenses and microbial homeostasis: role of microbial interactions. *Journal of Dental Research*, 68, 1567–1575.

Marsh, P.D., 2000. Role of the oral microflora in health. *Microbial Ecology in Health and Disease*, 12 (3), 130–137.

Marsh, P.D., Hunter, J.R., Bowden, G.H., Hamilton, I.R., McKee, a S., Hardie, J.M., and Ellwood, D.C., 1983. The influence of growth rate and nutrient limitation on the microbial composition and biochemical properties of a mixed culture of oral bacteria grown in a chemostat. *Journal of general microbiology*, 129 (3), 755–70.

Marshall, K.C., Stout, R., and Mitchell, R., 1971. Mechanism of the Initial Events in the Sorption of Marine Bacteria to Surfaces. *Journal of General Microbiology*, 68 (3), 337–348.

Massler, M., Emslie, R.D., and Bolden, T.E., 1951. Fetor ex ore. *Oral Surgery, Oral Medicine, Oral Pathology*, 4 (1), 110–125.

McKee, A.S., McDermid, A.S., Ellwood, D.C., and Marsh, P.D., 1985. The establishment of

reproducible, complex communities of oral bacteria in the chemostat using defined inocula. *Journal of Applied Bacteriology*, 59 (3), 263–275.

McKenzie, C., 2007. Perfusion biofilm model to screen compounds for antiglycolysis activity against cariogenic streptococci. University of the West of England.

McLean, R.J.C., Whiteley, M., Stickler, D.J., and Fuqua, W.C., 1997. Evidence of autoinducer activity in naturally occurring biofilms. *FEMS Microbiology Letters*, 154 (2), 259–263.

Merighi, M., Lee, V.T., Hyodo, M., Hayakawa, Y., and Lory, S., 2007. The second messenger bis-(3 -5)-cyclic-GMP and its PilZ domain-containing receptor Alg44 are required for alginate biosynthesis in Pseudomonas aeruginosa. *Molecular Microbiology*, 65 (4), 876–895.

Minsky, M., 1955. Confocal scanning microscope. *Rapport technique, Patent*, 3.

Minsky, M., 1988. Memoir on inventing the confocal scanning microscope. *Scanning*, 10 (4), 128–138.

Moorthy, S. and Watnick, P.I., 2004. Genetic evidence that the Vibrio cholerae monolayer is a distinct stage in biofilm development. *Molecular Microbiology*, 52 (2), 573–587.

Morita, M. and Wang, H.L., 2001a, Relationship Between Sulcular Sulfide Level and Oral Malodor in Subjects With Periodontal Disease. *Journal of Periodontology*. 72 (1), pp. 79–84.

Morita, M. and Wang, H.L. (2001b) Association between oral malodor and adult periodontitis: A review. *Journal of Clinical Periodontology*. 28 (9), pp. 813–819.

Mühlenhoff, U., Balk, J., Richhardt, N., Kaiser, J.T., Sipos, K., Kispal, G., and Lill, R., 2004. Functional characterization of the eukaryotic cysteine desulfurase Nfs1p from Saccharomyces cerevisiae. *Journal of Biological Chemistry*, 279 (35), 36906–36915.

Nagata, Y., Higashi, M., Ishii, Y., Sano, H., Tanigawa, M., Nagata, K., Noguchi, K., and Urade, M., 2006. The presence of high concentrations of free D-amino acids in human saliva. *Life Sciences,* 78 (15), 1677–1681.

Nakayama, S., Kelsey, I., Wang, J., Roelofs, K., Stefane, B., Luo, Y., Lee, V.T., and Sintim, H.O., 2011. Thiazole orange-induced c-di-GMP quadruplex formation facilitates a simple fluorescent detection of this ubiquitous biofilm regulating molecule. *Journal of the American Chemical Society*, 133 (13), 4856–4864.

Nakhamchik, A., Wilde, C., and Rowe-Magnus, D.A., 2008. Cyclic-di-GMP regulates extracellular polysaccharide production, biofilm formation, and rugose colony development by Vibrio vulnificus. *Applied and Environmental Microbiology*, 74 (13), 4199–4209.

Neu, T.R. and Lawrence, J.R., 2014. Advanced Techniques for In Situ Analysis of the Biofilm Matrix (Structure, Composition, Dynamics) by Means of Laser Scanning Microscopy, In:*Microbial Biofilms. Methods and Protocols* 4, 43-64.

Newell, P.D., Monds, R.D., and O'Toole, G.A., 2009. LapD is a bis-(3',5')-cyclic dimeric GMP-binding protein that regulates surface attachment by Pseudomonas fluorescens Pf0-1. *Proceedings of the National Academy of Sciences*, 106 (9), 3461–3466.

Newell, P.D., Yoshioka, S., Hvorecny, K.L., Monds, R.D., and O'Toole, G.A., 2011. Systematic analysis of diguanylate cyclases that promote biofilm formation by Pseudomonas fluorescens Pf0-1. *Journal of Bacteriology*, 193 (18), 4685–4698.

Newman, H.N. and Wilson, M., 1999. Dental plaque revisited : oral biofilms in health and disease, *Proceedings of a conference held at the Royal College of Physicians*, London, 3-5 November

1999. Cardiff, UK: BioLine.

O'Neill, J. F., Hope, C. K., & Wilson, M. (2002). Oral bacteria in multi-species biofilms can be killed by red light in the presence of toluidine blue. *Lasers in Surgery and Medicine*, *31*(2), 86–90.

Opoku-Temeng, C., Dayal, N., Miller, J., and Sintim, H.O., 2017. Hydroxybenzylidene-indolinones, c-di-AMP synthase inhibitors, have antibacterial and anti-biofilm activities and also re-sensitize resistant bacteria to methicillin and vancomycin. *RSC Advances*, 7 (14), 8288–8294.

Opoku-Temeng, C. and Sintim, H.O., 2016a. Potent inhibition of cyclic diadenylate monophosphate cyclase by the antiparasitic drug, suramin. *Chemical Communications*, 52 (19), 3754–3757.

Opoku-Temeng, C. and Sintim, H.O., 2016b. Inhibition of cyclic diadenylate cyclase, DisA, by polyphenols. *Scientific Reports*, 6, 1–8.

Osborn, M.J., 1969. Structure and Biosynthesis of the Bacterial Cell Wall. *Annual Reviews in Biochemistry*, 38, 501–538.

van Oss, C.J., 1995. Hydrophobicity of biosurfaces - Origin, quantitative determination and interaction energies. *Colloids and Surfaces B: Biointerfaces*, 5 (3–4), 91–110.

Pace, N.R., 1997. A molecular view of microbial diversity and the biosphere. *Science (New York, N.Y.)*, 276 (5313), 734–740.

Paraskevas, S., Danser, M.M., Timmerman, M.F., Van Der Velden, U., and Van Der Weijden, G.A., 2004. Amine fluoride/stannous fluoride and incidence of root caries in periodontal maintenance patients. *Journal of Clinical Periodontology*, 31 (11), 965–971.

Parsek, M.R. and Greenberg, E.P., 2005. Sociomicrobiology: The connections between quorum sensing and biofilms. *Trends in Microbiology*, 13 (1), 27–33.

Paster, B.J. and Dewhirst, F.E., 2009. Molecular microbial diagnosis. *Periodontology 2000*, 51 (1), 38–44.

Parveen, A., Smith, G., Salisbury, V., & Nelson, S. M. (2001). Biofilm culture of Pseudomonas aeruginosa expressing lux genes as a model to study susceptibility to antimicrobials. *FEMS Microbiology Letters*, *199*(1), 115–118.

Persson, S., Claesson, R., and Carlsson, J., 1989. The capacity of subgingival microbiotas to produce volatile sulfur compounds in human serum. *Molecular Oral Microbiology*, 4 (3), 169–172.

Pilch, S., Williams, M.I., and Cummins, D., 2005. Effect of a triclosan / PVM / MA copolymer / fluoride dentifrice on volatile sulfur compounds in vitro. *Oral Diseases*, 11, 57–60.

Pratt, J.T., Tamayo, R., Tischler, A.D., and Camilli, A., 2007. PilZ domain proteins bind cyclic diguanylate and regulate diverse processes in Vibrio cholerae. *Journal of Biological Chemistry*, 282 (17), 12860–12870.

Quirynen, M., 2003. Management of oral malodour. *Journal of Clinical Periodontology*, 30 (SUPPL. 5), 17–18.

Rasiah, I.A., Wong, L., Anderson, S.A., and Sissons, C.H., 2005. Variation in bacterial DGGE patterns from human saliva: Over time, between individuals and in corresponding dental plaque microcosms. *Archives of Oral Biology*, 50 (9), 779–787.

Redmile-Gordon, M.A., Armenise, E., White, R.P., Hirsch, P.R., and Goulding, K.W.T., 2013. A comparison of two colorimetric assays, based upon Lowry and Bradford techniques, to estimate total protein in soil extracts. *Soil Biology and Biochemistry*, 67, 166–173.

Roberts, A.P., Pratten, J., Wilson, M., and Mullany, P., 1999. Transfer of a conjugative transposon, Tn5397 in a model oral biofilm. *FEMS Microbiology Letters*, 177 (1), 63–66.

Roberts, W.R. and Addy, M., 1981. Comparison of the in vivo and in vitro antibacterial properties of antiseptic mouthrinses containing chlorhexidine, alexidine, cetyl pyridinium chloride and hexetidine: Relevance to mode of action. *Journal of Clinical Periodontology*, 8 (4), 295–310.

Robertson, C. A., Evans, D. H., & Abrahamse, H. (2009). Photodynamic therapy (PDT): A short review on cellular mechanisms and cancer research applications for PDT. *Journal of Photochemistry and Photobiology B: Biology*, *96*(1), 1–8.

Rølla, G., Løe, H., and Schiøtt, C.R., 1971. Retention of chlorhexidine in the human oral cavity. *Archives of Oral Biology*, 16 (9).

Romling, U., Galperin, M.Y., and Gomelsky, M., 2013. Cyclic di-GMP: the first 25 years of a universal bacterial second messenger. *Microbiology and Molecular Biology Reviews : MMBR*, 77 (1), 1–52.

Römling, U., Gomelsky, M., and Galperin, M.Y., 2005. C-di-GMP: The dawning of a novel bacterial signalling system. *Molecular Microbiology*, 57 (3), 629–639.

Rosenberg, M., Kulkarni, G. V, Bosy, A., and McCulloch, C.A.G., 1991. Reproducibility and Sensitivity of Oral Malodor Measurements with a Portable Sulphide Monitor. *Journal of Dental Research*, 70 (11), 1436–1440.

Rosenberg, M. and McCulloch, C.A.G., 1992. Measurement of Oral Malodor: Current Methods and Future Prospects. *Journal of Periodontology*, 63 (9), 776–782.

Rosenberg, M., Septon, I., Eli, I., Bar-Ness, R., Gelernter, I., Brenner, S., and Gabbay, J., 1991. Halitosis measurement by an industrial sulphide monitor. *Journal of periodontology*, 62 (8), 487–489.

Ross, B.M. and Esarik, A., 2013. The analysis of oral air by selected ion flow tube mass spectrometry using indole and methylindole as examples. *In*: *Volatile Biomarkers. Non-invasive Diagnosis in Physiology and Medicine*. Elsevier Oxford, England, 77–88.

Ross, P., Weinhouse, H., Aloni, Y., Michaeli, D., Weinberger-Ohana, P., Mayer, R., Braun, S., de Vroom, E., van der Marel, G.A., van Boom, J.H., and Benziman, M., 1987. Regulation of cellulose synthesis in Acetobacter xylinum by cyclic diguanylic acid. *Nature*, 325, 279.

Ryan, R.P., Andrade, M., Farah, C.S., Armitage, J.P., Ryan, R.P., Mccarthy, Y., Andrade, M., Farah, C.S., Armitage, J.P., and Dow, J.M., 2017. Correction for Ryan et al., Cell–cell signal-dependent dynamic interactions between HD-GYP and GGDEF domain proteins mediate virulence in *Xanthomonas campestris*. *Proceedings of the National Academy of Sciences*, 114 (7), E1303–E1303.

Rybtke, M.T., Borlee, B.R., Murakami, K., Irie, Y., Hentzer, M., Nielsen, T.E., Givskov, M., Parsek, M.R., and Tolker-Nielsen, T., 2012. Fluorescence-based reporter for gauging cyclic Di-GMP levels in Pseudomonas aeruginosa. *Applied and Environmental Microbiology*, 78 (15), 5060–5069.

Saad, S., Hewett, K., and Greenman, J., 2013. Use of an in vitro flat-bed biofilm model to measure biologically active anti-odour compounds. *Applied Microbiology and Biotechnology*, 97 (17), 7865–7875.

Saad, S.B.M., 2006. The study of the tongue biofilm and its role in oral malodour of microbial aetiology.University of the West of England.

Salako, N.O. and Philip, L., 2010. Comparison of the use of the halimeter and the oral chroma??? in

the assessment of the ability of common cultivable oral anaerobic bacteria to produce malodorous volatile sulfur compounds from cysteine and methionine. *Medical Principles and Practice*, 20 (1), 75–79.

Sambanthamoorthy, K., Gokhale, A.A., Lao, W., Parashar, V., Neiditch, M.B., Semmelhack, M.F., Lee, I., and Waters, C.M., 2011. Identification of a novel benzimidazole that inhibits bacterial biofilm formation in a broad-spectrum manner. *Antimicrobial Agents and Chemotherapy*, 55 (9), 4369–4378.

Sambanthamoorthy, K., Luo, C., Pattabiraman, N., Feng, X., Koestler, B., Waters, C.M., and Palys, T.J., 2014. Identification of small molecules inhibiting diguanylate cyclases to control bacterial biofilm development. *Biofouling*, 30 (1), 17–28.

Sambanthamoorthy, K., Sloup, R.E., Parashar, V., Smith, J.M., Kim, E.E., Semmelhack, M.F., Neiditch, M.B., and Waters, C.M., 2012. Identification of small molecules that antagonize diguanylate cyclase enzymes to inhibit biofilm formation. *Antimicrobial Agents and Chemotherapy*, 56 (10), 5202–5211.

Sanchez, C.J., Prieto, E.M., Krueger, C.A., Zienkiewicz, K.J., Romano, D.R., Ward, C.L., Akers, K.S., Guelcher, S.A., and Wenke, J.C., 2013. Effects of local delivery of d-amino acids from biofilm-dispersive scaffolds on infection in contaminated rat segmental defects. *Biomaterials*, 34 (30), 7533–7543.

Santos, D.E., Liu, G.J., and Takeuchi, H., 1995. Blockers for excitatory effects of achatin-I, a tetrapeptide having a d-phenylalanine residue, on a snail neurone. *European Journal of Pharmacology*, 272 (2), 231–239.

Scannapieco, F. a, 1994. Saliva-bacterium interactions in oral microbial ecology. *Critical reviews in oral biology and medicine : an official publication of the American Association of Oral Biologists*, 5 (3–4), 203–248.

Scheie, A.A., 2003. The role of antimicrobials. *Dental caries, the disease and its clinical management, 1st edn. Blackwell Munksgaard, Oxford*, 179–188.

Schlafer, S. and Meyer, R.L., 2015. Confocal microscopy imaging of the biofilm matrix. *Journal of Microbiological Methods*.

Schultz, J., Milpetz, F., Bork, P., and Ponting, C.P., 1998. SMART, a simple modular architecture research tool: Identification of signaling domains. *Proceedings of the National Academy of Sciences*, 95 (11), 5857–5864.

Seerangaiyan, K., van Winkelhoff, A.J., Harmsen, H.J.M., Rossen, J.W.A., and Winkel, E.G., 2017. The tongue microbiome in healthy subjects and patients with intra-oral halitosis. *Journal of breath research*, 11 (3), 36010.

Shannon, C.E., 1948, A Mathematical Theory of Communication. *Bell System Technical Journal* [online]. 27 (3), pp. 379–423.

Simm, R., Morr, M., Kader, A., Nimtz, M., and Römling, U., 2004. GGDEF and EAL domains inversely regulate cyclic di-GMP levels and transition from sessibility to motility. *Molecular Microbiology*, 53 (4), 1123–1134.

Simonson, L., McMahon, K., Clulders, D. and Morton, H. 1992 Bacterial synergy of Treponema denticola and Porphyromonas in a multinational population. *Oral microbiology and immunology*. 7,111–112.

Slater, H., Alvarez-Morales, A., Barber, C.E., Daniels, M.J., and Maxwell Dow, J., 2000. A two-component system involving an HD-GYP domain protein links cell-cell signalling to pathogenicity gene expression in Xanthomonas campestris. *Molecular Microbiology*, 38 (5), 986–1003.

Smith, D., 1992. The ion chemistry of interstellar clouds. *Chemical Reviews*, 92 (7), 1473–1485.

Smith, D. and Španěl, P., 2005. Selected ion flow tube mass spectrometry (SIFT-MS) for on-line trace gas analysis. *Mass Spectrometry Reviews*, 24 (5), 661–700.

Smith, D. and Španěl, P., 2011a. Ambient analysis of trace compounds in gaseous media by SIFT-MS. *The Analyst*, 136 (10), 2009.

Smith, D. and Španěl, P., 2011b. Direct, rapid quantitative analyses of BVOCs using SIFT-MS and PTR-MS obviating sample collection. *TrAC - Trends in Analytical Chemistry*, 30 (7), 945–959.

Socransky, S., Haffajee, A., Cugini, M., Smith, C. and Jr., K.R., 1998, Microbial complexes in subgingival plaque. *Journal of Clinical Periodontology*. 25 (2), 134–44.

Španěl, P., Ji, Y., and Smith, D., 1997. SIFT studies of the reactions of H3O+, NO+ and O2+ with a series of aldehydes and ketones. *International Journal of Mass Spectrometry and Ion Processes*, 165–166 (0), 25–37.

Spanel, P., Pavlik, M., and Smith, D., 1995. Reactions of H3O+ and OH-ions with some organic molecules; applications to trace gas analysis in air. *International Journal of Mass Spectrometry and Ion Processes*, 145 (3), 177–186.

Spangler, C., Böhm, A., Jenal, U., Seifert, R., and Kaever, V., 2010. A liquid chromatography-coupled tandem mass spectrometry method for quantitation of cyclic di-guanosine monophosphate. *Journal of Microbiological Methods*, 81 (3), 226–231.

Stahringer, S.S., Clemente, J.C., Corley, R.P., Hewitt, J., Knights, D., Walters, W.A., Knight, R., and Krauter, K.S., 2012. Nurture trumps nature in a longitudinal survey of salivary bacterial communities in twins from early adolescence to early adulthood. *Genome Research*, 22 (11), 2146–2152.

Stephens, D.J. and Allan, V.J., 2003. Light Microscopy Techniques for Live Cell Imaging. *Science*, 300 (5616), 82 LP-86.

Stoodley, P., Sauer, K., Davies, D.G., and Costerton, J.W., 2002. Biofilms as Complex Differentiated Communities. *Annual Review of Microbiology*, 56 (1), 187–209.

Sudarsan, N., Lee, E.R., Weinberg, Z., Moy, R.H., Kim, J.N., Link, K.H., and Breaker, R.R., 2008. Riboswitches in Eubacteria Sense the Second Messenger Cyclic Di-GMP. *Science*, 321 (5887), 411 LP-413.

Supuran, C.T., 2004. Carbonic anhydrases: catalytic and inhibition mechanisms, distribution and physiological roles. *In*: *Carbonic anhydrase*. CRC press, 13–36.

Tal, R., Wong, H.C., Calhoon, R., Gelfand, D., Fear, A.L., Volman, G., Mayer, R., Ross, P., Amikam, D., Weinhouse, H., Cohen, A., Sapir, S., Ohana, P., and Benziman, M., 1998. Three cdg operons control cellular turnover of cyclic di-GMP in Acetobacter xylinum: Genetic organization and occurrence of conserved domains in isoenzymes. *Journal of Bacteriology*, 180 (17), 4416–4425.

Tan, C.H., Koh, K.S., Xie, C., Zhang, J., Tan, X.H., Lee, G.P., Zhou, Y., Ng, W.J., Rice, S.A., and Kjelleberg, S., 2015. Community quorum sensing signalling and quenching: microbial granular biofilm assembly. *Biofilms and Microbiomes*, 1, 1–9.

Tangerman, a and Winkel, E.G., 2008. The portable gas chromatograph OralChroma^{TM}: a method of choice to detect oral and extra-oral halitosis. *Journal of Breath Research*, 2 (1), 17010.

Tatusov, R.L., 2001. The COG database: new developments in phylogenetic classification of proteins from complete genomes. *Nucleic Acids Research*, 29 (1), 22–28.

Taylor, B. and Greenman, J., 2010. Modelling the effects of pH on tongue biofilm using a sorbarod biofilm perfusion system. *Journal of Breath Research*, 4 (1), 17107.

Tchong, S.I., Xu, H., and White, R.H., 2005. L-cysteine desulfidase: An [4Fe-4S] enzyme isolated from Methanocaldococcus jannaschii that catalyzes the breakdown of L-cysteine into pyruvate, ammonia, and sulfide. *Biochemistry*, 44 (5), 1659–1670.

Ter Steeg, P.F., Van Der Hoeven, J.S., De Jong, M.H., Van Munster, P.J.J. and Jansen, M.J.H.,1988, Modelling the gingival pocket by enrichment of subgingival microflora in human serum in chemostats. *Microbial Ecology in Health and Disease*. 1 (2), 73–84.

Thomas, L., 1974. Recent developments and outstanding problems in the theory of the D region. *Radio Science*, 9 (2), 121–136.

Thormann, K.M., Duttler, S., Saville, R.M., Hyodo, M., Shukla, S., Hayakawa, Y., Spormann, A.M., Thormann, K.M., Duttler, S., Duttler, S., Saville, R.M., Saville, R.M., Hyodo, M., Hyodo, M., Shukla, S., Shukla, S., Hayakawa, Y., Hayakawa, Y., Spormann, A.M., and Spormann, A.M., 2006. Control of Formation and Cellular Detachment from Shewanella oneidensis MR-1 Biofilms by Cyclic di-GMP. *Microbiology*, 188 (7), 2681–2691.

Thorn, R.M.S. and Greenman, J., 2009. A novel in vitro flat-bed perfusion biofilm model for determining the potential antimicrobial efficacy of topical wound treatments. *Journal of Applied Microbiology*, 107 (6), 2070–2079.

Thrane, P.S., Young, A., Jonski, G., and Rölla, G., 2007. A new mouthrinse combining zinc and chlorhexidine in low concentrations provides superior efficacy against halitosis compared to existing formulations: A double-blind clinical study. *Journal of Clinical Dentistry*, 18 (3), 82–86.

Tielen, P., Strathmann, M., Jaeger, K.E., Flemming, H.C., and Wingender, J., 2005. Alginate acetylation influences initial surface colonization by mucoid Pseudomonas aeruginosa. *Microbiological Research*, 160 (2), 165–176.

Toledo-Arana, A., Valle, J., Solano, C., Arrizubieta, M.J., Cucarella, C., Lamata, M., Amorena, B., Leiva, J., Penades, J.R., and Lasa, I., 2001. The Enterococcal Surface Protein, Esp, Is Involved in *Enterococcus faecalis* Biofilm Formation. *Applied and Environmental Microbiology*, 67 (10), 4538–4545.

Tonzetich, J., 1971. Direct gas chromatographic analysis of sulphur compounds in mouth air in man. *Archives of Oral Biology*, 16 (6), 587–597.

Tonzetich, J., 1977. Production and Origin of Oral Malodor: A Review of Mechanisms and Methods of Analysis. *Journal of Periodontology*, 48 (1), 13–20.

Tonzetich, J., Eigen, E., King, W.J., and Weiss, S., 1967. Volatility as a factor in the inability of certain amines and indole to increase the odour of saliva. *Archives of Oral Biology*, 12 (10), 1167–1175.

Tonzetich, J. and Kestenbaum, R.C., 1969. Odour production by human salivary fractions and plaque. *Archives of Oral Biology*, 14 (7), 815–827.

Tonzetich, J. and McBride, B.C., 1981. Characterization of volatile sulphur production by pathogenic and non-pathogenic strains of oral Bacteroides. *Archives of Oral Biology*, 26 (12), 963–969.

Tonzetich, J. and Richter, V.J., 1964. Evaluation of volatile odoriferous components of saliva. *Archives of Oral Biology*, 9 (1), 39–45.

Tsuruoka, T., Tamura, A., Miyata, A., Takei, T., Inouye, S., and Matshuhashi, M., 1985. Second lytic target of β-lactam compounds that have a terminal d-amino acid residue. *European Journal of Biochemistry*, 151 (2), 209–216.

Tsuruoka, T., Tamura, A., Miyata, A., Takei, T., Iwamatsu, K., Inouye, S., and Matsuhashi, M., 1984. Penicillin-Insensitive Incorporation of D-Amino Acids into Cell Wall Peptidoglycan Influences the Amount of Bund Lipoprotein in Escherichia coli. *Journal of Bacteriology*, 160 (3), 889–894.

Tyrrell, K.L., Citron, D.M., Warren, Y.A., Nachnani, S., and Goldstein, E.J.C., 2003. Anaerobic bacteria cultured from the tongue dorsum of subjects with oral malodor. *Anaerobe*, 9 (5), 243–246.

Veech, J.A., 2013. A probabilistic model for analysing species co-occurrence. *Global Ecology and Biogeography*, 22 (2), 252–260.

Vesterlund, S., Paltta, J., Lauková, A., Karp, M., and Ouwehand, A.C., 2004. Rapid screening method for the detection of antimicrobial substances. *Journal of Microbiological Methods*, 57 (1), 23–31.

Vidal, O., Longin, R., Prigent-Combaret, C., Dorel, C., Hooreman, M., and Lejeune, P., 1998. Isolation of an Escherichia coli K-12 mutant strain able to form biofilms on inert surfaces: Involvement of a new ompR allele that increases curli expression. *Journal of Bacteriology*, 180 (9), 2442–2449.

Vollmer, W., Blanot, D., and De Pedro, M.A., 2008. Peptidoglycan structure and architecture. *FEMS Microbiology Reviews*, 32 (2), 149–167.

Wainwright, M. (2007). Phenothiazinium photosensitisers: V. Photobactericidal activities of chromophore-methylated phenothiazinium salts. *Dyes and Pigments*, *73*(1), 7–12.

Wayne, R.P., 2009. *R. P. Wayne 1985. Chemistry of Atmospheres. An Introduction to the Chemistry of the Atmospheres of Earth, the Planets, and their Satellites. xii + 361 pp. Oxford: Clarendon Press.*

Weidel, W., Frank, H., and Martin, H.H., 1960. The Rigid Layer of the Cell Wall of Escherichia coli Strain B. *Journal of General Microbiology*, 22 (1), 158–166.

Whitchurch, C.B., Tolker-Nielsen, T., Ragas, P.C., and Mattick, J.S., 2002. Extracellular DNA Required for Bacterial Biofilm Formation. *Science*, 295 (5559), 1487 LP-1487.

White, D.J., 1995. The Application of in Vitro Models to Research on Demineralization and Remineralization of the Teeth. *Advances in Dental Research*, 9 (3), 175–193.

White, J.G., Amos, W.B., and Fordham, M., 1987. An Evaluation of Confocal Versus Conventional Imaging of Biological Structures by Fluorescence Light Microscopy. *Cell*, 105 (1), 41–48.

Wiegand, A., Buchalla, W., and Attin, T., 2007. Review on fluoride-releasing restorative materials-Fluoride release and uptake characteristics, antibacterial activity and influence on caries formation. *Dental Materials*, 23 (3), 343–362.

Wilkinson, J.F., 1958. The extracellular polysaccharides of bacteria. *Bacteriological reviews*, 22 (1), 46–73.

Wilksch, J.J., Yang, J., Clements, A., Gabbe, J.L., Short, K.R., Cao, H., Cavaliere, R., James, C.E., Whitchurch, C.B., Schembri, M.A., Chuah, M.L.C., Liang, Z.X., Wijburg, O.L., Jenney, A.W., Lithgow, T., and Strugnell, R.A., 2011. MrKH, a novel c-di-GMP-dependent transcriptional activator, controls klebsiella pneumoniae biofilm formation by regulating type 3 fimbriae

expression. *PLoS Pathogens*, 7 (8).

Wilmes, P., Remis, J.P., Hwang, M., Auer, M., Thelen, M.P., and Banfield, J.F., 2009. Natural acidophilic biofilm communities reflect distinct organismal and functional organization. *ISME Journal*, 3 (2), 266–270.

Wilson, M., 2004. Lethal photosensitisation of oral bacteria and its potential application in the photodynamic therapy of oral infections. *Photochemical & Photobiological Sciences*, *3*(5), 412–418.

Wimpenny, J.W.T. and Colasanti, R., 1997. A unifying hypothesis for the structure of microbial biofilms based on cellular automaton models. *FEMS Microbiology Ecology*, 22 (February), 1–16.

Wingender, J., Neu, T.R., and Flemming, H.-C., 1999. *Microbial Extracellular Polymeric Substances: Characterization, Structure and Function*. Springer-Verlag.

Wu, A. na, Zhang, Y. fei, Zheng, C. li, Dai, Y. jie, Liu, Y. dong, Zeng, J., Gu, G. hua, and Liu, J. she, 2008. Purification and enzymatic characteristics of cysteine desulfurase, IscS, in Acidithiobacillus ferrooxidans ATCC 23270. *Transactions of Nonferrous Metals Society of China (English Edition)*, 18 (6), 1450–1457.

Xu, H. and Liu, Y., 2011a. D-Amino acid mitigated membrane biofouling and promoted biofilm detachment. *Journal of Membrane Science*, 376 (1–2), 266–274.

Xu, H. and Liu, Y., 2011b. Reduced microbial attachment by d-amino acid-inhibited AI-2 and EPS production. *Water Research*, 45 (17), 5796–5804.

Yaegaki, K. and Sanada, K.,1992, Biochemical and clinical factors influencing oral malodor in periodontal patients. *Journal of periodontology*. 63 (9), 783–789.

Yan, W., Qu, T., Zhao, H., Su, L., Yu, Q., Gao, J., and Wu, B., 2010. The effect of c-di-GMP (3 -5 -cyclic diguanylic acid) on the biofilm formation and adherence of Streptococcus mutans. *Microbiological Research*, 165 (2), 87–96.

Young, a, Jonski, G., Rölla, G., and Wåler, S.M., 2001. Effects of metal salts on the oral production of volatile sulfur-containing compounds (VSC). *Journal of Clinical Periodontology*, 28 (8), 776–781.

Zheng, Y., Zhou, J., Sayre, D.A., and Sintim, H.O., 2014. Identification of bromophenol thiohydantoin as an inhibitor of DisA, a c-di-AMP synthase, from a 1000 compound library, using the coralyne assay. *Chemical Communications*, 50 (76), 11234–11237.

Zhou, Y., Mihindukulasuriya, K. a, Gao, H., La Rosa, P.S., Wylie, K.M., Martin, J.C., Kota, K., Shannon, W.D., Mitreva, M., Sodergren, E., and Weinstock, G.M., 2014. Exploration of bacterial community classes in major human habitats. *Genome biology*, 15 (5), R66.

Zwaardemaker, H., 1895. *Die physiologie des geruchs*. .

Appendices

I. SIFT-MS settings (Profile3)

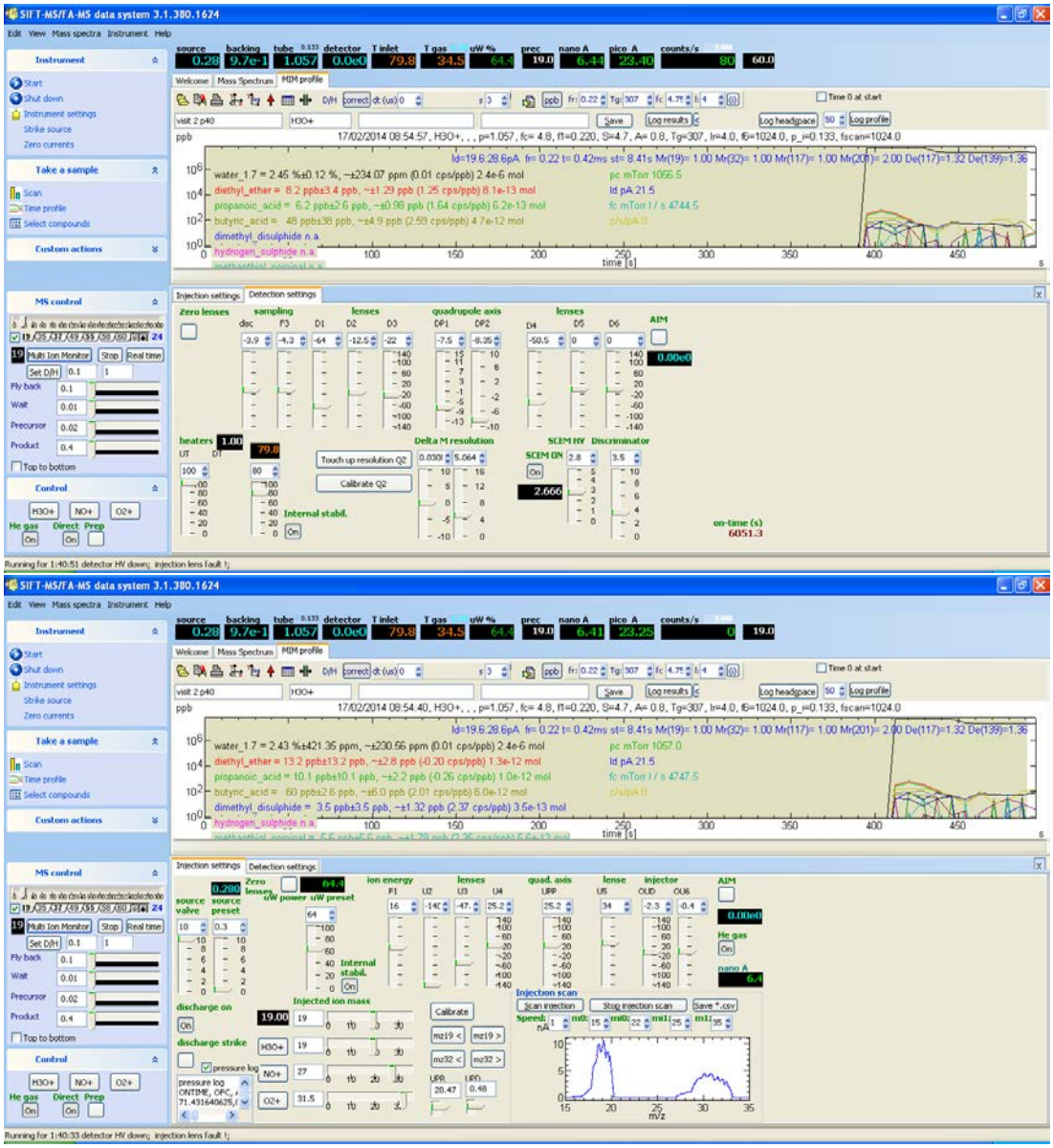

II. SIFT-MS settings (Voice200)

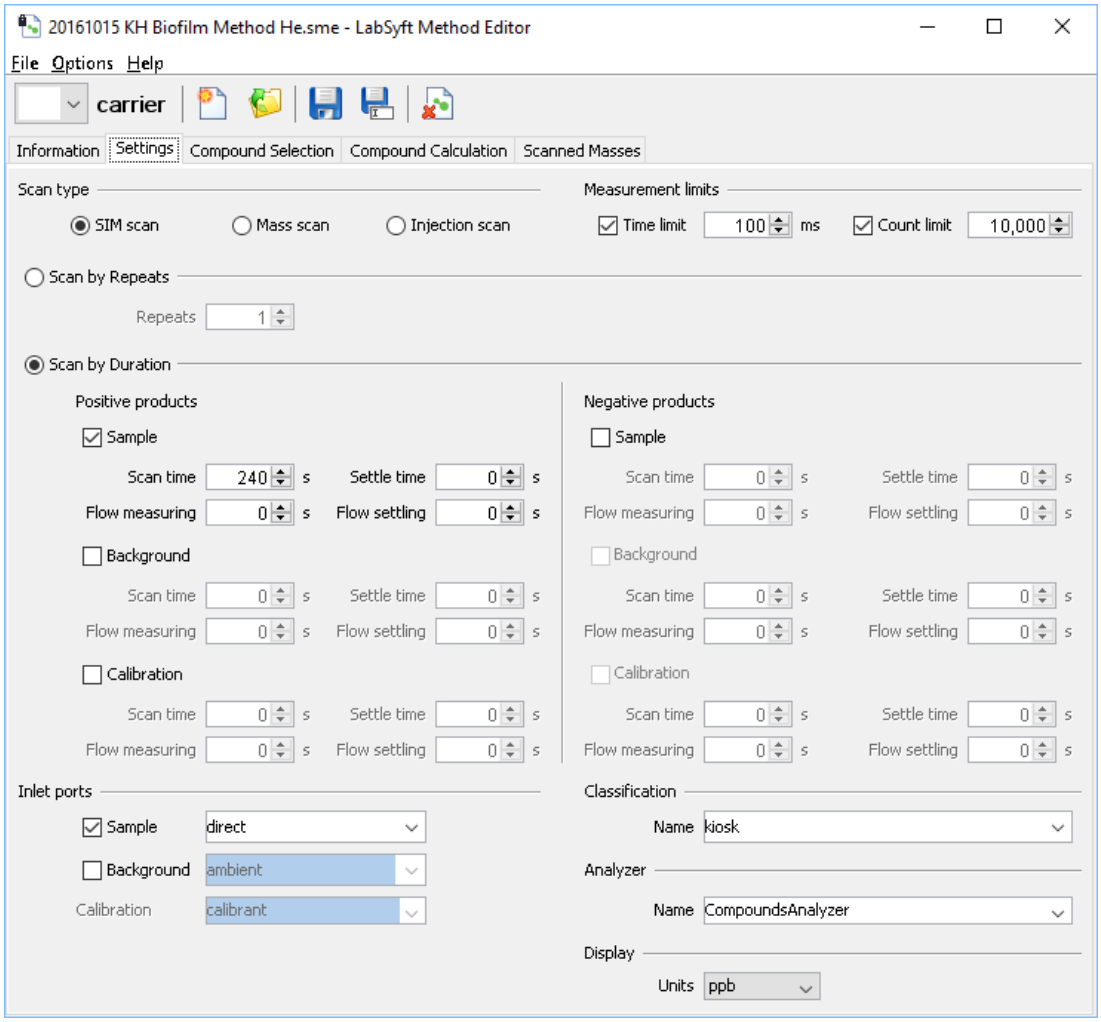

III. Incubator door panel and shelf plans

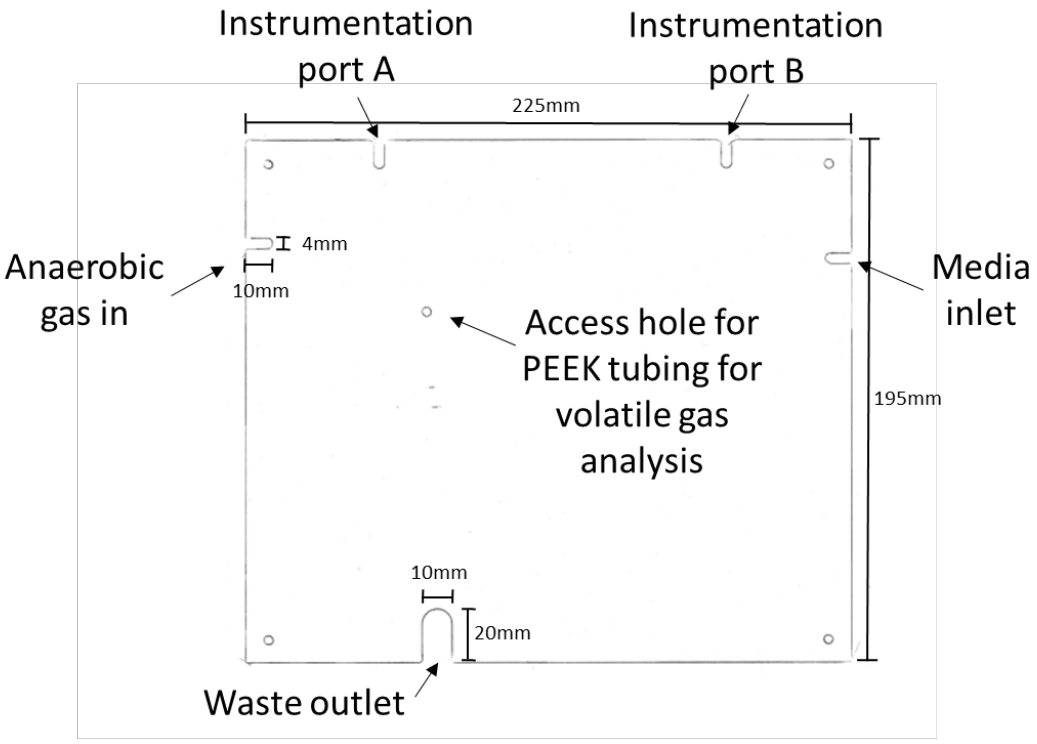

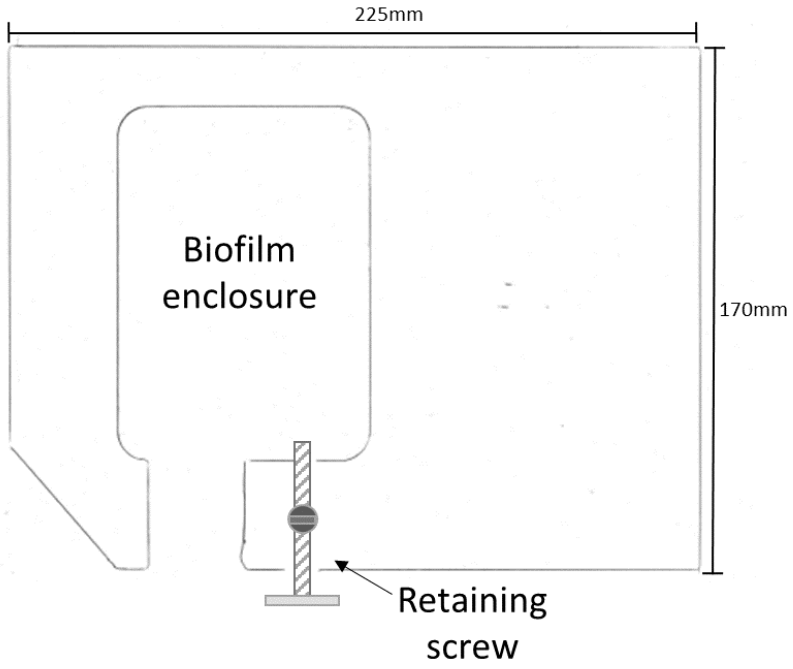

IV. Multivalve port Python code

```
import sys
import os
import gtk
import pango
import time
from Tkinter import *
import serial
from serial.tools import list_ports
import threading
from msvcrt import getch



class SequentialSampler2:


   def __init__(self):
      self.filename = None
      self.about_dialog = None
      list_ports.comports()
      self.ser = serial.Serial(
         port="COM4",
         baudrate=9600,
         parity=serial.PARITY_ODD,
         stopbits=serial.STOPBITS_TWO,
         bytesize=serial.SEVENBITS
         )
      self.locked = False
      self.cycling = False
      self.PortOpen = False
      self.OpenPort = 1
```

```
        self.RelayOn = "*RELAY 1%s ON<>0x0d>"
        self.RelayOff = "*RELAY 1%s OFF<>0x0d>"
        self.InitialisePorts = '*SET 0000010000000000\r\n'
        self.ResetPorts = "*SET 0000000000000000\r\n"
        spinbuttons =
["spinbutton1","spinbutton2","spinbutton3","spinbutton4","spinbutton5","spinbutton6"]
        GladeFile = "Sequential Sample 2.glade"
        LoadFailMsg = "Failed to load UI XML file:"
        self.ser.close
        self.ser.open

        # Set all relays to closed except number 1
        self.ser.write(self.InitialisePorts)

        # use GtkBuilder to build our interface from the XML file
        try:
            self.builder = gtk.Builder()
            self.builder.add_from_file(GladeFile)
        except:
            self.error_message(LoadFailMsg)
            sys.exit(1)

        # get the widgets which will be referenced in callbacks
        self.builder.connect_signals(self)
        self.window = self.builder.get_object("main_window")
        self.statusbar = self.builder.get_object("statusbar")
        self.text_view = self.builder.get_object("text_view")
        for spinbutton in spinbuttons:
            self.thisbutton = self.builder.get_object(spinbutton)
            self.thisbutton.set_value(5)
        self.statusbar_cid = self.statusbar.get_context_id("SeqSamp")
```

```
    self.reset_default_status()


# When the window is requested to be closed, we need to check if they have
# unsaved work. We use this callback to prompt the user to save their work
# before they exit the application. From the "delete-event" signal, we can
# choose to effectively cancel the close based on the value we return.
def on_window_delete_event(self, widget, event, data=None):
    if self.check_for_save(): self.on_gtk_save_activate(None, None)
    return False # Propogate event

# Called when the user clicks the 'New' menu. We need to prompt for save if
# the file has been modified, and then delete the buffer and clear the
# modified flag.
def on_gtk_new_activate(self, menuitem, data=None):

    if self.check_for_save(): self.on_gtk_save_activate(None, None)

    # clear editor for a new file
    buff = self.text_view.get_buffer()
    buff.set_text("")
    buff.set_modified(False)
    self.filename = None
    self.reset_default_status()

# Called when the user clicks the 'Open' menu. We need to prompt for save if
# thefile has been modified, allow the user to choose a file to open, and
# then call load_file() on that file.
def on_gtk_open_activate(self, menuitem, data=None):

    if self.check_for_save(): self.on_gtk_save_activate(None, None)
```

```
    filename = self.get_open_filename()
    if filename: self.load_file(filename)

# Called when the user clicks the 'Save' menu. We need to allow the user to choose
# a file to save if it's an untitled document, and then call write_file() on that
# file.
def on_gtk_save_activate(self, menuitem, data=None):

    if self.filename == None:
        filename = self.get_save_filename()
        if filename: self.write_file(filename)
    else: self.write_file(None)

# Called when the user clicks the 'Save As' menu. We need to allow the user
# to choose a file to save and then call write_file() on that file.
def on_gtk_save_as_activate(self, menuitem, data=None):

    filename = self.get_save_filename()
    if filename: self.write_file(filename)

# Called when the user clicks the 'Quit' menu. We need to prompt for save if
# the file has been modified and then break out of the GTK+ main loop
def on_gtk_quit_activate(self, menuitem, data=None):

    if self.check_for_save(): self.on_gtk_save_activate(None, None)
    gtk.main_quit()

# Called when the user clicks the 'Cut' menu.
def on_gtk_cut_activate(self, menuitem, data=None):
```

```
    buff = self.text_view.get_buffer();
    buff.cut_clipboard (gtk.clipboard_get(), True);

# Called when the user clicks the 'Copy' menu.
def on_gtk_copy_activate(self, menuitem, data=None):

    buff = self.text_view.get_buffer();
    buff.copy_clipboard (gtk.clipboard_get());

# Called when the user clicks the 'Paste' menu.
def on_gtk_paste_activate(self, menuitem, data=None):

    buff = self.text_view.get_buffer();
    buff.paste_clipboard (gtk.clipboard_get(), None, True);

# Called when the user clicks the 'Delete' menu.
def on_gtk_delete_activate(self, menuitem, data=None):

    buff = self.text_view.get_buffer();
    buff.delete_selection (False, True);

# Called when the user clicks the 'About' menu. We use gtk_show_about_dialog()
# which is a convenience function to show a GtkAboutDialog. This dialog will
# NOT be modal but will be on top of the main application window.
def on_gtk_about_activate(self, menuitem, data=None):

    if self.about_dialog:
        self.about_dialog.present()
        return

    authors = [
```

```
    "Keith Hewett <keith2.hewett@uwe.ac.uk>"
    ]

    about_dialog = gtk.AboutDialog()
    about_dialog.set_transient_for(self.window)
    about_dialog.set_destroy_with_parent(True)
    about_dialog.set_name("Sequential Sampler")
    about_dialog.set_version("1.3")
    about_dialog.set_copyright("Copyright \xc2\xa9 2014 Keith Hewett")
    about_dialog.set_comments("GTK+, Glade3 and Python")
    about_dialog.set_authors           (authors)
    about_dialog.set_logo_icon_name     (gtk.STOCK_EDIT)

    # callbacks for destroying the dialog
    def close(dialog, response, editor):
        editor.about_dialog = None
        dialog.destroy()

    def delete_event(dialog, event, editor):
        editor.about_dialog = None
        return True

    about_dialog.connect("response", close, self)
    about_dialog.connect("delete-event", delete_event, self)

    self.about_dialog = about_dialog
    about_dialog.show()

 # We call error_message() any time we want to display an error message to
# the user. It will both show an error dialog and log the error to the
# terminal window.
```

```
def error_message(self, message):

    # log to terminal window
    self.print_to_box  (message)

    # create an error message dialog and display modally to the user
    dialog = gtk.MessageDialog(None,
                        gtk.DIALOG_MODAL | gtk.DIALOG_DESTROY_WITH_PARENT,
                        gtk.MESSAGE_ERROR, gtk.BUTTONS_OK, message)

    dialog.run()
    dialog.destroy()

# This function will check to see if the text buffer has been
# modified and prompt the user to save if it has been modified.
def check_for_save (self):

    ret = False
    buff = self.text_view.get_buffer()

    if buff.get_modified():

        # we need to prompt for save
        message = "Do you want to save the changes you have made?"
        dialog = gtk.MessageDialog(self.window,
                            gtk.DIALOG_MODAL | gtk.DIALOG_DESTROY_WITH_PARENT,
                            gtk.MESSAGE_QUESTION, gtk.BUTTONS_YES_NO,
                            message)
        dialog.set_title("Save?")

        if dialog.run() == gtk.RESPONSE_NO: ret = False
```

```
        else: ret = True

        dialog.destroy()

    return ret

# We call get_open_filename() when we want to get a filename to open from the
# user. It will present the user with a file chooser dialog and return the
# filename or None.
def get_open_filename(self):

    filename = None
    chooser = gtk.FileChooserDialog("Open File...", self.window,
                                    gtk.FILE_CHOOSER_ACTION_OPEN,
                                    (gtk.STOCK_CANCEL, gtk.RESPONSE_CANCEL,
                                     gtk.STOCK_OPEN, gtk.RESPONSE_OK))

    response = chooser.run()
    if response == gtk.RESPONSE_OK: filename = chooser.get_filename()
    chooser.destroy()

    return filename

# We call get_save_filename() when we want to get a filename to save from the
# user. It will present the user with a file chooser dialog and return the
# filename or None.
def get_save_filename(self):

    filename = None
    chooser = gtk.FileChooserDialog("Save File...", self.window,
                                    gtk.FILE_CHOOSER_ACTION_SAVE,
```

```
                                (gtk.STOCK_CANCEL, gtk.RESPONSE_CANCEL,
                                 gtk.STOCK_SAVE, gtk.RESPONSE_OK))

    response = chooser.run()
    if response == gtk.RESPONSE_OK: filename = chooser.get_filename()
    chooser.destroy()
    filename = filename + ".mvl"
    return filename

# We call load_file() when we have a filename and want to load it into the
# buffer for the GtkTextView. The previous contents are overwritten.
def load_file(self, filename):

    # add Loading message to status bar and ensure GUI is current
    self.statusbar.push(self.statusbar_cid, "Loading %s" % filename)
    while gtk.events_pending(): gtk.main_iteration()

    try:
        # get the file contents
        fin = open(filename, "r")
        text = fin.read()
        fin.close()

        # disable the text view while loading the buffer with the text
        self.text_view.set_sensitive(False)
        buff = self.text_view.get_buffer()
        buff.set_text(text)
        buff.set_modified(False)
        self.text_view.set_sensitive(True)

        # now we can set the current filename since loading was a success
```

```
            self.filename = filename

        except:
            # error loading file, show message to user
            self.error_message ("Could not open file: %s" % filename)

        # clear loading status and restore default
        self.statusbar.pop(self.statusbar_cid)
        self.reset_default_status()

    def write_file(self, filename):

        # add Saving message to status bar and ensure GUI is current
        if filename:
            self.statusbar.push(self.statusbar_cid, "Saving %s" % filename)
        else:
            self.statusbar.push(self.statusbar_cid, "Saving %s" % self.filename)

        while gtk.events_pending(): gtk.main_iteration()

        try:
            # disable text view while getting contents of buffer
            buff = self.text_view.get_buffer()
            self.text_view.set_sensitive(False)
            text = buff.get_text(buff.get_start_iter(), buff.get_end_iter())
            self.text_view.set_sensitive(True)
            buff.set_modified(False)

            # set the contents of the file to the text from the buffer
            if filename: fout = open(filename, "w")
            else: fout = open(self.filename, "w")
```

```
            fout.write(text)
            fout.close()

            if filename: self.filename = filename

        except:
            # error writing file, show message to user
            self.error_message ("Could not save file: %s" % filename)

        # clear saving status and restore default
        self.statusbar.pop(self.statusbar_cid)
        self.reset_default_status()

    def reset_default_status(self):

        if self.filename: status = "File: %s" % os.path.basename(self.filename)
        else: status = "File: (UNTITLED)"

        self.statusbar.pop(self.statusbar_cid)
        self.statusbar.push(self.statusbar_cid, status)

    def LockButton_toggled(self,widget):
        if widget.get_active():
            self.locked = True
        if not widget.get_active(): self.locked = False

    def CycleButton_toggled(self,widget):
        if widget.get_active():
            print  ("Cycle Start")
            self.cycling = True
            self.StopTimer = False
```

```
        ##self.t2=threading.Thread(target=self.ESC_pressed())
        ##self.t2.start()
        self.t=threading.Thread(target=self.main_loop())
        self.t.start()

    else:
        print  ("Cycle Stop")
        self.cycling = False
        self.StopTimer = True


def print_to_box (self, prstr):
    buff = self.text_view.get_buffer()
    buff.insert_at_cursor(prstr+"\r")
    self.text_view.scroll_to_iter(buff.get_end_iter(),0.0, False, 0, 0)
    print prstr

def button_toggled(self, widget):
    self.ButtonToggled = gtk.Buildable.get_name(widget)[-1:]
    print ( "button toggled, current port is: " + self.ButtonToggled)
    if widget.get_active():
        SendText = self.RelayOn % self.ButtonToggled
        self.OpenPort = int(self.ButtonToggled)
        setstamp = True
    if not widget.get_active():
        SendText = self.RelayOff % self.ButtonToggled
        #if self.locked: widget.set_active(True)
        setstamp = False
    #if not self.locked:
    self.ser.write(SendText + '\r\n')
    out = ''
```

```
        ## device time delay
        time.sleep(0.5)
        while self.ser.inWaiting() > 0:
            out += self.ser.read(1)
        if out != '':
            print  ("Board responds:>> " + out)
        print  ("SWITCH: Port Number is now:" + str(self.OpenPort))
        if setstamp:
            stamp = str(int(time.time()*1000)) #time.strftime("%d/%m/%Y,%X",
time.localtime())
            stamp = stamp + "," + str(self.OpenPort)
            self.print_to_box (stamp)


    def switch_port(self, addport=1):
        if not self.PortOpen:
            print ("switch_port says port Number is:" + str(self.OpenPort))
            button = self.builder.get_object("button"+str(self.OpenPort))
            if button.get_active() == False:
                button.set_active(True)
            if self.OpenPort + addport < 7:
                self.OpenPort = self.OpenPort + addport
            else:
                self.OpenPort = self.OpenPort + addport - 6


    def ESC_pressed(self):
        print "t2 start"
        while self.cycling == True:
            key = ord(getch())
            if key == 27: #ESC
                print "ESC"
```

```
            self.cycling = False


    def main_loop(self):


        print "t1 start"
        while self.cycling == True:
            spinbutton = self.builder.get_object("spinbutton"+str(self.OpenPort))
            interval = spinbutton.get_value_as_int()
            self.switch_port(1)
            while gtk.events_pending():
                gtk.main_iteration()
            timestart = time.time()
            checkstop = open("checkstop.txt","r")
            if checkstop.read(4) == "STOP":
                self.cycling = False
            while time.time() - timestart < interval:
                stamp = str(int(time.time()*1000)) #time.strftime("%d/%m/%Y,%X",
time.localtime())
                stamp = stamp + "," + str(self.OpenPort-1)
                self.print_to_box(stamp)
                time.sleep(8.41)




    def on_window_destroy(self,object,data=None):
        self.ser.write(self.ResetPorts)
        self.cycling = False
        self.ser.close()
        self.print_to_box  ("quit with cancel")
```

```
        gtk.main_quit()

    def main(self):
        self.window.show()
        gtk.main()




if __name__ == "__main__":
    selector = SequentialSampler2()
    selector.main()
```

V. Documents relating to ethics and permissions

University of the West of England
BRISTOL

Study Number:

Patient Identification Number for this trial:

CONSENT FORM

Title of Project: The effects of oral formulations on oral malodour and tongue microbes

REC reference:

IRAS ID:

Name of Researcher:

Please initial box

1. I confirm that I have read and understand the information sheet dated ..... ☐ (version .....) for the above study. I have had the opportunity to consider the information, ask questions and have had these answered satisfactorily.

2. I understand that my participation is voluntary and that I am free to withdraw at any time, ☐ without giving any reason.

3. I understand that relevant sections of my medical notes and data collected during ☐ the study, may be looked at by individuals from Colgate-Palmolive and the University of the West of England, from regulatory authorities where it is relevant to my taking part in this research. I give permission for these individuals to have access to my records.

4. I understand that the information collected about me will be used ☐ to support other research in the future, and may be shared anonymously with other researchers.

5. I agree to take part in the above study. ☐

_____	_____	_____
Name of Patient	Signature	Date
_____	_____	_____
Name of Person taking consent (if different from researcher)	Date	Signature
_____	_____	_____
Researcher	Signature	Date

Health Questionnaire

Name:

Age:

Before beginning this study we need you to complete this form. Please tick or mark the appropriate boxes.

Are you presently participating in any other dental or medical study?

Yes/No

Has your medical status changed in any significant way since your last UWE breath odour trial? Yes/No

Do you suffer from any medical illness (heart disease, chest disease, liver disease, kidney disease, diabetes, intestinal disease)?

Yes/No

Are you taking any medically prescribed drugs or medicines for any reason?

Yes/No

Do you smoke and if so how many a day?

Yes (number)/No

Have you had any significant dental treatment since your last UWE breath odor trial?

(e.g. Rampant caries, crowns, caps, bridges, dentures, severe gingivitis, periodontal disease, dental abscesses, oral thrush)?

Yes/No

Are you taking any medicated sweets containing anti microbials?

Yes/No

Date of last visit to dentist

Date:

Please confirm that you agree to us retaining this information for 1 month after the trial has been completed. Thereafter, these forms will be destroyed. Information extracted from these forms will be devoid of any links to any individual (made anonymous). For instance we might report that 48% were male 52% were female, the median age was 32, none were taking medically prescribed drugs, all volunteers were in good health etc. but there would be no actual link to any named individual. Until destroyed, this form will be treated as confidential by the chief investigator and stored securely.

I agree to the short term (1-month) retention of the above information by the chief investigator

Signed: _____.

Date: _____.

Chief investigator: _____.

Invitation Letter

Participant Information Sheet

Project Title: The effects of oral formulations on bad breath and tongue microbes

This project has been reviewed and approved by NRES Committee North-West-Haydock

REC reference: 13/NW/0316

IRAS project ID: 178410

You are being invited to take part in the study "The effects of oral formulations on bad breath and tongue microbes"

Before you decide it is important for you to understand why the research is being done and what it will involve. Please take time to read the following information carefully and discuss it with others if you wish. Ask us if there is anything that is not clear or if you would like more information. Take time to decide whether or not you wish to take part.

1. Aim of the study

This three month study aims at looking at the potential changes in the numbers of microbes from the tongue, and in bad breath levels following the use of oral formulations; three test formulations plus two positive controls and one negative control.

2. Who are we, who is funding this study and why we are asking for your help?

We are the Centre of Oral malodour Research at UWE and have been working on this field for the last 22 years. This particular study is funded by a company in the UK Helperby Therapeutics Limited. Oral malodour or bad breath can affect any individual during their life and although not life threatening can cause a lot of distress in some. Bad breath may arise from microbes on the surface of the tongue. It is believed that certain types of microbes have the capacity to transform sulphur containing food into hydrogen sulphide and other malodorous gases. By measuring breath levels and sampling the tongue scrape for numbers associations may be seen between breath odour and quantity of microbes present on the surface of the tongue. The results obtained from this study could substantially influence the development of oral hygiene formulations (e.g. mouthwashes, lozenges or toothpastes) that could be used to reduce bad breath and subsequently relieve the stress and discomfort that this condition may cause in many humans.

3. Who can participate?

Anyone over the age of 18 and who has given informed consent**.** Participants should not have untreated caries or gum inflammation. Participants must not have received antibiotic therapy within at least one month prior to the study.

4. Do I have to take part?

Your participation in this study is entirely voluntary. If you decide to take part you will be given this information sheet and will be asked to sign a consent form. If you decide to take part you are still free to withdraw at any time without giving any reason.

5. What are we testing?

We are testing three different oral formulations and comparing them to two positive controls (Cordosyl and CB12) and to one negative control (Water). Of the three test formulations, one contains chlorhexidine diacetate, one contains zinc acetate, and the third contains HT61.

Some of the oral formulations you will be testing may or may not freshen the breath to the same extent as others.

6. What are the possible benefits of taking part?

Participation in this study may not benefit you personally. The results of this study may help other individuals in the future.

7. What are the side effects of any treatment received when taking part?

In general, no adverse side effects are anticipated from the use of either of these test toothpastes. However, you might experience tongue or gum irritation with the use of the test products. If either of these conditions occurs, it is expected they will be reversed upon cessation of the oral formulation use. If you experience any problems or any research related injury, you will have to contact Dr. Saliha BM Saad (117 328 2515 (day) or 07717723968 (mobile). You understand that if any physical injury results from your use of the test products, the funding company will be responsible for medical costs provided you seek medical attention as directed by the funding company or as directed by the Study Investigator (Dr. Saliha BM Saad).

8. What will happen to me if I take part?

Screening and Selection of Subjects: Candidates who have signed an Informed Consent Form and a Health Questionnaire will be screened by the examiner to identify those subjects who meet the inclusion / exclusion characteristics. Candidates will also be

examined by a qualified Dentist. The first 30 subjects that meet the inclusion/exclusion characteristics and sign an Informed Consent Form and a health questionnaire will be entered into the study. Baseline measurement described below will be completed at screening visit.

This crossover double-blind study will take place at the University of the West of England in our laboratory. A group of thirty participants will be taking part in this study which will last for three months. Before the start of the trial each participant will be examined by a qualified dentist who will assess their oral and dental status. The Dentist will advise each participant on the best way to use the oral rinse. Participants will be assessed and will use one type of treatment one day a week for six consecutive weeks. Each participant will receive one of the six oral formulations in a randomized manner. Neither the investigator, nor the participant will know which oral formulation has been allocated to you. You will be asked to visit the laboratory on six occasions, in the morning and afternoon for six consecutive weeks.

The study will be conducted as follows:

Prior to the study, you should continue with your normal oral hygiene routine (brushing your teeth and flossing using dental floss)

First visit to the laboratory:

The night before your first visit to the lab you must not consume any strong food (e.g. garlic, spices) and you must not drink alcohol.

You can brush your teeth at night before going to bed.

Morning of day1:

- You must not take food or drinks or brush your teeth
- You will have your breath assessed by a trained organoleptic judge
- You will have your breath measured by two different instruments
- You will give a tongue-scrape sample using a sterile toothbrush
- You will receive an oral formulation and you will be asked to use it straight away in the laboratory
- You will return to the lab 30 minutes, 3 hours and 6 hours after using the treatment to have your breath assessed by an organoleptic judge and by instruments
- You will be given a washout toothpaste to use twice a day for the duration of the trial

On day 7: The night before your second visit to the lab you must not consume any strong food (e.g. garlic, spices) and you must not drink alcohol.

You can brush your teeth at night before going to bed.

One day per week and for six consecutive weeks you will come to the lab to use one oral formulation and you will have to visit the lab four times on that same day (T0, 30 min, 3 hours and 6 hours after treatment).

Your sampling days will be: Day 1, Day 8, Day 15, Day 22, Day 29 and Day 36

9. How will anonymised samples be collected and mouth air analysed?

Each participant will be informed by email about the day and time of the visit at their convenience. On the day of the study, you will be asked to fill in a health questionnaire prior to your samplings and assessments and sign an informed consent form. This will be administered by the principal investigator.

Once you have consented to participate in the study, you will be asked to give a sample of your tongue scrape for microbiological analysis, and have your breath assessed by a trained breath judge and by instruments. Each sample taken (tongue scrape and breath) will be labelled with a code allocated to you. Thereafter, all samples are known by code number and not by name.

All these procedures will be performed under instruction and supervision of the investigator. All the samples and tests together should not take more than 30 minutes in total, so we hope that this should not interfere too much with your normal working day. You will need to visit our laboratory once a week in the morning only for three consecutive weeks.

On the sampling day you will be asked NOT to wear strongly perfumed cosmetics, nor to consume food associated with bad breath (for example garlic, onions, curry) on the day prior to and on the day of sampling. Your normal oral hygiene practice should continue the day before the study, but on the morning of testing you should not brush your teeth or use mouthwash or ingest food 2 hours prior to the tests. Drinks should be restricted to water during this period

10. What will happen next to my sample?

Coded microbial samples will be analysed using conventional microbiology methods and results (data) will be stored. Each sample will be coded. The results (data) from mouth air measurements will likewise be identified only by your code number, NOT your name.

Microbilogical samples will be disposed of, in accordance with the Human Tissue Act."

Any samples which are not correctly labelled with the code will be destroyed in accordance with the Human Tissue Act.

11. What happens next?

If having read the information (and any outstanding questions answered fully from our discussions) and you are happy to participate in the study, you may sign the consent form. This form states that you have read and understood this information sheet, that the participation is entirely voluntary, and that the samples are completely anonymised. You may also, if you prefer, take this information sheet away and think about whether you wish to take part**.** Please do not hesitate to contact me via the details below with any further questions and/ or when you are happy to consent.

Once consented you will be provided with; your protocol, your diary and appointment date & time for attending the laboratory, your informed consent code which needs to be written on any donated sample, and my contact details.

Consent forms will be kept for the duration of the study in a locked cabinet in a secure office. If at any point you wish to formally withdraw consent, please contact me (details below) and I will ensure your consent form is immediately destroyed and samples withdrawn and destroyed in accordance with the Human Tissue Act.

In the very unlikely event that an adverse reaction occurs in response to the procedure the University of the West of England will consider the possibility of no fault compensation without admitting liability. UWE confirms that it has in place all appropriate Professional Indemnity Insurance and Public Liability Insurance to cover any claims for negligence on the part of UWE staff and students in performing UWE's role in the study.

12. Who can I contact if I have any complaints?

In case you are not happy about the way the team dealt with you on the day of your assessment, or about the procedure used in this study, please do not hesitate to contact an independent person, the Research and Innovation Associate Dean: Pr Jenny Ames, University of the West of England, Frenchay Campus, Coldharbour Lane, Bristol e-mail: jenny.ames@uwe.ac.uk. Tel: 0117 3288409.

Oral Malodour Group would like to thank you for your time to help with the aims of our research. If at anytime you have further questions please do not hesitate to contact me.